ibvt-Schriftenreihe

Schriftenreihe des Instituts für Bioverfahrenstechnik
der Technischen Universität Braunschweig

Herausgegeben von Dietmar C. Hempel

Band 35

An analytic-synthetic approach combining mathematical modeling and experiments – towards an understanding of biofilm systems

Inhalt: Biofilme – mikrobielle Lebensgemeinschaften auf Grenzflächen – besitzen eine zentrale Bedeutung in der Natur, der Technik und auch für den Menschen. Die relevanten Prozesse, die das Wachstum von Biofilmen bestimmen, sind jedoch nicht gut verstanden. Das Ziel dieser Arbeit ist es, mathematische Modelle und experimentelle Methoden in engem Austausch zu kombinieren, um so die Zusammenhänge zu beleuchten, welche die zeitliche und räumliche Entwicklung von Biofilmen bestimmen. Hierzu kommen aktuelle Biofilmmodelle zum Einsatz, die die Entwicklung von Biofilmsystemen prognostizieren können. Diese Prognosen werden mit den Resultaten von langfristigen Biofilmkultivierungen quantitativ verglichen. So werden ein tieferes Prozessverständnis und Verbesserungen ebenso auf experimenteller Seite wie auf Ebene der Modellierung erreicht. Die so gewonnenen Ergebnisse bringen den Fokus dieser Arbeit auf die Untersuchung von Abtragsphänomenen in Biofilmsystemen. Hierzu wird ein mechanischer Ansatz präsentiert, der die Interaktion von Fluidströmung und Biofilmstruktur betrachtet.

Suchbegriffe: Biofilm, Biofilmstruktur, Biofilmwachstum, Abtrag, Modellierung, Biofilmreaktoren, Exopolymersynthese

Abstract: Biofilms – microbial communities on interfaces – are of central importance in nature, technosphere and also for human life. The processes underlying biofilm development, however, are currently poorly understood. The aim of this essay is to combine mathematical modeling and experimental methods in close interaction in order to shed light onto the coherences determining biofilm development in time and in space. Therefore, recent mathematical modeling tools come to application which allow prognoses about the behavior of biofilm systems. These prognoses are quantitatively compared with results of biofilm cultivations under comparable conditions. This leads to a better understanding of the processes and yields improvements on the experimental side as well as in terms of the model assumptions. These results bring the focus of this work to the detailed investigation of biofilm detachment phenomena. Here, a mechanical approach is presented regarding the interaction of fluid dynamics and biofilm structure.

Keywords: biofilm, structure, growth, detachment, modeling, reactors, EPS-production

An Analytic-Synthetic Approach Combining Mathematical Modeling and Experiments – Towards an Understanding of Biofilm Systems

Von der Fakultät für Maschinenbau
der Technischen Universität Carolo-Wilhelmina zu Braunschweig

zur Erlangung der Würde
eines Doktor-Ingenieurs (Dr.-Ing.)
genehmigte Dissertation

von Dipl.-Ing. Roland Bernhard Möhle
aus Braunschweig

FIT-Verlag für Innovation und Technologietransfer
Paderborn 2008

Die vorliegende Arbeit wurde als Dissertation angefertigt.

Prüfungsvorsitz:	Prof. Dr.-Ing. Dietmar C. Hempel
Referenten:	Prof. Dr. rer. nat. Rainer Krull
	Prof. Dr. rer. nat. Harald Horn
	Jun.-Prof. Dr.-Ing. Markus Böl
eingereicht am:	20. Juni 2008
mündliche Prüfung am:	11. Juli 2008

Meinen Eltern und meinem Großvater in Dankbarkeit gewidmet.

Bibliographische Information
Die Deutsche Bibliothek verzeichnet diese Publikation in der Deutschen Nationalbiografie; detaillierte bibliografische Daten sind im Internet über *http://dnb.ddb.de* abrufbar.

ISSN 1431-7230 ISBN 978-932252-42-6

Danksagung - Acknowledgement

Zahlreiche Personen und Institutionen haben entscheidend zum Gelingen dieser Arbeit beigetragen. Mein Dank gilt daher

- meinem Doktorvater Prof. Dr.-Ing. Dietmar C. Hempel für die Möglichkeit und die Freiheit, diese Arbeit anfertigen zu können, ebenso wie für seine stete Diskussionsbereitschaft,
- meinem Betreuer Prof. Dr. Harald Horn für die fachliche Betreuung meiner Arbeit und die damit verbundenen fruchtbaren Gespräche,
- Prof. Dr. Rainer Krull für die Hilfe in organisatorischen Fragen und die Übernahme des Referats,
- Prof. Dr. Andreas Haarstrick und Dr. Bernd Nörtemann insbesondere für ihre Hilfe in fachlichen Fragen,
- Frau Kahmann und Frau Oltmann für die reibungslose Abwicklung aller administrativen Angelegenheiten,
- den technischen Mitarbeitern des ibvt, namentlich Detlev Rasch, Yvonne Göcke, Sandra Hübner und Rochus Jonas, für ihre Hilfsbereitschaft und aktive Unterstützung bei den experimentellen Arbeiten,
- allen Mitarbeitern des ibvt, die zu der außergewöhnlich angenehmen Arbeitsatmosphäre im Institut beigetragen haben,
- den Mitarbeitern des Helmholtz-Zentrums für Umweltforschung in Magdeburg Dr. Thomas R. Neu, Marian Haesner, Kerstin Garny, Ute Kuhlicke und Dr. Barbara Zippel für die überaus gastliche wie herzliche Atmosphäre,
- Dr. João Xavier and Dr. Cristian Picioreanu who both taught me a lot about biofilm modeling; furthermore the research group in Delft and their head Prof. Mark van Loosdrecht for the hospitable atmosphere as well as the people I met there for crucially enriching these stays: Joana Xavier, Álvaro Oliveira Nappa, Daniel von der Schulenburg,

- Erik Alpkvist not only for the fruitful scientific cooperation but also for the excellent time we have spent together - let it be in Delft, Vienna, Leipzig, Berlin or Lund,
- Judith Arfsten, Stephanie Michel und Dr.-Ing. Ingo Kampen für die Möglichkeit, Messungen mit dem Nanoindenter des Instituts für Partikeltechnik durchführen zu können,
- Timo Geddert, Dr.-Ing. Wolfgang Augustin und Prof. Dr.-Ing. Stephan Scholl für die Möglichkeit, das FDG-Gerät des Instituts für Chemische und Thermische Verfahrenstechnik nutzen zu können,
- Herrn Jun.-Prof. Dr.-Ing. Markus Böl vom Institut für Festkörpermechanik für die angenehme und ertragreiche Zusammenarbeit im Bereich der Finite Elemente Modellierung und die Übernahme eines dritten Referats,
- Christopher Hamilton Cummiskey für die Korrektur des englischen Textes,
- den studentischen Hilfskräften Bin She, Congcong Zhang, Annelie Solether, Robert Westphal und Larissa Sahlmann für ihre tatkräftige Unterstützung,
- allen Studenten, die durch ihre Studien- und Diplomarbeiten zentral am Entstehen dieser Arbeit mitgewirkt haben: Judith Mechias, Timo Langemann, Katrin Zapf, Markus Kowalewski, Katrin Bierkandt und Kerstin Hage,
- der Deutschen Forschungsgemeinschaft DFG für die Finanzierung dieser Arbeit,
- der Oswald-Schulze-Stiftung OSS und der GlaxoSmithKline Stiftung für die finanzielle Unterstützung verschiedener Reisen sowie
- meinen Eltern und meinem Großvater Heinz Meißner für ihre stete Unterstützung in jeglicher Hinsicht. Ihnen sei diese Arbeit gewidmet.

Braunschweig, im Juli 2008 Roland B. Möhle

Teilergebnisse aus dieser Arbeit wurden mit Genehmigung der Fakultät für Maschinenbau in folgenden Beiträgen vorab veröffentlicht:

- Möhle RB, Langemann T, Haesner M, Augustin W, Scholl S, Neu T, Hempel DC, Horn H (2007) Structure and shear strength of microbial biofilms as determined with confocal laser scanning microscopy and fluid dynamic gauging using a novel rotating disc biofilm reactor. *Biotechnology and Bioengineering* 98(4):747-755.

Contents

1 Introduction

Living in biofilms –microbial communities on interfaces– is an evolutionary successful way of life for many microorganisms. Various phenomena, like specialization, communication, etc. which are responsible for the supremacy of multicellular organisms, can also be found in microbial biofilms. Hence, biofilms are present in a multitude of ecological niches and environments: from arctic piers to hot springs, from oil pipelines to phototrophic biofilms in dolomite stone.
In the technosphere, biofilms find application in highly efficient wastewater treatment plants. The biggest challenge in this research field though is provided by unwanted biofilms - biofouling - in technical devices or even more harmful: as medical biofilms on catheters or implants where they cause persistent infections of humans. Mainly due to historical reasons biofilm research is a young discipline and detailed knowledge about biofilm development is lacking. Biofilms in their environment are highly complex systems. Numerous processes –intrinsic as well as in exchange with the environment– are taking place simultaneously. The interaction of these processes emerge in the spatial and temporal development of biofilms. In pure experimental investigations these processes cannot be separated which makes the interpretation and explanation of experimental data difficult. The central idea of this work is to integrate relevant processes of biofilm development in mathematical modeling frameworks. In the numerical solution of these models biofilm properties shall emerge virtually and are quantitatively compared with experimental results obtained under comparable conditions. Basing on this idea, an iterative method is proposed combining the use of mathematical models and their validation with data from long-term biofilm cultivations. This procedure is of an analytic nature when focusing on single processes as well as synthetic when integrating these processes in comprehensive models. Thereby, a better understanding of the processes underlying biofilm development is reached. Furthermore, this approach leads to improvements of the experimental setup and the development of two novel reactor systems in this work.
The results of comparing quantitatively simulated and experimental data are shown

and discussed. From these considerations an intensive elaboration on biofilm detachment and its mechanical causes is needed. Due to the finding of detachment phenomena to be an important but poorly understood process, a basic approach on this topic is found.

2 Preliminary comments on microbial biofilms

2.1 Biofilm basics

Biofilms are one of the oldest forms of life. The first fossil records are stromatolites which date back up to 3.5 billion years [15, 220]. They are relicts of consortia of phototrophic cyanobacteria. Precipitated or entrapped minerals in these microbial mats led to the formation of cauliflower-like rocks as displayed in **figure 2.1** [122, 123]. By producing molecular oxygen as a metabolic by-product their photosynthetic metabolism caused one of the most important changes in life. Over the millions of years, the atmosphere changed from reductive to oxidative conditions allowing the development of life as it is known today. It may become obvious in this chapter that biofilms are still of great importance and can be found in numerous environments: they are ubiquitous.

Figure 2.1: 240 million year old stromatolite as fossil record of cyanobacterial colonies (picture taken at Heeseberg, 35km south-east from Braunschweig, Germany)

Generally, biofilms can be defined as microbial communities on interfaces [160]

meaning any interface including solid-liquid, gaseous-liquid, solid-gaseous or liquid-liquid. The focus of this study are biofilms growing on solid-liquid interfaces and subjected to fluid flows. This is representative of several topics, i.e. technical (piping systems, heat exchangers), natural (benthic/riverine biofilms) and also medical (intravascular catheters) issues. Microbial communities in biofilms are enclosed in a matrix constituted by slimy extracellular polymeric substances (EPS) of microbial origin.
In numerous articles and books, biofilms are termed as for example *"...the prevailing microbial lifestyle."* [238]. It is usual to find statements like *"The fact that microbes appear to grow predominantly on surfaces..."* [115] or *"...biofilm microbiologists had concluded that bacteria grow preferentially in matrix-enclosed communities adherent to surfaces."* [38]. Even though these assertions are criticized, for example D.L. Kirchner mentions the high amount of -although low concentrated- planktonic bacterial biomass in the oceans (see correspondence in *Nature* **413**, 772; 2001), the biofilm mode of life obviously is a successful evolutionary approach of microbial life (cp. section 2.4).

2.1.1 Constituents

Surely, microbial cells are the key components of biofilms. Numerous different species of unicellular organisms from prokaryotes (bacteria, archaea) to eukaryotes (fungi, protista) are inhabiting and/or constituting biofilms. Even several metazoa (e.g. rotifers, nematodes, mites) are adapted to live in or on biofilms, respectively. However, they are by far not the only constituents. The term extracellular polymeric substances (EPS) is used to sum up all the polymers of microbial origin in a biofilm (outside the cells) [216, 25, 67]. Several different types of polymers can occur - originating from different species or even from one species under different conditions. Predominantly, polysaccharides seem to build up the biofilm matrix and constitute their structural stability but also proteins (e.g. exoenzymes: belonging to so-called active EPS), nucleic acids and lipids are found [160, 68, 129]. Extracellular DNA (eDNA) may also have a structural role in biofilm formation [241]. Furthermore, biofilms are favoring the exchange of genetic information by horizontal

gene transfer. High biomass concentrations and spatial proximity of the cells could also increase the probability for transformations (Gene transfer without conjugation by transfer of DNA through the liquid between cells). This would explain the presence of eDNA in biofilms as well. Moreover, particulate matter is found as detritus (rests of structural cell elements, discarded pili or flagella, etc.) or inorganics (e.g. trapped or precipitated minerals as of special importance for the encrustation of urethral catheters [213]). Recently, also membrane vesicles are found to be occuring in biofilms in high numbers [203]. Their function, however, is not yet definitely resolved.
The vast number of options combining the different constituents already indicates that biofilms are in the most seldom cases homogeneous and easily describable entities.

2.1.2 Biofilm structure and heterogeneity

The terms biofilm structure and heterogeneity are often used unexact. It is spoken about biofilm structure and implicitly meant heterogeneity. In this study biofilm structure shall mean the 3D spatial structure of the biofilm. For later discussions it is distinguished between three spatial scales: (1) microscale - from bacterial dimensions to the size of microcolonies (1 to several 10μm), (2) mesoscale - in the dimension of biofilm thickness (up to several 100μm) and (3) macroscale - in the dimension of reactor size. It is well known and also central issue of this thesis that biofilm structure is of big importance as the determinant for mass transfer at the bulk/biofilm interface [177], mechanical stability (cp. chapter 6), etc. In turn, biofilm structure is determined by environmental conditions and can also change in time [128, 29].
Following Bishop and Rittmann [16] heterogeneities in biofilms can be regarded as *"...spatial differences in any parameter we regard as important."*. They distinguish four groups of heterogeneities for which experimental evidence is found [246]: (1) *Geometrical heterogeneities* (biofilm thickness, roughness, porosity, etc.) are clearly revealed by microscopic studies (e.g. CLSM). (2) In particular, the use of microelectrodes has shown *chemical heterogeneities* for a number of compounds,

for example oxygen concentration. (3) Different reaction types are also found to be dependent on structural properties. In mixed culture biofilms Denaturing Gradient Gel Electrophoresis (DGGE) analyses reveal a high microbial diversity emphasizing *biological heterogeneity* [108]. (4) The variability of *physical heterogeneities* (density, rheological properties, stability, etc.) will be discussed explicitely in chapter 6.

The occurence of these heterogeneities is often caused by diffusion limitation of compounds into the biofilm. This leads to a stratification of the aforesaid parameters [27]. Thus, several parameters are found to depend mainly on the coordinate perpendicular to the substratum (usually z) [258, 211]. All these structural properties can change when environmental conditions (flow, substrate, pH, temperature, etc.) vary [225, 250, 134, 90].

2.1.3 Biofilm development

Development in this context generally means morphological changes of biofilms in time and/or space. Principally, it is about the temporal development of biofilms from cells initially adhering to a surface up to the formation of a mature biofilm with its specific complex structure. This can be seen as the emerging result of different processes which are partially presented in section 3.2. **Figure 2.2** shall demonstrate important stages of this development briefly[1]. Detailed treatises can be found for example in [32, 27]. Every surface in natural aquatic systems is covered by sorption processes with a (mono)layer of organic molecules, the so-called "conditioning film" (1) [32]. Effectively, this is the surface microorganisms are interacting with. Suspended microbial cells (2) can adsorb reversibly due to e.g. intermolecular forces (van-der-Waals) (3) or pili [111] (5) and also desorb again (4). After adhering irreversibly (6) the cells can proliferate, excrete EPS and thereby form microcolonies (7). From the mature biofilm (8) biomass can be released by detachment processes (9) (cp. section 3.2.3).

[1] Sincere thanks are given to Thomas Neu for providing this graphic. *http://www.ufz.de/index.php?en=1788*

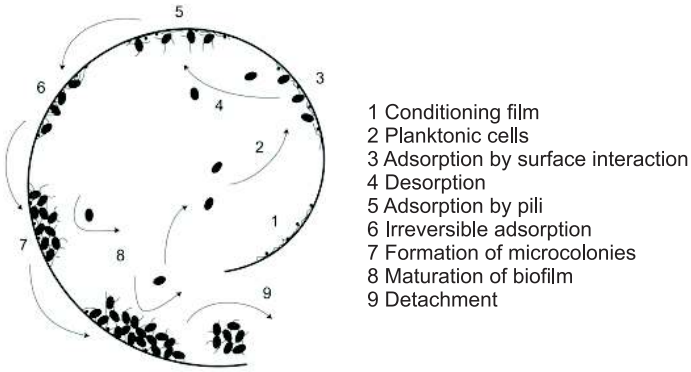

Figure 2.2: Model of biofilm development according to Thomas R. Neu (explanations in the text)

2.2 Biofilms in nature, technosphere and medicine

2.2.1 The role of biofilms in natural ecosystems

Biofilms are present in soils, sediments, on stones, plants, animals and also humans. They can inhabit environments from glaciers to hot springs. Furthermore, they are involved in global cycles of matter (carbon, nitrogen, oxygen, etc.). Per se, biofilms have evolutionary advantages in numerous ecological niches. They can deal with varying substrate conditions and find protection against mechanical, chemical or biological attacks by their EPS matrix. The spatial proximity of different microbial species provides the possibility of forming microbial consortia. In this way complex metabolic tasks can be solved together: synergistic collaborations allow the degradation of complex substrates even under difficult conditions (e.g. absence of oxygen). Examples can be found in many places like microbial mats [74], anaerobic digestion [12] or phototrophic biofilms [247].

Solids as nutrient sources for microbes

Biofilms are predestined for the use of solids as a nutrient source. Solid organic polymers like for example cellulose must first be hydrolyzed before they can be

assimilated by the cell. For this task the cell excretes hydrolytic enzymes [204]. These exoenzymes can accumulate as active EPS in the diffusion limited regime of the biofilm. Thereby the enzymes are available in high concentrations and the products of the enzymatic reaction are directly disposable for the biofilm cells [78]. Some microbes, e.g. *Geobacteriaceae* are capable of utilizing solid metal minerals as electron acceptors or energy source. Due to comparable reasons an adhered way of living is favored in order to optimize electron transport. Interestingly, pili are used as nanowires for electron transfer between cell and substratum [140, 188]

2.2.2 Biofilms in industrial applications

In process biotechnology only a few application fields are present where biofilms come to use. Artificially immobilized microorganisms or mammalian cells are not assigned to be biofilms in this sense [73]. One of the earliest processes is the production of vinegar (acetic acid) by microbial biofilms with wood chips as substratum [33]. Moreover, bioleaching in copper mining is a process in which biofilms are of great significance [24, 196, 166]. Production of bacterial polysaccharides is carried out with biofilm-forming microbes [55, 54]. The most important appearance of biofilms in industry, however, is found in detrimental aspects summed under the term "biofouling" - including numerous negative topics concerning biofilm growth in industrial plants. Fortunately, even beneficial aspects can be found as for example in wastewater treatment.

Biofouling

Biofouling is defined as the unwanted deposition and growth of biofilms [66]. Several different branches of industry like paper, chemical, or food industry suffer from biofouling. The impacts reach from a decrease in efficiency (e.g. in heat exchangers) over contamination of products (paper industry) and as far as the distribution of pathogens via drinking water distribution networks [234]. Moreover, biofilms can accelerate corrosion processes which is summarized under the term microbially influenced corrosion (MIC) [82, 174].
The strong adhesion of biofilms to a substratum makes their removal laborious and

cost-intensive. In these circumstances a consolidated knowledge might help in controlling or avoiding the growth of unwanted biofilms.

Wastewater treatment

Although trickling filters were the first wastewater treatment reactors (section 2.3), currently activated sludge systems are well established and are widely used in the treatment of municipal wastewater [245]. In biofilm reactors diffusion limitation causes a decline in reactor performance [233]. However, they provide quite a number of advantages. Not only they are stable in operation [52] and also need less installation size but also their energy demand can be much lower in comparison to that of activated sludge systems ($150 - 350 Wh/m^3$ for activated sludge systems in contrast to $30 - 60 Wh/m^3$ for trickling filters whereas biofilters can also reach values of more than $350 Wh/m^3$) [7]. Due to the decoupling of bacterial growth rate μ and dilution rate D higher throughputs can be realized, and the flow rate is no longer creating an evolutionary pressure. This allows for the existence of slow growing organisms which are capable of degrading persistent compounds like phenols [114], naphthalenesulphonic acids [121], chelating compounds [84, 167] or others (for a detailed treatise see [83, 245]). Furthermore, the biofilm matrix can provide sorption sites which improves the biodegradability of xenobiotic compounds. Also the spatial proximity of microbial consortia favors symbiotic degradation pathways (e.g. xenobiotics, nitrification, anaerobic digestion). Higher organisms like protozoa (ciliates, amebae) or metazoa (rotifers, nematodes, mites) can better survive in the reactor by grazing on the biofilm (see also section 3.2.3) and thereby reduce sludge production. Furthermore the existence of certain rotifers (e.g. *Philodina spec.*) yields a clearer effluent.
Airlift reactors with particle fixed biomass [161, 21] have proved its value in this context because of their good mixing (good mass transfer of oxygen) and fluidisation properties. Here, inorganic particles (e.g. broken sand, [114], pumice [22], etc.) function as substratum and effect a good settlability of the biomass. But also other reactor types come to use in this field: biofilters [23, 93], rotating biological contactors [167], etc. Recently, several innovative wastewater treatment processes make use of biofilms. Enhanced biological phosphorus removal is possible with biofilm

reactors [158]. Biofilms growing on gas-permeable membranes (Membrane Biofilm Reactors) can be supplied with hydrogen or oxygen gas improving for example simultaneous nitrification-denitrification [193, 219, 146]. Henceforth, a further step would be not only to get rid of undesirable compounds but also to bring them to good use for human purposes [112]. One very interesting approach is to use biofilms in the form of granular sludge in bubble column reactors. Aerobic granules in sequencing batch reactors emerge to be a promising technology for advanced wastewater treatment allowing the simultaneous removal of organics, nitrogen and phosphate [51]. Thereby feast-famine periods favor the microbial production of Polyhydroxyalkanoates (PHAs) as storage compounds [255] which are important for the formation of granules and can further be used as raw material for the synthesis of bioplastics [191].

Microbial Fuel Cells

Microbial Fuel Cells (MFCs) provide a promising technology for directly converting chemical energy to electric energy at ambient environmental conditions (concerning temperature, pressure, etc.) [186]. Recent studies reveal the important role of biofilms concerning performance and stability of MFCs [108, 139, 171]. A very interesting application is found in wastewater treatment where the biological degradation of wastewater compounds is combined with generation of electrical power [136, 81]. Nonetheless, the performance of current systems is still far from technical application. The highest area-specific power could be found in Rabaey et al. [186] with $3.6 W/m^2$ substratum area which the same author lists as $216 W/m^3$ reactor volume.

2.2.3 Medical biofilms

Humans and microbes live in coexistence with microorganisms, e.g. on the skin or even in symbiosis like in the gastrointestinal tract. It is well known that they can cause infections, too - needless to say also in the form of biofilms: Cystic fibrosis pneumonia is mainly caused by *Pseudomonas aeruginosa* and *Burkholderia cepacia*, biofilms of dental plaque (acidogenic gram-positive cocci like *Streptococcus spec.*)

effect the accumulation of acids which in turn attack the enamel surface resulting in cavities (caries) [69]. Persistent infections are caused by biofilms growing on medical devices like catheters or implants in the human body [75, 190].

Diverse causes can be appointed for the resistance of bacteria in biofilms against antibiotic therapies [41, 198]: (1) Mass transfer processes can influence the penetration of antibiotics into the biofilm. Not only the diffusion of large molecules is retarded in the biofilm matrix. Also organic molecules can adsorb in the EPS matrix which is favored when positively charged antibiotics like aminoglycosides (e.g. gentamicin, streptomycin, etc.) come in contact with the often negatively charged EPS. (2) Mainly due to diffusion limitation bacterial growth in the biofilm is retarded or even stopped (vegetative dormancy). So, antibiotics targeting the growth-related processes like cell wall synthesis (e.g. β-lactams like Penicillin) lose their effectiveness. (3) The spatial proximity favors the exchange of genetic information by horizontal gene transfer promoting the distribution of antibiotic resistances. (4) Differences in gene regulation between planktonic and sessile bacteria can deactivate metabolic pathways of biofilm bacteria which are the targets of antibiotic drugs [69].

Different studies investigate the host immune response against bacterial biofilms [132, 30]. They reveal a high resistance against antibody-mediated phagocytosis (for example using Interferon-γ and human leukocytes in Leid et al. [132]). However, a good explanation for these observations is lacking. Regarding the fact of a long co-evolution of microbial biofilms and protozoa or metazoa which use the biofilm biomass as food source ("grazing", cp. section 3.2.3), it is a small step to think that biofilm microbes might have developed mechanisms to protect against phagocytosis. Recent experimental findings are affirming this assumption and indicate, moreover, a quorum sensing regulation of these traits [147, 240, 185]. Here, a possible target for future drugs might be suspected [86]. That natural compounds being capable of inhibiting quorum sensing (so-called quorum quenchers) can be found is promising regarding the aspect that phototrophic organisms like e.g. algae or plants might protect themselves from being overgrown and thereby deteriorating light intensity. An auspicious substance is already found produced by the red alga *Delisea pulchra* [109, 142, 87] and also in polyphenols [103].

2.3 Historical Aspects

The sections before have shown the spectacular importance and ubiquity of biofilms. Nevertheless, biofilm research is a quite young discipline (around 30 years). Researchers recently working on it are coming from distinct fields of sciences like microbiology, microbial ecology, mechanical engineering, civil engineering, mathematics, etc. An explanation for this can be found in the history of biofilm research. The major cause why biofilms were widely neglected are the pioneer works of microbiology - mainly in the field of medical bacteriology [207], combined with the establishment of methods originating from Robert Koch and having the focus on planktonic cells in single-species cultures [201, 38]. An early work emphasizing sessile bacterial growth is found in Zobell [262] who analytically approached and described the attachment and growth of sessile bacteria in dilute nutrient solutions like sea water. In the 1970's the works of Marshall et al. [143, 144] focussed on sorption of bacteria on surfaces and in 1978 the Scientific American published an article about slime enclosed microbial communities [39] - later called "biofilms".
Early bacteriology in the late 19th century also revealed that pathogenic germs, like *Vibrio cholerae*, are distributed by contaminated water originating from human feces. A remedy is therefore found in a controlled draining of sewage and later on wastewater treatment (section 2.2.2). Transferring the known self-purification capabilities of soils into technical application yielded in early biofilm reactors: porous media, e.g. sand, overgrown by biofilms [113, 245]. This brought engineers to be interested in biofilms since they are relevant for engineering applications but also because biofouling causes severe damage in technical plants (section 2.2.2).
Concluding, different researchers have different aims and educational backgrounds which results in at least two challenges. At first a common language must be found. Moreover, biofilm systems are determined by processes originally assigned to physics, chemistry, biology, etc. Only their interaction results in the emergent properties we can observe (section 3.1.1). Thus, a generalistic knowledge is needed for their understanding.

2.4 Perceptions of biofilm systems

The methods applied to investigate natural systems determine their perception. Costerton et al. [40], for example, have coined the term "mushroom" structure of biofilms. This special kind of finger-like biofilm structure with open channels for water flow is usually found for *Pseudomonas aeruginosa PAO1*-biofilms in flow-cell reactors under certain environmental conditions . In mixed culture biofilms developed from sewage sludge or river/benthic biofilms "mushrooms" are, however, found seldomly (Harald Horn, personal communication).
Different authors try to compare biofilms with other real entities like mushrooms (see above), houses [67] and cities [238]. Besides these metaphoric views, it is known that biofilms already existed billions of years before the appearance of multicellular organisms.

An alternative to multicellularity?

Several evolutionary concepts have proved to be very successful in nature. One of them is multicellularity which also led to the Cambrian Explosion - a rapid rise of biological diversity around 545 million years ago [187]. The example of the eye which approximately has evolved 20 times during evolution up to now indicates that successful concepts are repeated in nature when they favor colonizing ecological niches ("convergent evolution", see [187]). So, can we directly compare the biofilm lifestyle and multicellular organisms? Might there be a higher level of complexity or organization, respectively, which we have overlooked [38]? Historically, microorganisms like bacteria are regarded as autarkic units. In natural systems, however, bacteria usually exist in communities. Already numerous examples for complex multicellular behavior are found in the world of microbes [207] - not only for the model organism *Dictyostelium spec.* showing both mono- and multicellular behavior [107]. Shapiro [207] gives examples for different species like *Rhizobium spec.*, *Anabaena spec.* or *Myxococcus xanthus* and states that most, perhaps virtually all, bacteria lead multicellular lives. Even a common evolution of distinct species is possible [80]. Particularly, the recently emerging evidence of intercellular

communication in biofilms, let it be by quorum sensing [46, 168] or horizontal gene transfer [70] suggests a coordinated behavior of cells in biofilms.
As a working hypothesis biofilms are regarded in the same way as multicellular organisms [115] so that checking the different criteria attributed to multicellular organisms [49] lets us test this hypothesis. *Aggregation* of cells is elementary for biofilm formation. Generally, aggregation provides evolutionary advantages, e.g. protection or centralized information, which might let accept limited resources. In multicellular organisms *differentiation* of cells leads to metabolic specialization and thereby a "division of work". This phenomenon is also typical for microbial communities - with the difference that the cells do not necessarily derive from a unique cell but can belong to different species. *Pattern formation* can be regarded as e.g. stratification and is also found in nitrifying biofilms [146]. *Reproduction* with the aim of spreading can be found in the form of biofilm detachment (cp. section 3.2.3) [131].

3 Methodology and modeling

3.1 Methodology

3.1.1 Systems, Emergence and Complexity

Systems consist of objects which are connected by specific interactions. Thus, properties are exhibited which cannot be attributed to the components of the system. In that way, new, so-called emergent properties arise on a higher spatial scale [50, 37]. An example can be carbon whose macro-scale (emergent) properties like density, color and hardness derive from the interactions of its atoms: the manner how carbon atoms are connected in the crystal lattice determines whether it will be diamond or graphite.

In addition, complex systems are constituted by a high number of objects and numerous interactions. So, it is hard to ascribe their emergent properties to specific components or interactions [205]. Every biological system is complex and in billions of years of evolution life has developed an enormous degree of complexity [183]. In order to substantiate this aspect and its implication in biofilm research, a concrete example is presented. In **figure 3.1** a graphic biofilm model is outlined which relates components of a biofilm system (relevant parameters) by interactions (processes). A hemispherical biofilm microcolony is growing on a substratum surrounded by a flowing liquid bulk phase. In a thought experiment, the flow field in the bulk phase $\vec{w}$ is perturbed by changing flow rate through the system (e.g. a biofilm reactor). As can be stated a priori, at least two central mechanisms will be directly influenced: mass transfer at the bulk/biofilm interfaces and partly within the biofilm (parameter k_L) as well as mechanical stresses (in normal direction σ and shear τ) on the biofilm (cp. section 3.2.2). Thus, several different process chains are affected: mass transfer determines distribution of substrates $c_{S,i}$ which influences growth rate μ of biomass X but can also act as selective pressure favoring micoorganisms with different (more or less) stable EPS. EPS stability, however, is a major determinant of the resistivity against mechanical stresses σ, and so forth. Concluding, a perturba-

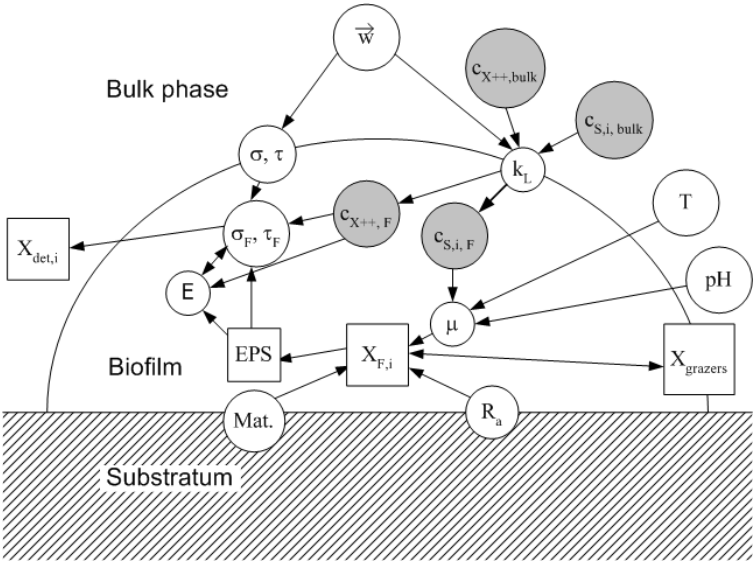

Figure 3.1: A graphic biofilm model (constituents in rectangles and parameters in circles - concentrations highlighted in gray)

tion of a single parameter like flow rate influences numerous processes. Emergent traits, i.e experimental results, can hardly be interpreted nor attributed to changes in one of these processes. Hence, it becomes evident that profound and useful explanations cannot be derived from a pure descriptive experimental approach. So, a method is developed accepting the high degree of complexity and using computational methods as a tool for its understanding.

3.1.2 Iterative Method

The method proposed and applied in this study is straightforward basing on the considerations made in the last section. It does not fundamentally differ from the conventional scientific methodology [232]. There, hypotheses are used to generate prognoses which are tested by comparison with experimental results. If the comparison is not successful the hypotheses can be falsified. However, the match of

prognosis and experimental result can be interpreted as evidence or coincidence but never as a proof. This is due to reasons of logic: truth can be transferred from premisses (hypotheses) to conclusion (prognosis) (*modus ponens*) but not vice versa. Falsity, however can be transferred from conclusion to premisses (*modus tollens*) [181]. Thus, the term "verification" which is usually used for the search after proofs in science will not be used in this work. It is substituted by "validation" which is explained later on.
For complex systems a methodological variation is needed because the observable phenomena emerge from many interactions of a plethora of components. So, it is not easily possible to test a single hypothesis at the outcome of an experiment. Experimental results are hard to interpret and the gain in knowledge when solely using experimental methods might be poor as discussed in section 3.1.1.
Hence, a method is developed which takes into account the challenges provided by biological systems with high complexity. It is comparable with the approach of systems biology [20]. Its basic idea is that from the virtual representation of relevant system components and interactions *in silico* the same phenomena are emerging which can also be observed in reality. A scheme with the chronological proceeding of this iterative method is presented in **figure 3.2**. The procedure is started with the collection of assumptions, processes and hypotheses considered as important in terms of determining the behavior of the system (I). These assumptions are then translated into mathematical equations (II) yielding a system of differential and algebraic equations. To be precise, in individual based models some of the processes cannot be written as equations but are realized in the form of computer algorithms - e.g the spreading algorithm (see section 3.3.2). This system of equations is solved by computers using numerical approximation procedures (III) and delivers simulation results. They are used to specifically design the experimental setup (IV) and moreover chose the range of all adjustable parameters which must mimic the conditions of the *in silico* experiment. After conducting the experiment raw data are transferred into comparable values (see section 3.4.2). Now, experimental and simulation results are compared quantitatively (V). This process of model testing is termed as model validation. The same logical aspects as already explained above are responsible for the fact that a match in this step is not a proof for the correctness

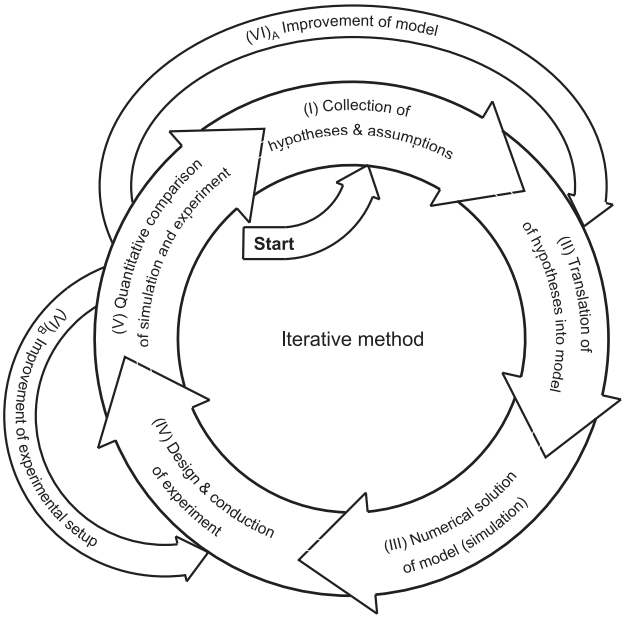

Figure 3.2: Iterative Method

of the model. A mismatch, however, reveals the need for a change of the model $(VI)_A$ or the experimental setup, respectively $(VI)_B$. The application of this method and the results thereby acquired are presented in chapter 5.

In literature some studies can be found where experimental and simulation results from one-dimensional biofilm models are directly compared [96, 97, 99, 101], only few however are known with the aim of validating multidimensional biofilm models [253, 4, 146] as also performed in this study (chapter 5).

3.2 Biofilm processes

The purpose of this section is to sum up and discuss all the processes that are assumed to be relevant in order to develop a suitable biofilm model. One of the central questions in biofilm research surrounds the old discourse of "nature vs. nurture" on a microscale [115]. In the following explanation, processes are therefore distinguished between intrinsic and environmental. A recommended compilation of microbial processes is found in Pirt [179] where diverse aspects in this section are taken from.

3.2.1 Intrinsic processes

Microbial growth

The predominant reproduction mechanism of microorganisms is cell division. Under ideal conditions biomass X can grow with a specific growth rate μ.

$$\frac{dX}{dt} = \mu X \tag{3.1}$$

This equation has the form of an autocatalytic reaction and its analytical integration gives an exponential function rising in infinity. In real systems, however, nutrients like carbon or energy sources are usually depleted or limited which retards growth rate. A well established approach describing the substrate dependency of growth rate is proposed by Monod [156] (equation (3.2) for growth on n substrates) with a maximum growth rate μ_{max}, the concentration of the limiting substrate c_S, the half-saturation constant K_S and compound i.

$$\mu = \mu_{max} \prod_{i=1}^{n} \frac{c_{S,i}}{K_{S,i} + c_{S,i}} \tag{3.2}$$

The values for growth determining parameters μ_{max} and K_S are species-specific and should be known for modeling purposes as they strongly influence the simulation results. For low concentrations of different substrates μ might be due to mathematical reasons stronger reduced than for only one limiting substrate. For biological reasons cells will be limited by only one of several low concentrated substrates. This

effect can be compensated by applying MIN-functions for the distinct Monod terms (C. Picioreanu, personal communication). Nevertheless, the limiting substrates in microbe cultivations must be known for modeling.

Due to a lack of adequate experimental methods the real values for microorganisms in biofilms are not measured but assumed to be the same as in planktonic culture. The latter can easily be determined in continuous culture (CSTR) [179]. The validity of this assumption is, however, uncertain. Computations performed by Wagner and Hempel [233] indicate that the diminution of overall growth rates in biofilms can directly be explained by mass transfer processes . More recent studies, however, show differences in genetic regulations between planktonic and sessile life forms of the same species [182]. A difference in metabolism and thereby growth rate can thus be concluded.

Moreover, realistic mixed-culture systems as they are the subject of this work can reveal a huge number of different species present in the biofilm [1, 108, 76]. To be exact, all these species should be identified and characterized in terms of their kinetic parameters. The complexity of this undertaking is easy to imagine. So, all species or groups of metabolic similar species are merged by one or several growth determining values which generally are fitted to measured data [96]. A biological argument for this simplification is additionally the high rate of horizontal gene transfer observed in biofilms [70]. Thus, different species obtain comparable metabolic capabilities for specific environments and can therefore be described by similar kinetic parameters.

In order to maintain conservation of mass, growth of biomass must be related to consumption of organic substrates. The coupling parameter is the substrate yield coefficient $Y_{\frac{X}{S}}$.

$$Y_{\frac{X}{S}} = -\frac{\frac{dX}{dt}}{\frac{dc_S}{dt}} = -\frac{r_X}{r_{c_S}} \tag{3.3}$$

$Y_{\frac{X}{S}}$ is also species-specific and a measure for the efficiency with which cells are using substrates for the production of new biomass. Especially under limited conditions as they often occur in biofilms due to mass transfer processes growth rate of cells decreases and comparatively more substrate is needed as energy source for the maintenance of cell structure and function (e.g. for active transport mecha-

nisms). Substrate consumption can then be extended with a maintenance coefficient k_m [95, 179].

$$\frac{dc_S}{dt} = -\left(\frac{\mu}{Y_{\frac{X}{S}}} + k_m\right) X \tag{3.4}$$

In biofilm cultivations this effect can be observed as a decrease of apparent yield coefficient at increasing biofilm thickness (meaning an increase of limited regions in the deeper layers of the biofilm).

Internal mass transfer

In the gel-like biofilm matrix all solutes, as for example nutrients or oxygen, are transported by diffusive mass transfer processes. Interstitial voids in heterogeneous biofilms may serve as channels or pores promoting convective mass transfer which yields in a better penetration of the biofilm under fast flow conditions [48, 47]. The importance of convective mass transfer in biofilm voids, however, is unclear. A good argument favoring its negligibility is expressed by Picioreanu and van Loosdrecht [175]. Convection in biofilm voids only occurs at very high flow rates. In that case, fluid-induced mechanical stresses (cp. chapter 6) result in dense and compact biofilm structures with only few pores. For this study only laminar flow conditions are considered during biofilm development. So, convective mass transfer in biofilms will be disregarded.
Diffusive mass transfer perpendicular to the substratum, i.e. in z-direction, can be described by Fick's 1st law.

$$j = -D_F \frac{dc}{dz} \tag{3.5}$$

It is generally assumed that the presence of extracellular polymers and cells does retard the diffusion process in biofilms [209]. A measure for this effect is found in the ratio $f_D = \frac{D_F}{D_W}$ which relates diffusion coefficient in the biofilm D_F to the one in water D_W. Values for f_D are found in wide ranges, e.g. for oxygen from 0.08 to 0.95 [33]. It is shown in modeling studies that internal mass transfer is influenced by biofilm structure [148]. This might explain the strong deviation of measured values for f_D in Horn and Morgenroth [98] who try to validate empirical approaches [63, 259] experimentally.

For the non-stationary case which is needed for modeling dynamic behavior of substrate distributions in biofilms Fick's 2nd law is used [33].

$$\frac{\partial c}{\partial t} = D_F \frac{\partial^2 c}{\partial z^2} \tag{3.6}$$

Diffusion is a comparably slow process. So, it often occurs that concentrations of nutrients are depleted in biofilms albeit remarkable concentrations are present in the bulk phase. This effect is summed under the term diffusion limitation and is responsible for a number of phenomena in biofilm systems. Because of its low solubility in water, this is often the case for oxygen. Thus, oxygen concentration in biofilms can decrease or reach values of zero which might lead to stratified microniches of aerobic, anoxic or anaerobic conditions in biofilms. Assuming a zero-order kinetic for consumption of substrate i, equation (3.7) can be derived giving penetration depth δ - the depth as far as concentration c_i is higher than zero [254, 169].

$$\delta = \sqrt{\frac{2 D_F c_{i,surf} Y_{\frac{X}{S_i}}}{\mu X}} \tag{3.7}$$

Inserting typical values for oxygen ($D_{O2} = 2.1 \cdot 10^{-4} m^2/d$; $c_{O_2,surf} = 8 g/m^3$; $Y_{X/O_2} = 0.5 gX/gO_2$; $\mu = 5 d^{-1}$; $X = 30 kg/m^3$) results in a penetration depth of $\delta = 106 \mu m$ meaning that deeper than around $100 \mu m$ anoxic or - under absence of other electron acceptors like NO_3^-, PO_4^{3-}, etc. - also anaerobic conditions prevail. The concentration $c_{i,surf}$ of substance i at the biofilm surface, furthermore, is strongly dependent on flow conditions (see section 3.2.2, s.v. external mass transfer).

Decay of Microorganisms

As just discussed mass transfer phenomena can cause depletion of substrates in the biofilm. Under these conditions, several processes like decay, lysis, maintenance or endogenous respiration, may gain importance. In van Loosdrecht and Henze [226] a detailed discussion about the microbial causes of these processes is found for activated sludge modeling. In biofilm modeling, processes in which active biomass is converted either to soluble substrates (lysis) or to inert biomass (death, inactivation

or inertization [56]) are frequently used. Generally, these processes are described by an inhibition kinetic as shown by Horn and Hempel [95].

$$r_{X,decay} = -k_{decay} \cdot X \prod_{i=1}^{n} \frac{K_{S,i}}{K_{S,i} + c_{S,i}} \tag{3.8}$$

The lower substrate concentration $c_{S,i}$ the higher decay rate gets whereas the maximum of $r_{X,decay} = -k_{decay} \cdot X$ is reached at $c_{S,i} = 0$. Here, two parameters (k_{decay} and $K_{S,i}$) are needed which should be directly measured [200] but usually are fitted with experimental data.

However, a possible option is to simplify this process by a first order decay rate which only needs one parameter (for arguments on model simplification see section 3.4). Cells in the active layer of the biofilm only have a short solid retention time [224] - especially under high detachment regimes. Hence, time-dependent decay will not have a high influence. In the deeper layers of the biofilm where substrate is depleted, the inhibition term in (3.8) will become one and the maximum rate of decay is reached [95].

$$r_{X,decay} = -k_{decay} \cdot X \tag{3.9}$$

The decay coefficient k_{decay} is taken from literature [200] or fitted to experimental data.

Production of extracellular polymeric substances EPS

The term EPS comprises numerous different types of polymers which mainly are synthesized and excreted by living cells. Hence, EPS formation kinetics must be dependent on biomass X. Generally, a product formation kinetic according to Luedeking-Piret can be applied [239, 93].

$$\frac{dc_{EPS}}{dt} = \alpha \frac{dX}{dt} + \beta X \tag{3.10}$$

The coefficients α of the growth-dependent part and β of the biomass-dependent part, respectively, are empirical parameters and must be determined experimentally. As comparable to growth kinetic parameters (see above), they are supposed to be measured in chemostat culture as presented in comparison with simulations by Kommedal et al. [116]. Experimental studies reveal, however, that EPS-synthesis

can be regulated in dependence on environmental conditions [244]. Studies performed by Davies et al. [44, 45] demonstrate an up-regulation of alginate synthesis by adhered *P. aeruginosa* cells. Moreover, the level of productivity seems to be determined by surface properties of the substratum [28]. Thus, the approach chosen in this study is to directly use data about EPS-distributions in biofilms for the validation of a structural biofilm model (see section 5.5).
Kommedal et al. [116] propose and successfully test an EPS production kinetic with an inhibition term for substrate (equation (3.11)). In that case EPS will particularly be produced under substrate depletion [116, 99].

$$\frac{dc_{EPS}}{dt} = k_{EPS} \cdot Y_{EPS/X} \cdot \frac{K_S}{K_S + c_S} \cdot X \tag{3.11}$$

The yield coefficient $Y_{\frac{EPS}{X}}$ is directly comparable to α in equation (3.10).
Substrate depletion often occurs in deeper layers of biofilms due to diffusion limitation. With such an EPS formation kinetic, the higher amount of EPS in these regions as found by Staudt et al. [211] could be explained. But why should microbes follow such a metabolically demanding task when nutrients are lacking? Here, several explanations are possible. (1) The EPS-matrix can provide sorption sites for organic compounds in aqueous solutions which can be used as substrates. More EPS- especially when leading to roughly structured surfaces - could in this case increase the sorptive capacity of the biofilm matrix [65]. (2) It is known that production of EPS can yield evolutionary advantages in biofilms [251]. Here, microbes could especially be adapted to survive in microniches with low substrate conditions (k-strategists) as they are present in deeper regions of biofilms. (3) Very interesting is an approach which brings to the fore inter-species competition. The synthesis of whatever kind of EPS needs a carbon source for which microbes are competing. Especially when other nutrients (e.g. nitrogen, phosphorus) are not sufficiently available the soluble carbon source could be transformed into insoluble polymers and thereby removed from bulk phase [228].

3.2.2 Exchange with the environment

The substratum - adhesion

Primarily, two important aspects about the substratum as a surface which is colonized by biofilms can be itemized. One of the first steps in biofilm development (see section 2.1.3) is the interaction of suspended bacteria or aggregates (flocs), respectively, with the substratum or - in natural aquatic environments - with a layer of adsorbed macromolecules (conditioning film) [262, 160, 208]. Numerous studies can be found about phenomena of initial adhesion [27] because technologies are promising to hinder or to even avoid biofouling. Also in terms of further biofilm development initial adhesion processes might be relevant. Differences in substratum material may trigger variations in composition of initially adhering species. The surface topography can play a role for adhesion of microbes [229, 149]. Also (twitching) motility of biofilm forming organisms at this state in biofilm development might determine later biofilm structure and propagation [85, 172].
Surely, all experiments - let them be real or virtual - start with an inoculation of the system with suspended biomass. It is however assumed that in established mature biofilms (ages from months to years) these processes do not play any more an important role.
The second aspect which may be relevant in longterm biofilm cultivations lies in the mechanical connection between substratum and biofilm - the adhesion strength. Experimental evidence for the systems investigated in this study, however, demonstrate that cohesion is smaller than adhesion strength [151]. So, influences of adhesion phenomena on biofilm detachment are neglected in the following analysis.

Solutes in bulk phase

The available solutes in the bulk are one of the important environmental factors determining biofilm development. Experimental [97] as well as theoretical studies [176] demonstrate that substrate conditions strongly influence biofilm structural development. Oxygen concentration can influence structure development as demonstrated with *P. aeruginosa* biofilms [248]. The spatial distribution of nutrients in the biofilm, in turn, is strongly dependent on internal and external mass transfer pro-

cesses and thereby also on biofilm structure, hydrodynamics, etc. Regarding the complexity of these mutual interactions it is obvious that no simple relation can be announced and experimental data are hard to be interpreted [77]. Qualitatively, a higher substrate supply leads to lower biofilm densities and conversion rates [97]. The availability of multivalent ions (Mg^{2+}, Ca^{2+}, Fe^{2+}/Fe^{3+}, etc.), furthermore, affects mechanical properties of the biofilm by cross-linking of polysaccharides in the EPS-matrix [120, 151].

Effects of Hydrodynamics

Hydrodynamic conditions strongly influence biofilm development [97, 138]. Several parameters depend on hydrodynamics whereas usually no clear dependencies can be formulated [93]. This can also be explained by the high complexity of biofilm systems. Qualitatively, biofilm density - a parameter which is often announced as a measure for biofilm compactness and activity - obviously is dependent on hydrodynamic conditions. This statement is affirmed by **figure 3.3** using literature data from different studies [150] and showing an increase of biofilm density when hydrodynamic stresses increase. Here, two central impacts of varying hydrodynamics can be directly named: external mass transfer and mechanical stresses. Both will affect further processes (cp. section 3.1.1).

External mass transfer

In contrast to internal mass transfer (see above), external mass transfer refers to transport processes through the concentration boundary layer outside the biofilm. The thickness of this layer is dependent on flow conditions in a way that faster flow decreases boundary layer thickness and thereby increases mass transfer [124]. The dependence of external mass transfer on flow conditions is experimentally studied in extense by Wäsche et al. [250] . This study is conformed by modeling studies which also show a dependency of external mass transfer on biofilm structure, especially surface roughness [59, 177]. Mathematically, external mass transfer can be formulated in empirical relationships for the Sherwood number that is dependent on the Reynolds and Schmidt number $Sh = f(Re, Sc)$ [202]. Wäsche et al. [249, 250] introduced a factor Ω to consider structural properties of the biofilm.

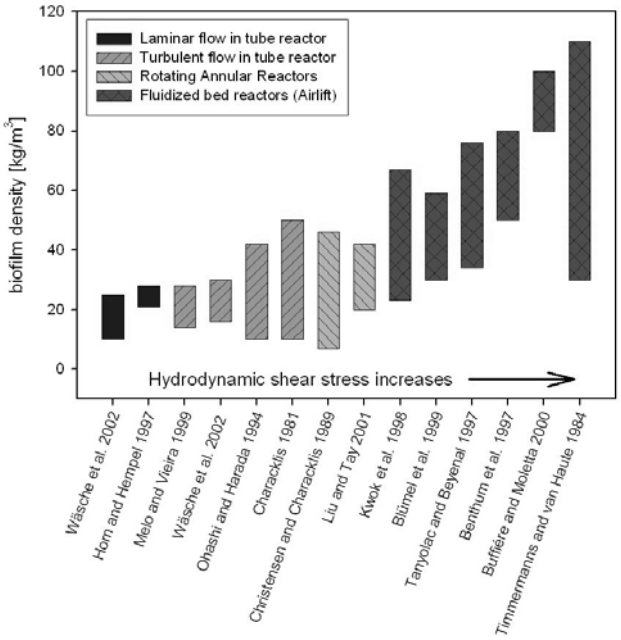

Figure 3.3: Biofilm density depends on hydrodynamic stresses in the system; adapted from Horn [93], references can be found there

Fluid induced mechanical stresses

Fluids (usually liquids) flowing past biofilm structures are imposing mechanical stresses on them as investigated in chapter 6. There, fluid-structure interactions and mechanical stresses in biofilms are regarded. At this point, however, the impact of forces and stresses on biofilms and specially on therein embedded microbes is in the focus.

At first, an evolutionary approach is proposed for multispecies biofilms. For high flow velocities species are favored which are embedded in a stable and thereby resistant EPS-matrix. So, species that can excrete such polymers possess an evolutionary advantage (see also section 3.2.3). Secondly, another impact is connected with the recent research field of cellular stress response. For numerous different cell types, e.g. human [163], mammalian [157], plant [34] and also microbial cells like fungi

[43] or bacteria [199, 155] the ability to respond to mechanical stresses are identified. Hence, it suggests itself to suspect these abilities also for biofilm forming microorganisms. So, Liu and Tay [137] postulate metabolic responses of biofilms to a variation in shear stress. The mechanism underlying their experimental observations, however, cannot clearly be identified and might also be referred to other phenomena like external mass transfer. Moreover, stresses must propagate into the biofilm structure in a way that cells can sense it. An experimental investigation of these phenomena in biofilms seems challenging and demands the application of biomolecular methods.

3.2.3 Biofilm detachment

Biofilm detachment - the disruption and discharge of biomass originating from the biofilm - is accepted to be one of the major determinants in biofilm development but also one of the least understood processes [8, 170, 93]. Detachment is of special importance in terms of reactor performance and stability [254], dispersal of pathogens in aquatic environments [131, 79] and also for the removal of unwanted biofilms. Furthermore, it may determine species composition of biofilms [159].

Detachment processes

The distinction of detachment into four different processes according to Bryers [26] is well established: (1) erosion, (2) sloughing, (3) abrasion and (4) grazing. Erosion (1) is the continuous removal of small particles (cells or small cell aggregates) from the biofilm surface whereas sloughing (2) is understood as periodic loss of large biofilm patches [192]. To be precise, erosion and sloughing both are of discrete nature. Biomass particles (possibly cells as smallest entities) are detaching from the biofilm. Both processes are assumed to be a result of the mechanical interaction of external forces and internal strength of the biofilm (cp. chapter 6). Thereby, the distinction may be arbitrary [212]. This can explain different distinction sizes found in literature between erosion and sloughing reaching from around $10\mu m$ (small cell aggregates) over $0.25mm$ (exclusion size of sieve analysis [164]) up to the dimension of biofilm thickness [159]. Abrasion (3) is caused by particle collisions and not

by fluid induced stresses. It is especially important for fluidized bed reactors [21] but may also occur in reactors with recirculation, e.g. Rotating Annular Reactors (RARs) or Biofilm Tube Reactors (BTRs) (see chapter 4), [153] but will not be considered in this work. Biofilms themselves can serve as a food source for predators like protozoa (amoebae, ciliates) but also metazoa (rotifers) which is summarized under the term grazing (4) [217, 105].

Biological aspects

Regarding detachment from a biological point of view it turns out that detachment can provide several evolutionary advantages. Xavier et al. [256] show in a modeling study that at higher detachment rates net biomass production is higher. Biofilm detachment leads furthermore to a spreading of species - especially in flow dominated aquatic systems [131]. Detached biofilm particles can serve as birthplace for a new biofilm which can be interpreted as a reproductive mechanism. Hunt et al. [104] show that detachment can also be triggered under nutrient starvation which can be interpreted as an adaptive behavior . This leads to the interesting question whether microorganisms in biofilms are generally capable of actively adapting to environmental conditions, especially to variations in flow (cp. section 3.2.2).

Mechanical aspects

A priori, biofilm detachment can always be regarded as a mechanical process. That means that the cause of detachment is a matter of force balance: (1) external forces are acting on biofilm structures; (2) thereby internal stresses in the structure are effected what in turn will result in strains; (3) if the internal strength of the biofilm matrix is not large enough to resist these stresses the structure will disrupt and parts of the biofilm will detach. This means that detachment can be induced by variations on both sides - a change in external forces or changes in biofilm material properties. Mechanical stresses can vary due to changes of flow rate in fixed bed reactors, particle number or aeration rate in airlift reactors [225, 83]. The weakening of matrix strength can happen internally, e.g. due to induced detachment [184], gas vacuoles [164] or also lysis products. Externally, the matrix can be weakened by different agents such as enzymes [252] or detergents [125]. Multivalent ions also influence

matrix strength [151]. A profound investigation of these aspects is presented in chapter 6.

Mathematical description

In order to capture the interaction of mechanical stresses and biofilm strength, plenty of data as well as computational power are needed [57]. For the description of biofilm cultivations and reactors, thus, empirical approaches to describe biofilm detachment are used of the following type.

$$r_{X,det} = f(\rho_F, L_F, \tau_W, \mu, u_F, ...) \tag{3.12}$$

Tabular listings of different detachment models are found in literature [212, 170, 159, 93]. The existence of diverse approaches regarding different parameters like biofilm density ρ_F, thickness L_F, theoretical wall shear stress τ_W, growth rate of microorganisms in biofilm μ, biofilm growth speed u_F, etc. already indicates that the mathematical description of biofilm detachment has not yet succeeded. Furthermore, it can be hypothesized that an empirical description of biofilm detachment is not sufficient to describe the complex mechanical interaction. In order to understand detachment, a more detailed investigation is needed as presented in chapter 6.
For the representation of detachment rates and thickness development in 1D-models, however, an approach regarding biofilm growth velocity u_F has proved to be the best choice [237, 95, 93].

$$\left(\frac{dL_F}{dt}\right)_{det} = k_{det} \cdot u_F \tag{3.13}$$

Detachment velocity $\left(\frac{dL_F}{dt}\right)_{det}$ as applied in the AQUASIM model [237] can be transformed to detachment rate via biomass concentration in the biofilm (biofilm density).

$$r_{X,det} = \left(\frac{dL_F}{dt}\right)_{det} \cdot X_F \tag{3.14}$$

The detachment coefficient k_{det} can obtain values between 0 and 1 which corresponds to the ratio between grown and detached biomass (cp. section 5.4). So, k_{det} is a measurable parameter.

3.3 Biofilm models

Here, different frameworks are introduced in which the processes as explained before can be implemented. In their basic structure, biofilm models are quite similar: Solids (e.g. biomass, inerts, EPS, etc.) and solutes (e.g. nutrients, oxygen, signaling compounds, etc.) are treated separately. The solutes are subjected to mass transfer processes (convection in bulk phase, diffusion in biofilm). The central topic of biofilm model development, however, is how to represent the solid fraction of the biofilm and how to describe its change in volume due to growth, decay or other processes. Together with the number of dimensions considered in the model this is the major criterion of distinction for biofilm models.
This section shall serve as a short introduction to biofilm modeling, focusing on the two models applied in this study: (1) the continuum 1D-model of Wanner and Gujer [235] and (2) the multidimensional particle-based biofilm model as developed by Picioreanu et al. [173]. A detailed treatise on biofilm modeling is the book of Eberl et al. [57], a short survey is also found in Horn [93].

3.3.1 Microscopic mass balance for solute compounds

The microscopic (differential) mass balances of dissolved compounds - i.e. the mass balance with the biofilm or biofilm elements, respectively, as control volume - are equal for all biofilm models [57]. Assuming diffusion as a single mass transfer process the mass balance for dissolved compound i can be written as in equation (3.15) for 3D and 1D case in equation (3.16), respectively, in Cartesian coordinates.

$$\frac{\partial c_i}{\partial t} = D\left(\frac{\partial^2 c_i}{\partial x^2} + \frac{\partial^2 c_i}{\partial y^2} + \frac{\partial^2 c_i}{\partial z^2}\right) + r_i \tag{3.15}$$

$$\frac{\partial c_i}{\partial t} = D\frac{\partial^2 c_i}{\partial z^2} + r_i \tag{3.16}$$

Rate r_i can be substituted by any process, as for example microbial consumption of nutrients, which can be derived from equation (3.3).
Macroscopic (integral) mass balances describing mass fluxes through the reactor

are presented in section 3.4.2. Generally, the reactor bulk phase is regarded as completely mixed.

3.3.2 Representation of particulate components

Continuum approaches

The most common used software for biofilm modeling is AQUASIM [235, 237, 236]. Therein the model of Wanner and Reichert [237] comes to application which applies a continuum representation for particulate components of the biofilm matrix. The microscopic mass balance for particulate compounds is formed in straight analogy to the one for dissolved compounds.

$$\frac{\partial X_i}{\partial t} = -\frac{\partial j_{X_i}}{\partial z} + r_{X_i} \tag{3.17}$$

The mass flux j_{X_i} is determined by an advective velocity u_F which describes the expansion or shrinking velocity, respectively, along the z-axis perpendicular to the substratum.

$$j_{X_i} = u_F \cdot X_i \tag{3.18}$$

This velocity u_F is in turn determined by all processes r_{X_i} of growth, decay, etc. that are defined for all particulate components X_i with density ρ_{X_i}.

$$u_F = \frac{1}{1-\phi_l} \cdot \int_0^{L_F} \left(\sum_{i=1}^{n} \frac{r_{X_i}}{\rho_{X_i}} \right) dz \tag{3.19}$$

Continuum models are also extended to multidimensionality [53, 58, 5]. As "real" mathematical models they provide several advantages: their stability can be mathematically analyzed and, particularly, dependencies of parameters can be investigated [3].

Discrete approaches

Individual based biofilm models are developed as multidimensional models to describe structural biofilm development. Early Multi-D (2D or 3D) models are using

the Cellular Automaton (CA) approach to represent particulate biomass [176, 89]. Although they reveal severe drawbacks, especially in biomass spreading, they are still in use nowadays [31]. This is predominantly because they are simple and easy to program. Kreft et al. [118] developed an individual based model which regarded single cells as the smallest particulate units with the aim that biofilm properties should emerge from the behavior of single cells in the biofilm. An extension of this approach which is less computationally demanding is found in the particle-based biofilm model by Picioreanu et al. [173] that also comes to use in this study. There, biomass is discretized as spherical biomass particles for which biofilm growth is realized by their expansion. Thereby two or more particles can overlap which in turn is released by the so-called shoving mechanism. To be exact, this model is not a mathematical model but a computer model. So, no mathematical expression for biofilm growth can be written. Xavier et al. [255, 256] have extended this model by implementing detachment and production of capsular EPS.

3.3.3 Finite Element Modeling

The Finite Element Method (FEM) provides frameworks for the integration of any kind of process into multidimensional models [260]. Here, a FE model for the fluid-structure interaction of biofilms in a tube reactor is developed using a commercial FEM kit (ANSYS). FEM simulations are performed by Markus Böl, Institute of Solid Mechanics, TU Braunschweig. Only mechanical interactions of the tubular flow field and biofilm structure are considered. Linear elastic behavior of the biofilm matrix is assumed. For more detailed information see Böl et al. [17]

3.4 Model development and simulation

3.4.1 Aspects of model development

Simplicity is a desirable criterion of scientific theories and "Occam's razor" has become a terminus technicus as an economizing tool of theory development (see also chapter 7 "Simplicity" in [181]). In mathematical modeling, moreover, further aspects of model's simplicity ought to be considered. Additionally to the choice of processes, the number and quality of parameters is of central importance. This becomes evident when regarding the uncertainty and specificity of parameters from literature and also the method of fitting simulation results to experimental data. Following parameters' citations backwards from one article to another it occurs often that they might just be estimated. Fitting of parameters to data is a helpful method but might also be dangerous in terms of losing track of reality - especially for highly parametrized models [261]. Every additional parameter or process increases the degree of freedom of the model. Thus, a more complex model with more equations can better describe any set of experimental data. This effect can easily be imagined when trying to fit a set of experimental data (x/y-data pairs) with a power function of the type $y = f(x) = \sum_{i=0}^{n} x^i$. The higher the value of n the higher regression coefficient will get and the -putative- better the data will be described. Here, special care must be applied in order not to lose track of reality.
Not all processes and parameters might be important for the model outcome. Sensitivity analysis can help here in order to achieve an economic model reduction.

3.4.2 Data Analysis

Characteristic Parameters

As major characteristic parameters, biofilm thickness L_F and biofilm density ρ_F are established. They are derived from wet and dry biomass from reactor samples as

shown in equation (3.20) and (3.21), respectively.

$$L_F = \frac{m_{F,w}}{\rho_{F,w} A_F} \tag{3.20}$$

Due to the high water content of biofilms, wet density is assumed to be $\rho_{F,w} = 1050 \frac{kg}{m^3}$ It has to be taken into account that biofilm thickness L_F here is a mean thickness assuming a cuboid-like shape of the biofilm. Thickness as determined by CLSM is the height of CLSM stacks. Hence, L_F is a maximum thickness.

$$\rho_F = \frac{m_{F,d}}{V_{F,w}} = \frac{m_{F,d}}{\frac{m_{F,w}}{\rho_{F,w}}} \tag{3.21}$$

Biofilm density, relating dry biomass and wet volume, is a sum parameter regarding all solids in the biofilm (e.g. active biomass, EPS, etc.). Thus, it is often used as indicator for conversion capacity (active biomass) or stability (EPS content) of biofilms. Furthermore, ρ_F is a central parameter in biofilm modeling. For the model of Wanner and Reichert [237] it must be mentioned that ρ_F is comparable to the biomass concentration X in the biofilm. The biofilm density implemented in the model, however, is representative for a volume element completely filled with solid material (cells, etc.) - so, it represents a maximum biofilm density. Here, values around $300 \frac{kg}{m^3}$ are derived from measured cell densities [10] and are similar to densities derived from a method in which CLSM and gravimetry are combined [211].

Macroscopic mass balances

Overall mass balances of biofilm reactors are slightly different from CSTR systems with planktonic biomass [9]. From mass balances with the whole reactor as a control volume, global (overall) rates are computed. In biofilm reactor systems rates are generally related to the area of substratum surface A_F. Mass balances of biofilm reactors are based on the substrate yield coefficient $Y_{\frac{X}{S}}$ (equation (3.3)) which relates biomass production rate to substrate consumption rate. In this work glucose is always provided as sole carbon source (see also section 4.5) for growth of heterotrophic microorganisms. Therefore substrate yield coefficients are related to glucose consumption. So, for continuous biofilm reactors mass balances can be developed.

The uptake rate r_{c_i} of substrate i is resulting from the difference of inlet and outlet concentration c_i and the volumetric flow rate Q through the reactor with the volume V_R (equation (3.22)). It is assumed that all substrate is taken up to be consumed by microbial processes. Therefore this rate equals the consumption rate for solute compounds (mainly glucose and oxygen).

$$r_{c_i} = \frac{V_R}{A_F}\frac{dc_i}{dt} = \frac{Q}{A_F}(c_{i,in} - c_{i,out}) \tag{3.22}$$

In biofilm reactors the biomass produced remains either in the biofilm or gets detached. So, biomass production rate can be split in accumulation and detachment rate.

$$r_{X,prod} = r_{X,acc} + r_{X,det} \quad \text{with} \quad r_X = \frac{dX}{dt} \tag{3.23}$$

For the evaluation of experimental data mass balances are calculated using gravimetrically determined values of dry biomass. Rates are then computed from discrete measured values according to

$$\frac{dX}{dt} \approx \frac{\Delta X}{\Delta t} = \frac{X_2 - X_1}{t_2 - t_1} \tag{3.24}$$

Development of parameter sets

As in chapter 3.1.2 proposed modeling and simulation are the first steps of the iterative method proposed. In order to compare simulation and experimental results quantitatively specific values of high reliability are needed for the model parameters. They are either directly taken from the experimental setup (e.g. reactor volume, substratum area) or from literature (e.g. kinetic constants, yield coeffients). The latter are generally system- and often species-specific which is specially providing challenges in the work with mixed-culture biofilms in non-sterile systems. Furthermore, the values found in literature often deviate strongly (see [92]). Therefore, kinetic parameters in this work are determined by fitting to experimental data and regarding value ranges from literature.

4 Reactor development and operation

Against the background of the methodology proposed in the previous chapter, the need for an experimental system is obvious which can deliver data in the desired quality for the quantitative comparison of simulation and experiment. Due to several reasons a tube reactor system seems to be the best choice.

Requirements on biofilm reactors in research applications

For the cultivation of microbial biofilms in laboratory experiments different experimental setups have been established, i.e. flow cells [11], Rotating Annular Reactors (RARs) [130, 71], Airlift Reactors [221, 22] and Tube Reactors [91, 92, 94]. Regarding the considerations already made, it should have become obvious that environmental or cultivation conditions, respectively, are major determinants of biofilm development, structure and activity (section 3.2.2). Hence, in biofilm cultivations their specification and adjustability must be assured. That means that physicochemical parameters such as temperature, pH, flow and substrate conditions must be well adjustable with the chosen reactor system. For the aim pursued in this study - to quantitatively compare simulation results and experimental data - overall mass balances of the reactor must completely be closed. Thereby all rates and certain parameters, as for example detachment coefficient, mean growth rate, apparent yield coefficients, etc. can directly be computed and be compared with simulated values. Furthermore, the geometry of the carrier used as substratum might play a role. Microscopic or other methods might need planar substrata. A listing of these requirements and how they are satisfied by different reactor types is presented in section 4.4, table 4.1.

4.1 Flow in tube reactors

Tube reactors fulfill well the requirements of adjustability of physicochemical parameters - especially in terms of flow conditions. One of the major advantages of using inner walls of tubes as substratum surface is the rotational symmetry of the flow field as visualized in figure 6.3. Disregarding inlet and outlet zones of the tube any spot of the tube's inner wall experiences equal theoretical flow and shear conditions. Moreover, an analytic solution for Navier-Stokes equations is available which allows the computation of the tubular flow field as well as of the fluid forces acting on biofilm structures (detailed discussion and computations in chapter 6). In addition, the diffusion distance from the axis of the tube in any perpendicular direction is equal. So, depletion of substrate in edges of square-shaped geometries does not occur [60, 4].
Using an elaborate reactor design a well working reactor is developed in this study whose experimental results (chapter 5) confirm the correctness of the considerations above.
As a base for the upcoming considerations the macroscopic flow field of tubes which are flown through by aqueous solutions is examined. Certain aspects can usually be found in any textbook about engineering fluid mechanics (recommended can be White [243], chapter 6). In this work only laminar flow conditions are considered due to the existence of an analytical solution for the Navier-Stokes-equation and also because effects of wall roughness can be neglected. The latter is evidently affected by biofilm structure (section 2.1.2) which in turn is dependent on diverse parameters and can change wall roughness in time.

Flow patterns

From dimensional analysis the Reynolds number Re_T for flow in tubes can be defined.

$$Re_T \equiv \frac{\bar{u} \cdot d_T}{\nu} \tag{4.1}$$

Re_T is the primary parameter affecting the transition from laminar (parallel streamlines) to turbulent flow (unstructured patterns). The accepted Reynolds number for

transition to turbulence in tubes is $Re_T = 2300$. The transition can be imagined as a stability problem meaning that the flow patterns can oscillate between laminar and turbulent flow at Reynolds number of about $10^3 < Re_T < 10^4$ (a detailed discussion is found in [202]).
It is important to realize that a change of the tube diameter, which can result from biofilm growth, will change Re_T and potentially the flow conditions. This effect is regarded in the derivation of the following equations.

Inlet and outlet zone

Usually a volumetric flow is created by a pump and from there flowing into a tube. At the inlet of the tube the flow field is not yet showing the expected profile. Entrance length L_e where the flow profile develops can be estimated depending on tube's diameter and Re_T.

$$\text{laminar} \qquad \frac{L_e}{d_T} \approx 0.06 Re_T \tag{4.2}$$

$$\text{turbulent} \qquad \frac{L_e}{d_T} \approx 4.40 Re_T^{\frac{1}{6}} \tag{4.3}$$

At the outlet of the tube the diameter is reduced again to fit with the subsequent conducts. This can lead also to effects which perturb the flow field in the near of the outlet. Hence, it can be concluded that the sampling of the biofilm should not occur in these regions.

Flow field

As an analytical solution of the Navier-Stokes equation the law of Hagen-Poiseuille can be derived which is valid for laminar flow.

$$u(r) = \frac{1}{4\eta}\left(-\frac{dp}{dx}\right)(R^2 - r^2) \tag{4.4}$$

For a constant volume flux Q through the tube u_{max} remains constant according to equation (4.5). Biofilm growth on the inner surface of the tube, however, can yield a reduction of the tube diameter and thereby of the cross sectional area $A = \pi R^2$. This phenomenon has more effect when using tubes with smaller diameter.

$$\bar{u} = \frac{u_{max}}{2} = \frac{Q}{A} \quad \text{with} \quad u_{max} = -\left(\frac{R^2}{4\eta}\right) \cdot \frac{dp}{dx} \tag{4.5}$$

So, u is only dependent on radius r and the radial profile reveals a parabolic shape (see also figure 6.3). The propagation of biofilm surface due to growth decreases the tube radius. With the biofilm thickness L_F the hydraulic radius R is substituted by $R = R_T - L_F$.

Pressure difference along tube

In order to get a solution for the equations shown the pressure gradient $\frac{dp}{dx}$ along the axial direction of the pipe must be known. For a pipe with the length L the gradient from inlet $x = 0$ to outlet $x = L$ is determined by the pressure drop Δp.

$$\frac{dp}{dx} = -\left(\frac{\Delta p}{L}\right) \tag{4.6}$$

Combining equation (4.5) and equation (4.6) gives equation (4.7) which relates pressure drop and volume flux Q in a pipe with the length L.

$$\frac{\Delta p}{L} = \frac{8\eta Q}{\pi(R_T - L_F)^4} \tag{4.7}$$

The selection of gear pumps provides the advantage of widely maintaining constant volume fluxes when pressure drop of the tube increases due to biofilm growth which in turn causes a reduction of cross sectional area.

Fluid shear

For Newtonian fluids (such as water) wall shear stress τ is proportional to the flow velocity gradient $\frac{du}{dr}$ according to equation (4.8) with radial coordinate r and the dynamic viscosity η as a proportionality coefficient [243].

$$\tau = -\eta\frac{du}{dr} \tag{4.8}$$

Inserting equation (4.4) into equation (4.8) regarding equation (4.6) and (4.7) gives the wall shear stress at r in a pipe at laminar flow (equation (4.9)).

$$\tau = \frac{r}{2}\left(-\frac{dp}{dx}\right) = \frac{r}{2}\left(\frac{8\eta Q}{\pi(R_T - L_F)^4}\right) \tag{4.9}$$

4.2 The Biofilm Tube Reactor (BTR)

An established system using the advantages of tubular flow is the biofilm tube reactor (BTR) as it is developed by Horn [91]. It is easy to handle, well applicable for microelectrode measurements and has shown its flexibility in several studies [135, 94, 249, 250, 134]. **Figure 4.1 (A)** presents a flow chart of the systems as it is also used by Haesner [77, 76]. Flow rate through the tube is maintained by a gear pump. The tube itself is divided in segments for an easier disassembling according to different investigative purposes. It is mounted vertically in order to provide equal influences of gravity to each side of the tube. A mixing vessel allows to provide aeration and nutrient supply. An outlet is responsible for constant reactor volume. In that way continuous process control is realized.

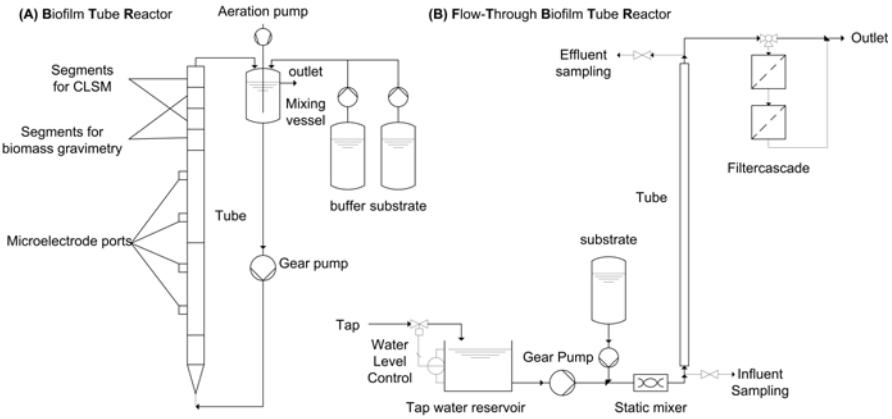

Figure 4.1: Sketch of Biofilm Tube Reactor (BTR) (A) and Flow-through Biofilm Tube Reactor (FTBTR) (B)

4.2.1 Development of CLSM-segments

In order to combine the advantages of tubular flow and the applicability of CLSM to tubular systems (which is not trivial), special tube segments (so-called "CLSM-

segments") are ad hoc designed for this work. Design and realization are displayed in **figure 4.2**. In order to apply the same substratum material as in former studies with the RAR [211] the half slides are made of Polycarbonate whereas the carrier is constructed from PE or PVC. The substratum surface is sandblasted to assure good adhesion of the biofilm to the substratum. For microscopic investigations the segments are dismounted from the reactor and subjected to the CLSM-method according to STAUDT ET AL. [211].

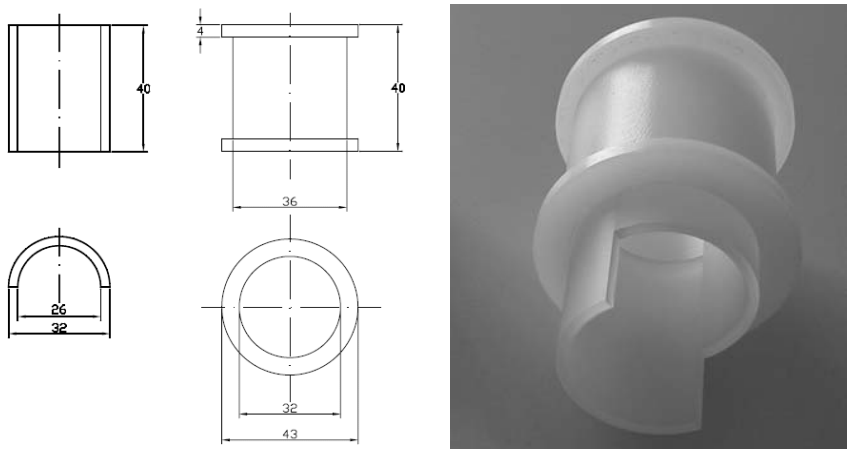

Figure 4.2: CLSM-segments in Biofilm Tube Reactor (BTR): drawing (left) and picture (right, taken by M.Haesner)

4.2.2 Operation of BTR in long-term biofilm cultivations

Here, an experiment is presented which is conducted in order to provide experimental data to directly compare simulation and experimental results as described in section 3.1.2. Therefore, a biofilm is cultivated under low substrate supply (starting at substrate loading $B_A = 1\frac{g}{m^2 d}$ and shifted to $B_A = 2\frac{g}{m^2 d}$ on day 27) and moderate flow conditions ($Re_T = 2000$). During the cultivation biofilm samples are taken and gravimetry (wet and dry weight) as well as CLSM (see Appendix B.1) is performed. Detached biomass is collected by a fluted filter which is changed daily. In filtered

samples concentrations of Chemical Oxygen Demand (COD) are measured. Furthermore, light microscopy is applied to samples from detached biomass in order to observe occurrence of protozoa [257]. From these data several parameters and rates are computed (cp. section 3.4). **Figure 4.3** presents the temporal development of biofilm thickness and density during the cultivation.

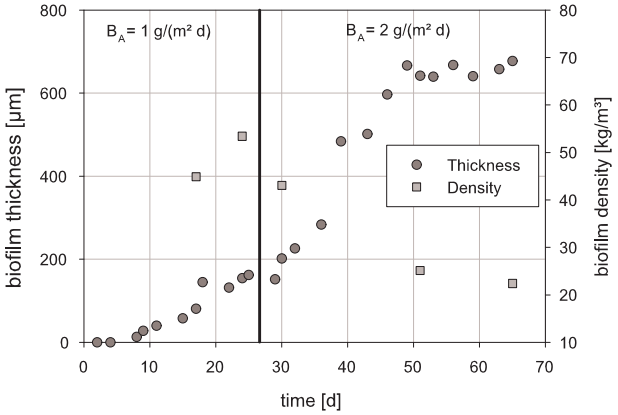

Figure 4.3: Development of biofilm thickness and density in BTR over cultivation time

The progress of biofilm thickness corresponds to a typical biofilm growth curve. It increases - faster when substrate supply is raised - and reaches steady state around day 50. It is generally observed that low substrate supply leads to dense biofilms (section 3.4.2, [250]). Thus, the decrease of biofilm density after increase of substrate loading is not surprising. Here, no particular observations can be made. This, however, will change when regarding the temporal development of detachment rate as presented in **figure 4.4**. As can be seen, detachment rate is oscillating with a high amplitude at the beginning which decreases during cultivation time. **Figure 4.5** emphasizes this observation where the averaged detachment rate over five days and its standard deviation is displayed. An exponential fit is applied to demonstrate the decrease of standard deviation to zero after $45d$. A possible explanation becomes evident when taking into account regular maintenance events as given as perpen-

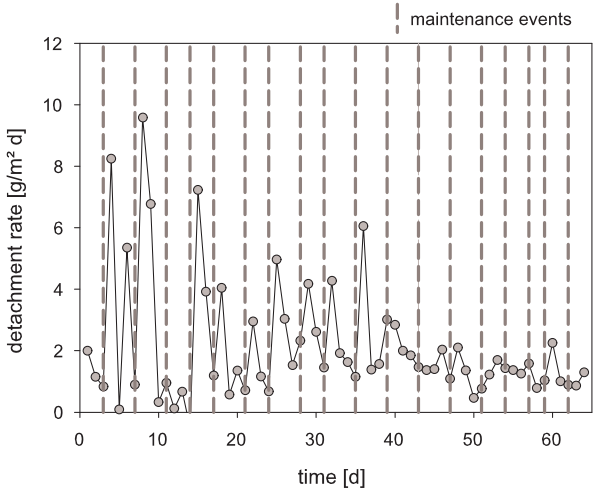

Figure 4.4: Development of overall detachment rate and maintenance events of reactor

dicular lines in figure 4.4. It is striking that detachment rate dramatically increases after maintenance events. During such a maintenance event the reactor is slowly drained and all conduits, mixing vessel and the pump are cleaned in order to remove unwanted biofilm growth. That means that the biofilm gets in contact with air, temporarily lacks nutrients and is mechanically stressed by draining and refilling. It is evident that such a procedure is applying a definite stress on the biofilm. Hence, it is assumed that by performing regular reactor maintenance the biofilm is damaged in a way that parts of the biomass are being easily detached afterwards.
The magnitude of this phenomenon is decreasing over time which can be interpreted as adaptation of the biofilm to the regular stimulus connected with reactor maintenance works. It is hypothesized that this evolutionary pressure favors the presence of stable matrix forming species which allows the biomass in the biofilm to resist better against stresses of maintenance events. Assuming biofilm stability is connected to its density in a way that higher density means higher stability, one would expect an increase of biofilm density over time. This could not be observed in this experiment because the change of substrate supply may overlap this effect. But

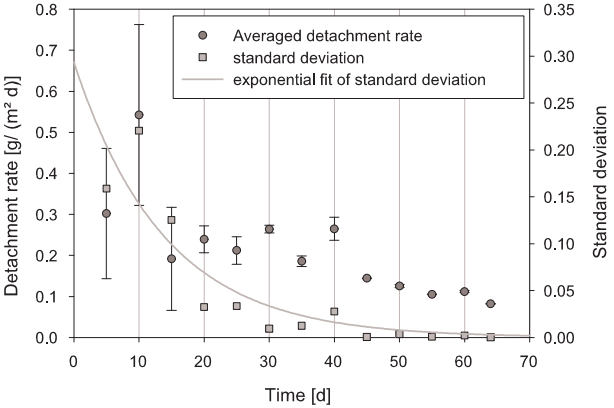

Figure 4.5: Mean and standard deviation of overall detachment rate

in other experimental studies this phenomenon, termed as "biofilm consolidation" could be observed [133]. For the experimental results shown here it seems that biofilm consolidation might be an artefact caused by regular maintenance works which in turn is necessary due to the existence of a recirculation loop in the reactor.
A recirculation of the tube outlet causes further negative influences which are summarized:

Recirculation

- Detached biofilm particles accumulate in bulk phase (growth in suspension, abrasion due to collisions, re-attachment).
- Soluble compounds accumulate in bulk phase (intermediates, signaling compounds, etc.).
- Biofilm growth in pipes and pump deteriorates mass balances and demands regular maintenance.

Maintenance of reactor

- Regular mechanical stress are applied on biofilm system by maintenance (draining, substrate lack and direct contact with air).
- High working load during experiments is needed (around 30h/week).

Substrate conditions
- After removing unwanted biofilms during maintenance, more substrate gets available. So, substrate loading might vary.
- Substrate inlet concentration is decreased when reactor segments are dismounted. Thus, substrate availability may vary.

It is obvious that this reactor system can not fulfill the requirements listed at the beginning of this chapter. Thus, the BTR is not suitable for a direct comparison of simulation and experimental results.

4.3 The Flow-through Biofilm Tube Reactor (FTBTR)

To use a once-flow-through tubular system is the direct consequence of the experiences made up to this point. Thereby, the negative traits of recirculative process control are removed whereas the advantages of a tubular flow field are still present. This concept is realized in the FTBTR: the Flow-through Biofilm Tube Reactor. A flow chart of the system is displayed in figure 4.1 (right). Water is now supplied by the tap. In order not to directly connect the biofilm system with the drinking water distribution net it is interrupted by a level controlled water reservoir. Flow rate is maintained by a gear pump as in the BTR. The substrate supply for the biofilm, however, is realized by a continuous injection of a sterilized and concentrated substrate solution (see section 4.5 for its composition). Liquid sampling is possible before and after the tube whereas solid samples originating from detached biomass can be separated according to particle size in a filter cascade. Thus, mass balances for solutes as well as solids can be closed and samples of the biofilm can be taken by removing parts of the tube. They are used for gravimetric biomass determination and CLSM investigations.
Chapter 5 reveals the high quality and consistency of experimental data acquired with this system in detail. However, a challenge is provided by the comparably small amount of biomass in the system combined with the short residence time of

the fluid in the reactor (e.g. $\tau = 33s$ at $Re_T = 1500$). This leads to small differences of inlet and outlet substrate concentration which in turn demand sensitive analytical methods. DOC and COD measurements do not yield the success whereas HPLC is more useful. Additionally, microelectrode measurements are more challenging than with the BTR.

4.4 Evaluation of reactor setups in biofilm research

Based on the experiences made in this study (see also section 5.1) and literature studies concerning reactor types that have not been used here [71, 162, 11] an evaluation of biofilm reactor setups in research applications is presented in **table 4.1**.

Criterion	Flow cell	Airlift	RAR	RDR	BTR	FTBTR
Flow field	-	–	–	+	++	++
Substrate cond.	++	+	+	+	+	++
Mass balance	+	+	–	-	-	++
Planar substrata	++	–	++	++	+	+
Work load	++	+	+	-	–	++
Sterile operation	++	-	-	-	+	–

Table 4.1: Evaluation of biofilm reactors in research applications (++ very good, + good, - satisfactory, -- insufficient)

A discussion on the Rotating Disc Reactor (RDR) is found in Appendix C and in Möhle et al. [151]. The distinct reactor types are evaluated according to different criteria which are important for fundamental research on biofilm development. Research on Airlift Reactors, however, is more aiming on a Scale-Up for industrial processes. The table shows that the distinct reactors are unequally well appropriate for different research tasks. In this work, the FTBTR reveals to be the best choice which is affirmed by its results as they are presented in chapter 5.

4.5 Concept of substrate solution composition

In many cases the concept of a substrate solution's composition in biofilm cultivations is unclear. Especially in mixed-culture biofilm cultivations, however, the available substrates determine microbial composition and thereby possibly biofilm structural development (section 3.2.2). For modeling microbial growth it is of central importance to know the limiting substrate so that growth kinetics can be successfully applied. Hence, complex media like the common Luria-Bertani (LB) medium [102] cannot be used. Under limiting conditions, furthermore, filamentous microorganisms, e.g. *Microthrix parvicella*, may gain a chance to dominate the population (cp. bulking sludge phenomena in wastewater treatment plants) and overgrow compact biofilm microorganisms. The filamentous structures can grow into the bulk phase where fluid flow can cause oscillating movements of the filaments. This effect improves advective transport and thereby essentially decreases mass transfer limitations [206, 145]. Here, a minimal medium is developed that shall assure only glucose as limiting substrate and provide all further nutrients in sufficient amounts. Glucose can be metabolized by all microorganims (in glycolysis pathway). So, no selection of species shall occur. The use of tap water simplifies the preparation of the medium by providing trace elements and minerals but special care is needed if tap water composition might change, e.g. when cultivating at different locations. In addition to carbon and energy sources further compounds are needed for the cells to grow and maintain their metabolism. Nitrogen and sulphur are constituents of amino acids and hence of proteins. Phosphorus is used in the energy metabolism of the cell (in ATP, NADP, etc.). Several metals are needed as functional elements of enzymes (e.g. for Cytochromes in the respiratory chain) [141].

In **table 4.2** averaged results from elementary analyses of bacterial biomass are listed [141] and an example for cellular demands of distinct elements is shown when $20\frac{g}{m^3}$ glucose is fed as inlet concentration.

Applying this concept the concentrations of supplementary added substances are coupled to the inlet concentration of carbon source. Regarding the composition of

Table 4.2: Elementary composition of prokaryotic cells [141] and estimated demand for a cultivation with $20\frac{gGlc}{m^3}$ compared to available nutrients in tap water, **bold**: elements that might not be supplied in sufficient amounts by tap water

Element	Content [%DM]	$c_{needed}[\frac{g}{m^3}]$	$c_{tap}[\frac{g}{m^3}]$
Carbon	50	8	-[1]
Oxygen	20	3.2	-[2]
Nitrogen	14	2.24	1.37[3]
Hydrogen	8	0.64	-[2]
Phosphor	3	0.48	**0.033**[4]
Sulfur	1	0.16	8.87[5]
Potassium	1	0.16	0.9
Calcium	0.5	0.08	19.1
Magnesium	0.5	0.08	2.8
Chlorine	0.5	0.08	9.5
Iron	0.2	0.032	**0.02**
Others	0.3	-	-

[1] Carbon is usually not measured and assumed to be undegradable (not microbially metabolized under presence of glucose); [2] sufficient hydrogen and oxygen are available in water; [3] from sum of NH_4^+, NO_2^- and NO_3^{2-}; [4] from PO_4^{3-}; [5] from SO_4^{2-}

tap water in Braunschweig, Germany[1] following substances are added: urea (as nitrogen source which can easier be taken up than nitrate contained in the tap water), Sodium phosphate, iron sulphate (mainly as iron source because iron is removed in the drinking water purification process) [2]
As a result of this work und other studies [120] multivalent ions, e.g. Ca^{2+}, Fe^{2+}/Fe^{3+} can play an important role in terms of mechanical stability of the biofilm matrix. This effect is extensively discussed in section 6.1.3. Fe_2SO_4 solution is prepared as saturated stock solution. In presence of oxygen Fe^{2+} ions will oxidize to Fe^{3+} resulting in the precipitation of insoluble $Fe(OH)_3$. This process occurs within minutes. Using a photometric iron cell test (Merck 14549) iron concentration is measured over time and is identified to be constant at $390 mg/l\ Fe$. Also iron concentration in the substrate solution remains constant. So, no further precipitation of iron in the biofilm is expected. All further necessary elements can be found sufficiently in the tap water. Substrate inlet concentration $c_{S,in}$ is coupled to the substrate loading rate.

$$B_A = \frac{c_{S,in} Q}{A_F} \tag{4.10}$$

To be precise, not all glucose taken up by the cell is used to generate new biomass. A fraction which is determined by the substrate yield coefficient (see equation (3.3)) is used for energy generation. Thus, more substance is provided than needed.

[1] *http://www.bs-energy.de/index.php?id=339 (5/13/07)*
[2] http://www.forum-trinkwasser.de/fragenundantworten/fragenundantworten.html (5/13/07)

4.6 Characterization of inoculum

Several causes favor the usage of sewage sludge as biofilm inoculum in laboratory cultivations of undefined mixed culture biofilms which shall mimic realistic conditions. Activated sludge flocs contain biofilm forming microorganisms of diverse species. Several types of mesophilic, aerobic, heterotrophic and also autotrophic bacteria are present. But like in many aquatic environments also fungi, algae or proto- and metazoa are found. In this study, activated sludge samples from the wastewater treatment plant Gerwisch in Magdeburg, Germany are used as in a parallel project [76]. In former studies [250, 134, 211] samples from wastewater treatment plant Steinhof in Watenbüttel, Germany are applied but show neither in particle size analysis nor microscopy significant differences to the ones from Magdeburg.

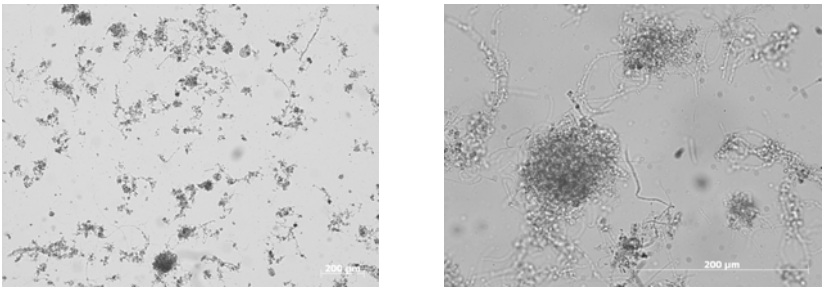

Figure 4.6: Microscopic images of Activated Sludge used as inoculum from wastewater treatment plant Gerwisch in Magdeburg, Germany (left: 5x/0.12 NA objective lense and right: 20x/0.5 NA objective lens)

Microscopic analysis

Figure 4.6 provides light microscope images with different magnifications of an activated sludge sample. As can clearly be seen, biomass is existent in different forms: aggregates and flocs of different sizes as well as single cells. Furthermore, filamentous structures are visible. After inoculation of biofilm reactors both flocs and cells may adhere and provide initial sites for biofilm development. This might affect further structural development decisively (see section 5.6).

Particle size distribution of flocs

Using laser diffraction spectroscopy (see Appendix B.2), volume distribution of activated sludge inocula is measured. Before inoculation samples are homogenized.

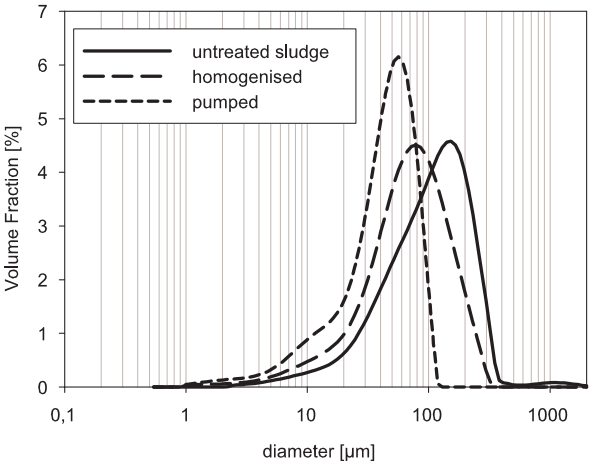

Figure 4.7: Particle size analysis of sewage sludge used as inoculum from WWTP Gerwisch, Magdeburg, Germany

After addition of inoculum the reactor is in closed recirculation for one night which means that the suspended biomass is also mechanically stressed. As **figure 4.7** reveals, the particle size distribution thereby becomes narrower and the maximum is moved toward smaller particle sizes.

5 Biofilm development in model and experiment

5.1 Applicability of biofilm reactors for experimental validation

The results of this section are summarized in table 4.1.

RAR cultivations

Experimental data from long-term cultivations with chemoautotrophic biofilms in a Rotating Annular Reactor performed by STAUDT [210] (experiment *Amm07*) are used for the validation of a biofilm growth model. Based on the reactor mass balance, the experimental setup and literature values a set of well fitting parameter is developed. The simulations with a one-dimensional model (realized in AQUASIM) represent the global reactor balances satisfyingly.
When transferring the processes and parameters from the 1D to the multidimensional model similar results for the mass balances are achieved. However, the simulated biofilm structure appears to be always flat and compact which does not agree with the experimental results of the CLSM investigations (see [211, 210]). Generally, a rough surface structure of the biofilm on the microscale is observed experimentally but could not be reproduced in simulations. Heterogeneous structures are only predicted by multidimensional biofilm models when at least one substrate is limiting [176, 256]. Here, this is not the case. But how can the heterogeneous surface structure then be explained? One explanation approach is found against the background of flow-induced biofilm detachment which is known to influence biofilm structure and can effect rough biofilms (section 3.2.3). The RAR is known for its complex and badly describable flow field [124, 71] which is suspected to effect heterogeneities. Especially the occurrence of Taylor eddies provides additional mechanical stresses. The corresponding influences, however, are not assessable.

Hence, data of biofilm cultivations with RARs do not provide the desired quality for the experimental validation as it is traced in this work.

BTR cultivations

Due to reasons that are itemized in section 4.1 a well-established tube reactor system promising a better describable flow field than the RAR is chosen. However, as already presented in section 4.2 mass balances cannot be closed and biofilm development is strongly influenced by regular reactor maintenance. Hence, the experimental setup must be improved in order to provide the required data.

FTBTR cultivations and limitation phenomena

As discussed in chapter 4 the need for a novel reactor system emerges and the FTBTR (see section 4.3) is successfully tested. Based on these experimental results (presented later in this chapter), a 1D growth model is developed with the same model equations as shown in table 5.1 but assuming a flat biofilm geometry [117]. Even with a simple approach the development of biofilm thickness and density is well describable. Overall rates derived from reactor mass balances, however, do not yield the same behavior as predicted by the simulations. Experimental rates are increasing throughout the whole experiment (cp. figures 5.3 and 5.4) whereas simulated rates begin leveling off around $t = 15d$ and then become constant around $t = 25d$. Constant rates occur when parts of the biofilm are no longer penetrated by the limiting substrate. In that case only the biomass in the active layer grows which causes a linear increase of biofilm thickness and the constancy of all relevant rates. Summarizing, the FTBTR provides useful data for the experimental validation of biofilm models. So, these considerations bring the focus to the question how the increasing observed rates can be described in the model.

5.2 Model construction

The way how the numerical solutions of the mathematical models discussed in the following chapters are acquired is summarized in appendix A. Before presenting the constituting processes and parameters of the model as well as the experimental conditions, mesocale structural properties of biofilms must be regarded as far as they are of importance for the upcoming considerations (see also Appendix C).

5.2.1 Biofilm mesoscale structure

The results presented in appendix C.2 indicate that it may not be sufficient to collect data on macroscale (gravimetry and chemcial analyses at reactor level) and microscale (CLSM and DIA) to completely capture relevant structural properties of the biofilm. **Figure 5.1** illustrates this conclusion by comparing CLSM visualizations and photographs of the experiment presented in section 4.2.2 at two points of time. The visualizations of the CLSM pictures do not show the patchy growth of the biofilm on the scale of several *mm* (i.e. mesoscale) shown by the photographs which is probably caused by substrate limitation and also by the initial adhesion as small flocs from the inoculum. They only provide an image of a relatively small fraction of the biofilm (covering an area of $(500 \times 500)\mu m^2$) where a completely different structure may be observed.
Generally, a more heterogeneous biofilm structure can influence biofilm activity and development. A rough structure yields an increase in surface area and may thereby improve mass transfer processes in dependence on flow conditions. For the experiment presented in the following a patchy growth on the mesoscale is observed. Thus, it is assumed that an increased mass transfer leads to a better penetration of the biofilm with substrates and delays the point of time in which limitations occur.
This effect of heterogeneous growth is modeled as biofilm growth in hemispherical microcolonies. This can already be realized in a 1D model and is recognized as biofilm area A_F as a function of the space coordinate z [189].

$$A_F = 4\pi n_{spheres}(r_{particle} + z)^2 \tag{5.1}$$

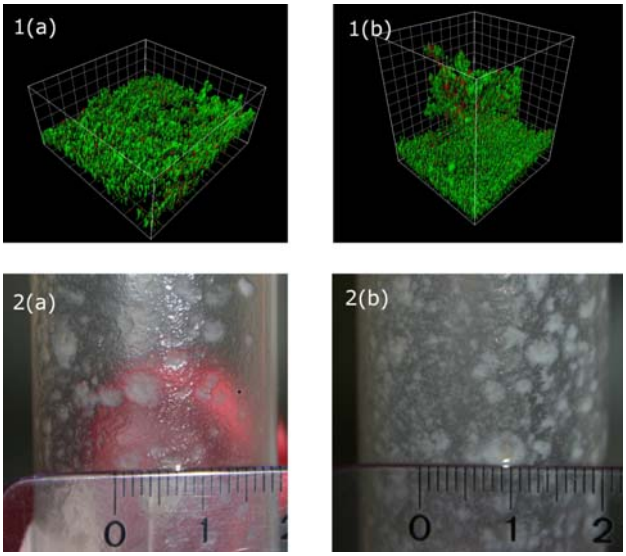

Figure 5.1: Biofilm structure in different spatial scales: (1) 3D-visualizations of CLSM stacks (red: cells, green: EPS glycoconjugates, grid length: $50\mu m$ and (2) photographs from outside the tube; taken at (a) $t = 8d$ and (b) $t = 24d$, respectively

Due to the fact that mass transfer only happens in the direction of radial coordinate r and not perpendicular to it, the hemispherical colonies can be represented in the model as spheres ($n_{spheres}$) with $n_{colonies} = 2 \cdot n_{spheres}$. Equation 5.1 is valid for a spherical biofilm growing on a spherical particle with a radius $r_{particle}$. For numerical reasons a radius of $r_{particle} = 10^{-8}m$ is chosen which is different from zero.
Regarding the fact that sewage sludge is used as inoculum this approach seems quite reasonable. Sludge flocs may adhere to the substratum and form microcolonies which can grow under good external mass transfer in any direction resulting in a hemispherical shape of the colonies. Later they might confluently grow together and form a compact biofilm. This, however, is probable to occur relatively late because of low substrate supply.
This approach requires an additional parameter together with the initial diameter of the colony (relating to initial biofilm thickness $L_{F,ini}$): the number of colonies $n_{colonies}$. In order to gain information about a value of these two parameters, particle

size distributions of the inoculating biomass are determined as presented in figure 4.7. After exposure to homogenization and pumping, a narrow distribution of particle sizes with a maximum around $50\mu m$ diameter of equivalent sphere is present. Using this value as initial diameter of microcolonies in the model, however, yielded no good results.
Regarding the large amount of biomass in the inoculum and the comparably small surface area of the reactor it is likely that only a small portion of biomass can adhere. The fraction of inoculum that is adhered cannot be characterized with respect to the size and number of colonies. Best results in this study are achieved with an initial diameter of $200\mu m$ which complies well with the untreated sludge in figure 4.7. In further studies the initial sizes of colonies ought to be determined experimentally which in turn requires special experimental methods (e.g. optical approaches).
It is also possible to apply distributions of initial colony sizes in the model. This is tested in this study (data not shown) but does not give better results. Furthermore, it complicates the model by the number of parameters.
It has to be mentioned at this point that this colony-like growth is observed under laminar flow and low substrate supply. Under other cultivation conditions these structures may not occur and other modeling approaches might be a better choice.

5.2.2 Processes and Parameters

Table 5.1 shows the stoichiometric matrix of the model presented in the following with the processes of growth and decay of cellular biomass as well as growth-coupled EPS-production (see section 3.2.1). In **table 5.2** parameters of the model are listed. The considered solutes are organic substrate c_S and oxygen c_{O_2} as well as the particular components of the biofilm heterotrophic biomass X_H, EPS X_{EPS} and inert biomass X_I.

Inactivation (also termed as inertization) is chosen as decay process. The decayed cells remain in the biofilm but completely lose their metabolic activity. This will not change biofilm density and is therefore in accordance with the experimental observations (see figure 5.2). Surely, it can be assumed that these inactive cells preferably lyse and thereby release parts of their cytoplasm as degradable substrates which can

Table 5.1: Stoichiometric matrix

Process	dissolved		particulate			Rate r_i
	$\mathbf{c_{O_2}}$	$\mathbf{c_S}$	$\mathbf{X_H}$	$\mathbf{X_{EPS}}$	$\mathbf{X_I}$	
Growth	$1 + Y_{\frac{EPS}{X}} - \frac{1+Y_{\frac{EPS}{X}}}{Y_{\frac{X}{S}}}$	$-\frac{1+Y_{\frac{EPS}{X}}}{Y_{\frac{X}{S}}}$	1	$Y_{\frac{EPS}{X}}$	0	$\mu_H \frac{c_S}{K_S+c_S} \frac{c_{O_2}}{K_{O_2}+c_{O_2}} X_H$
Decay	0	0	−1	0	1	$k_{decay} X_H$

Table 5.2: Model parameters

Parameter		Value	Source
Kinetic constants			
Decay coefficient	k_{decay}	$0.025 d^{-1}$	[100]
Detachment coefficient	k_{det}	$0.97 d^{-1}$	exp. data
Diffusion coefficient glucose	D_S	$5.8 \cdot 10^{-5} \frac{m^2}{d}$	[100]
Diffusion coefficient glucose	D_{O_2}	$2.1 \cdot 10^{-4} \frac{m^2}{d}$	[100]
Maximum growth rate	μ_H	$4.8 d^{-1}$	[235] and fit
Monod constant glucose	K_S	$2.3 \frac{g}{m^3}$	[235] and fit
Monod constant oxygen	K_{O_2}	$0.1 \frac{g}{m^3}$	[100]
Number of spheres	$n_{spheres}$	200000	estimated
Yield coefficient	$Y_{\frac{X}{S}}$	$0.42 \frac{gX}{gS}$	[100] and fit
Yield coefficient EPS	$Y_{\frac{EPS}{X}}$	$0.25 \frac{gEPS}{gX}$	estimated
Experimental settings			
Oxygen inlet concentration	$c_{O_2,in}$	$8 \frac{g}{m^3}$	saturation
Substrate inlet concentration	$c_{S,in}$	$6 \frac{g}{m^3}$	measured
Flow rate	Q_in	$1.017 \frac{m^3}{d}$	$Re_T = 1500$
Model values			
Initial fraction of cells	$\epsilon_{S,ini}$	0.1	estimated
Initial fraction of EPS	$\epsilon_{EPS,ini}$	0.15	estimated
Initial fraction of Inerts	$\epsilon_{I,ini}$	0	estimated
Density cells	ρ_{X_H}	$240000 \frac{g}{m^3}$	[10, 211]
Density EPS	$\rho_{X_{EPS}}$	$40000 \frac{g}{m^3}$	estimated
Density Inerts	ρ_{X_I}	$240000 \frac{g}{m^3}$	[10, 211]

subsequently be metabolized by other biofilm inhabitants. Simulation results, however, reveal the negligibility of this substrate source due to comparably small masses (data not shown). For modeling of biofilm detachment an approach as presented in equation (3.13) is chosen.

Experimental conditions

The data presented in the following sections are derived from an experiment with the FTBTR under constant hydrodynamic ($Re_T = 1500$) and substrate conditions ($c_{Glc,in} = 2.5\frac{g}{m^3}$ (presented in Möhle et al. [152])). The reactor is treated as described in section 4.3. Overall rates are computed using the equations presented in section 3.4.2.

5.3 Biofilm growth and activity

Figure 5.2 gives the experimental and simulation results of biovolume and biofilm density. The characteristic parameter of biofilm thickness (see section 3.4.2) is here replaced by the volume of the biofilm, termed as biovolume. When growing as hemispheres the term biofilm thickness refers to the radius of the colonies and not to the mean biofilm thickness. Thus, biovolume is a more adequate parameter of comparison.
The rising behavior of biovolume during the cultivation is excellently described by the simulation. With the hemispherical model an exponential growth is predicted which coincides well with the experimental results. Interestingly, biofilm density remains widely constant throughout the cultivation at $30\frac{kg}{m^3}$. All cultivation conditions remained constant during the experiment. Thus, it might not be surprising to find a constant biofilm density. In some studies, however, a time dependent process is postulated and termed as "biofilm consolidation" effecting an increase of biofilm density with time [164, 128, 29]. This is not observed here which demonstrates the need for more experimental work on this subject. In experiments with the BTR (sec-

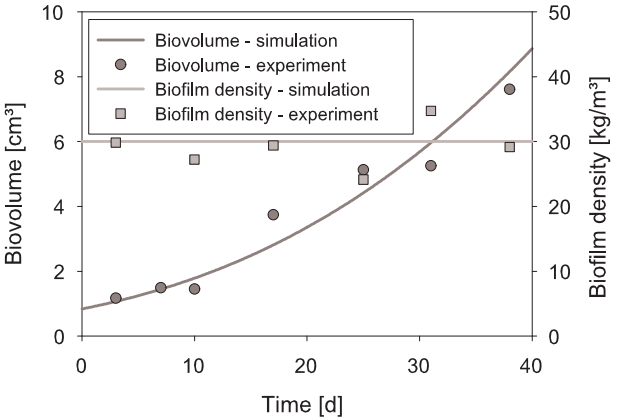

Figure 5.2: Temporal development of biovolume and biofilm density in FTBTR

tion 4.2) this compaction process of the biofilm may be explained by the adaptation to the regular stress of reactor maintenance.

When looking at consumption rates, it becomes obvious that the model is also capable of representing biofilm activity. Due to hemispherical growth, rates do not level off to constant consumption rates as mentioned in section 5.1 but rise throughout the cultivation as shown in **figure 5.3**. Substrate consumption rate is underestimated by the simulation. With high probability this can be ascribed to the analytics used for the measurement of substrate concentration. In this case, Chemical Oxygen Demand (COD) is measured and several disadvantages become evident. At first, not only glucose concentration which is considered in the simulated consumption rates is determined but virtually all oxidisable compounds in tap water which may vary in concentration. These compounds are supposed to be persistent and are not degraded by microbes under presence of glucose. Secondly, the difference of substrate inlet and outlet concentration is small caused by the low hydraulic retention time in the reactor. Random errors thereby gain high influence on the value of substrate consumption rates. Moreover, absolute values of concentrations are relatively small (several ppm). Thus, measurements are performed in the lower region of COD test

sensitivity. An alternative approach is to apply HPLC methods where first tests already showed promising results.
Amperometric measurement of oxygen concentration with electrodes, however, yields more reliable values. The computed rates are therefore more trusted and the model indeed explains well the rise of oxygen consumption rate throughout the cultivation.

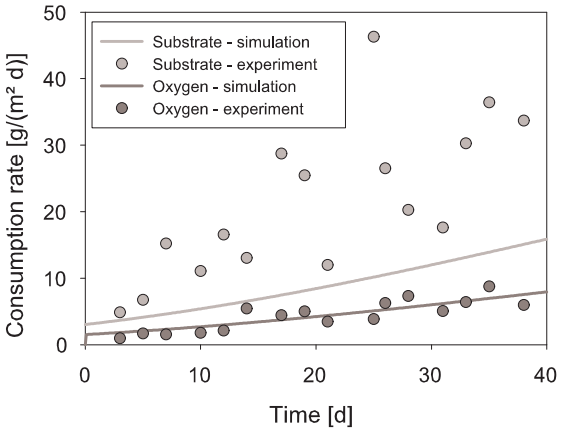

Figure 5.3: Overall consumption rates of organic substrate and oxygen in FTBTR

5.4 Biofilm detachment

Overall rates of biofilm detachment and accumulation computed with equations (3.23) and (3.24) are displayed in **figure 5.4**. In this case, experimental rates are well described by the simulation results, too. The graph clearly shows that the rate of detachment is much higher than the one of accumulation. The detachment coefficient which relates the biomass production to the detachment rate can be directly

computed from the experimental results and is in average $k_{det} = 0.97 \pm 0.04$ meaning that around 97% of newly grown biomass is detached from the biofilm. Due to the once flow through it is furthermore assured that all detached biomass originates from the biofilm.

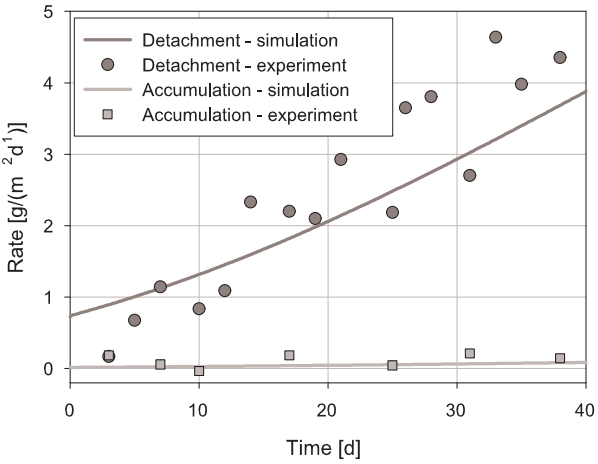

Figure 5.4: Temporal development of overall biofilm accumulation and detachment rate

This result seems surprising but is in accordance with results of flow cell studies [13, 215]. Biofilms are often regarded as sessile communities, or even as "microbial houses" (cp. section 2.4). To speak in this metaphor: Why throw away 97% of building material and "workers" when constructing a house? A probable explanation approach with evolutionary background is already discussed in section 3.2.3: A high detachment rate allows for more net biomass production and the distribution of biomass into new habitats. Especially under the environmental conditions in this experiment with low substrate supply a spreading of off-spring to search for better living spaces seems adequate. In **figure 5.5** values for the detachment coefficient k_{det} from this and further experiments with the FTBTR (performed by Kerstin Garny, UFZ Magdeburg, Germany) are presented. Despite the high standard deviation at

higher substrate concentrations which is due to more frequent sloughing events a decrease of detachment rate at increasing substrate supply can be hypothesized. This is in accordance with literature [104] and supports the explanation approach above. On the other hand it is known that EPS production can increase under low substrate supply (see section 3.2.1). Given that a higher EPS content effects a higher biofilm stability the contrary would be expected.

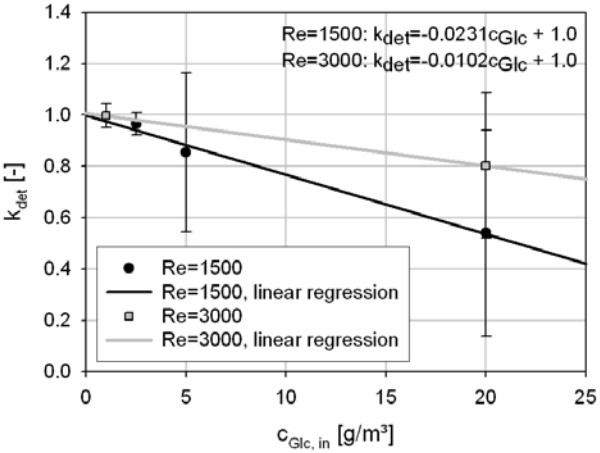

Figure 5.5: Detachment coefficient in dependence on substrate inlet concentration (using further data from Kerstin Garny, UFZ Magdeburg, Germany)

The evolutionary explanation approach may explain how these traits may have developed and how they added to the success of the biofilm mode of life. A process which can be quantitatively formulated, however, is thus not derivable. The development of a substantiated hypothesis will be central subject of chapter 6. At this point it can only be stated that a growth-coupled approach is well suitable of describing the overall detachment rate. The underlying processes, however, are not yet captured.

A better understanding might be indicated when investigating erosion and sloughing separately. So, sieve analysis results of detached biomass are presented as overall

erosion and sloughing rates in **figure 5.6** and **5.7**, respectively.

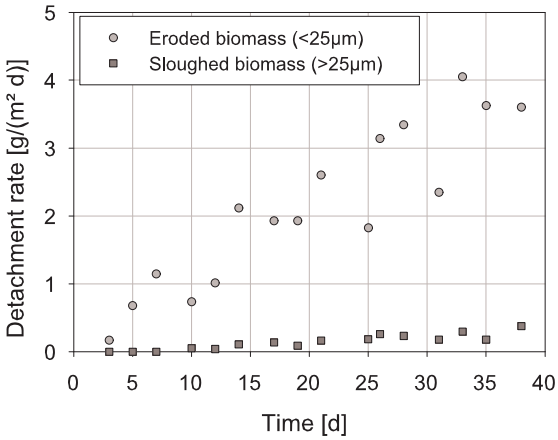

Figure 5.6: Erosion and sloughing rates

It is evident that erosion amounts for the -by far- major part of detached biomass in this experiment - erosion is in average 16 times higher than sloughing rate. *Erosion* is a surface phenomenon meaning that detached biomass originates from the biofilm surface. The highest microbial activity is found there because of best substrate availability. Thus, at the biofilm surface newly grown cells will detach with a high probability. It is hypothesized that these cells are not easily integrated into the biofilm matrix when located at the biofilm surface. From other studies it is known that cell surface properties may vary depending on growth state [2, 14]. Latter play a role in cell adhesion [227] but may also affect the integration of cells into the biofilm matrix.

This hypothesis would be supported if the erosion rate could be correlated to the surface area of the biofilm. Due to several weaknesses of the CLSM method no good data of biofilm surface area is available (see also section 5.5 and [76]). However, the well validated model as presented in this chapter allows for a comparison of simulated data which is given in **figure 5.8**. It becomes obvious that the detachment rate

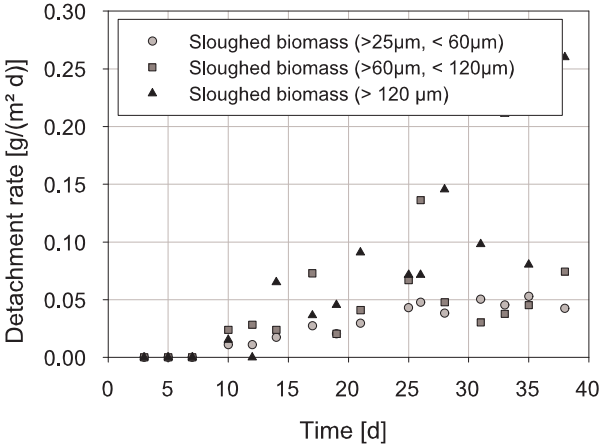

Figure 5.7: Sloughing rates separated in size classes

(here predominantly erosion) can be well correlated to the biofilm surface area, i.e. the surface area of the hemispherical colonies, in this simulation with exponential biofilm growth. This result is not trivial. In the model detachment is coupled to biofilm growth which is not directly related to the biofilm surface area. Thus, the importance of biofilm spatial structure may also be given in terms of detachment phenomena. Nonetheless, a profound explanation of the observed erosion phenomena is lacking but may be found in a more detailed investigation on mechanical interactions of fluid flow and structure in biofilm systems as presented in chapter 6. Regarding the rate of *sloughing* separated by particle sizes (figure 5.7) it can be seen that sloughing starts at day 10 and the rates show a rising tendency with strong deviations. These findings are in accordance with the mechanical explanation approach as developed in chapter 6 and discussed in section 6.4. There, it is proposed that sloughing occurs as a disruption of exposed biofilm structures which grow from the base into the flowing liquid. This results in an augmentation of internal stresses in the structure and effects the break-off of this part of the biofilm. These structures must first grow to a certain size until the internal stresses exceed the strength of the matrix. So, sloughing may first occur after a certain lag phase as observed

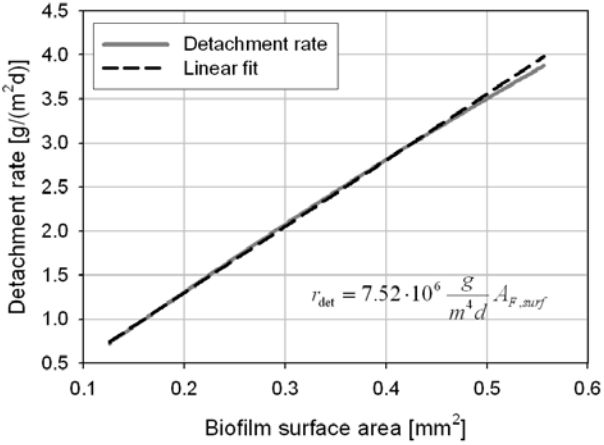

Figure 5.8: Correlation of simulated detachment rate and biofilm surface area

here. From external observation these sloughing events seem to occur stochastically which also causes the high deviation of the observed values.

5.5 EPS-Production

At this point, the model is broadly validated on macroscale which means that all global rates can be represented by the simulation results. Now, a first attempt is made to validate the EPS production process by CLSM data. Before, wet volume from gravimetry and volume from CLSM are compared in order to find out whether a quantitative comparison is reasonable. **Figure 5.9** shows the pairs of values for different measurements during the cultivation. The biofilm volume determined by CLSM is interpolated to the whole reactor.

The values obtained from CLSM and treated by Digital Image Analysis (DIA) (appendix B.1) partially show high deviations and do not necessarily follow a clear trend. Nevertheless, a linear function is chosen in order to gain a portion factor

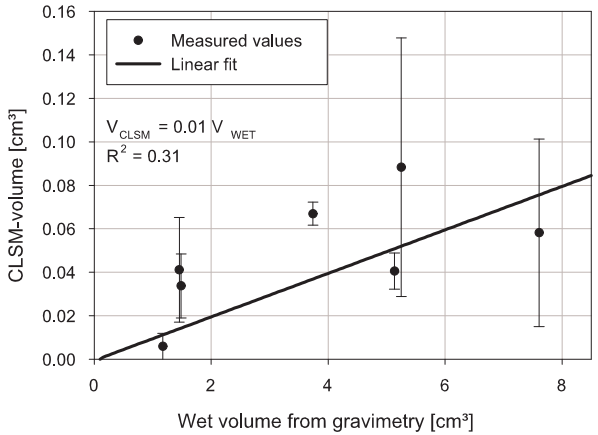

Figure 5.9: Calibration of CLSM volume with wet volume from gravimetrical data

relating CLSM and wet volume assuming that the portion of stained biovolume is constant over cultivation time. This assumption, however, has to be discussed critically. Haesner [76] shows by Denaturing Gradient Gel Electrophoresis (DGGE) that microbial composition of biofilms in BTRs changes over time which probably means that also EPS composition changes. The specificity of lectins (here originating from *Aleuria aurantia* which is specific to fucose [211]) might then cause a variation of stained biovolume over time. Referring to figure 5.9 a high standard deviation of certain values favors the presence of a high spatial heterogeneity of biovolume which does not allow any assured conclusion from microscopic images to the whole reactor. These drawbacks result in a low portion factor and correlation coefficient, respectively, of $0.01 \frac{m^3(CLSM)}{m^3(wet)}$. Assuming that CLSM and wet volume are directly comparable this would mean that only 1% of the gravimetrically determined volume is found by CLSM. The direct comparison is valid when all water in the biofilm is present as hydrate water bound to the EPS. However, interstitial voids and channels in the biofilm are not detected by CLSM but definitely by gravimetry. Thus, the real staining efficiency is supposed to be higher than 1%.
Applying this correction factor, the CLSM data for EPS volume can be compared

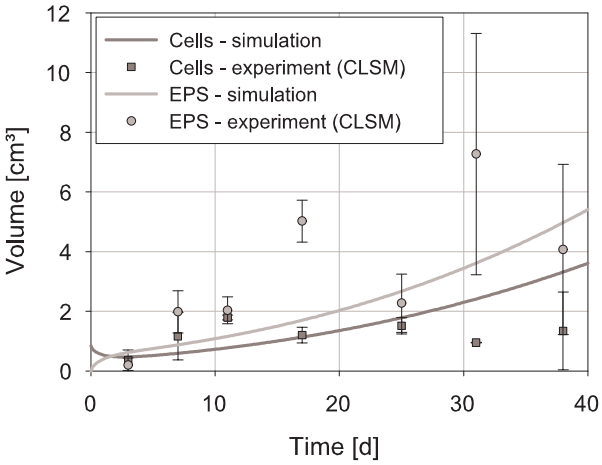

Figure 5.10: Simulation results of EPS volume in biofilm with an approach relating production to growth rate and without decay of cells

to simulation results as presented in **figure 5.10** and **figure 5.11**. The processes of EPS production as presented in section 3.2.1 are tested in this study. Best results are achieved with an approach with a dependency of EPS production rate to growth rate (see table 5.1). Figure 5.10 shows the corresponding outcome. Here, the development of cell volume is overestimated by the simulation. Hence, the process of cellular decay is implemented into the model (see sections 3.2.1 and 5.2.2). With this combination both cell and EPS volumes in the biofilm are well represented by the simulation (see figure 5.11) although CLSM results cannot be trusted. Finally, the question of how to model EPS production cannot be resolved in this work. DGGE-analyses of comparable mixed species biofilms under similar conditions reveal the high diversity of microorganisms [76]. Their specific synthesis pathways for excreted polymers and the specificity of the lectin-staining method [211] yields a small fraction of stained biomass only. The direct comparison of simulation results and CLSM-data in terms of EPS contents and distribution is thereby not helpful. Furthermore, it has to be mentioned that the amount and type of EPS will determine stability and mechanical properties of the biofilm matrix which has major implica-

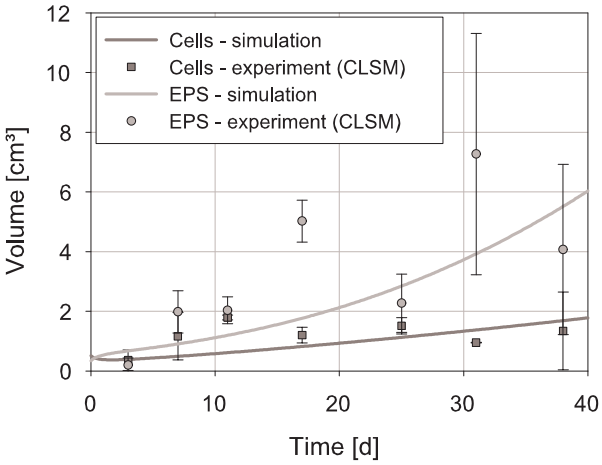

Figure 5.11: Simulation results of EPS volume in the biofilm with additional process of cell decay

tions on detachment phenomena (cp. section 6.1).
These results demonstrate the need for an improvement of the CLSM method or a usage of chemical analyses [195]. A possible solution of this problem may be found in the usage of monocultures as biofilm forming microorganisms. In that way a defined biofilm matrix containing one type of cells and EPS can be obtained. This approach however not only complicates reactor operation and control but also creates an rather artificial laboratory system. By far most real systems are undefined mixed culture systems what particularly challenges systematic investigations.

5.6 Structural development

In order to model the development of biofilm spatial structure a multidimensional model approach is applied as introduced in section 3.3.2. In such a bottom-up approach, biofilm structure in the simulations emerges from the processes and param-

eters implemented in the model. Firstly, biofilm growth in hemispherical colonies shall be modeled in order to allow the comparability with the 1D model already presented. These kinds of structures are observed in simulations with only few inoculating particles (sludge flocs), low detachment forces and no external mass transfer limitations so that each direction of growth is equally preferred. **Figure 5.12** shows the structural development in a simulation based on the processes and parameters as listed in section 5.2.2 without implementation of a detachment process. As can be seen, a colony-like growth of the biofilm in hemispheres can be well achieved.

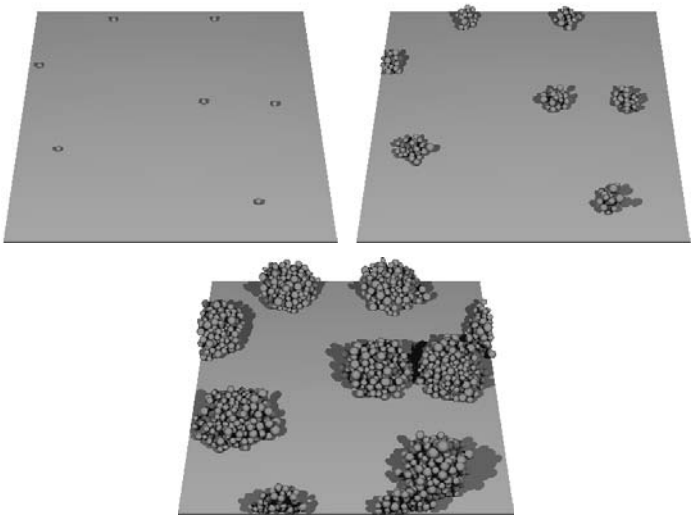

Figure 5.12: Development of biofilm structure in 3D simulations without detachment can effect hemispherical growth

In a next modeling step detachment of biomass is implemented. The challenge is now to find an empirical detachment function (of a type as given in equation (3.12)) that describes a high detachment rate and still effects hemispherical growth. This goal could not be achieved in this work. Biofilm structures always developed as shown in **figure 5.13**. In the example shown here, a simulation with a detachment function depending on the coordinate z perpendicular to the substratum and biofilm

density ρ_F is applied [255].

$$r_{det} = k_{det} \cdot \frac{z^2}{\rho_F} \tag{5.2}$$

The detachment coefficient k_{det} is varied manually in a way such that growth and detachment rate reach values as observed experimentally. In the model, detachment forces act from above the biofilm in z-direction. So, biomass is preferably detached from the top of the structures. Biofilm growth predominantly occurs in regions with lower detachment forces so that the biofilm covers the substratum in a flowing manner effecting a smooth and flat biofilm structure.

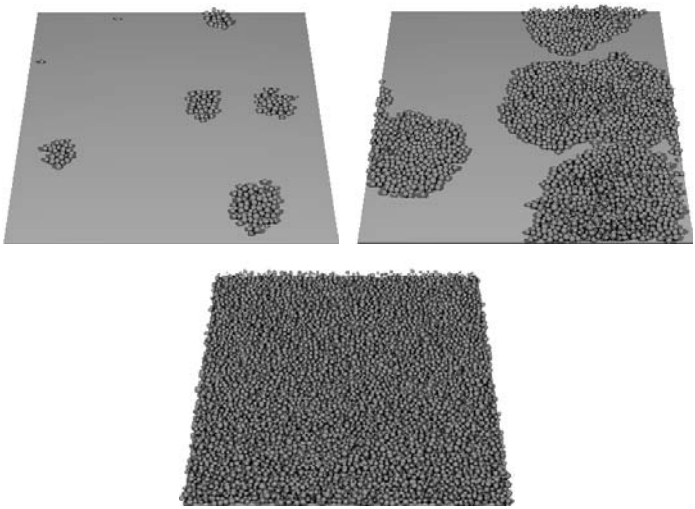

Figure 5.13: Development of biofilm structure in 3D simulations with high detachment rate yields flat and compact biofilm structures

Furthermore, in a 2D modeling approach several different empirical detachment functions are tested relating detachment to either local growth rate $\mu(x, z)$, EPS concentration $X_{EPS}(x, z)$, biofilm density ρ_F or space coordinate z and also to combinations of these parameters. At the high detachment rate that ought to be represented in the experiment always flat biofilm structures emerge in the simulations as already shown in figure 5.13. This result confirms the assumption made earlier in this chap-

ter: empirical approaches for the mathematical description of biofilm detachment prove to be too simplistic. Hence, the complex interaction of fluid flow and biofilm structure considering mechanical aspects must be taken into account.
Another important factor influencing the development of biofilm structure is widely neglected in biofilm research. Grazing of protozoa or metazoa definitely changes biofilm structure but, to the knowledge of the author, this phenomenon has not yet been intensively studied. In mixed culture biofilm cultivations as they are presented in this work grazing organisms are always observed. Due to the insufficient knowledge this effect is not considered in this work.
Concluding this investigation it is an unsatisfying result that a highly sophisticated model as presented is not able to reproduce the observed detachment phenomena. Basic changes in the modeling framework may lead to the wanted structural development in the simulation results. This proceeding, however, will not lead to the desired gain in knowledge. Biofilm detachment results from an interaction of several processes and its mathematical description is obviously not trivial. So, a more detailed and spatially resolved analysis of biofilm detachment is needed. It is desirable that after this excursion to modeling approaches with higher complexity simpler relationships describing biofilm detachment can be deduced for a more practical application in future biofilm models.

6 Mechanics of biofilm detachment

The aim of this chapter is to approach an understanding of the processes underlying biofilm detachment. A priori, detachment is assumed to be a matter of mechanics. Fluid flow past a biofilm surface induces stresses on the biofilm structure which in turn effect strains. If the strength of the matrix cannot resist the internal stresses, parts of the biofilm will disrupt and detach. These considerations are generally accepted for sloughing events but may also explain erosion.
In this chapter, analytical and numerical computations of force balances in biofilm systems regarding fluid-structure interactions are presented. Firstly, an analytical model is developed in order to show by which parameters detachment is determined and to give an idea of the dimensions of values on both sides - internal strength and stresses due to external forces. If they are in the same range a mechanical explanation approach of detachment may be reasonable. To assure the validity of the conclusions drawn from this estimation, realistic values for the model parameters are needed. The derivation of the model is found in Appendix D.
In this work, only fluid induced forces are considered. In Airlift reactors which are used in wastewater treatment also particle-biofilm collisions on biofilms can happen [225]. This kind of mechanical exposure can be much higher than fluid-induced stresses acting on biofilm structures.

6.1 Mechanical properties of biofilms

Several studies demonstrate viscoelastic behavior [110] of monospecies [231, 197], defined mixed species [214] and also undefined mixed culture biofilms ([223], this study). Values for biofilm mechanical parameters can be found in literature and are also measured in this work (for a tabular listing see [151]). The high variation between parameter values originating from different literature sources is obvious. Several causes can hereto be listed.
In mixed culture biofilms different species can produce one or more different matrix

polymers with potentially different mechanical properties. Depending on cultivation conditions certain species are favored so the type and amount of EPS in the biofilm is likely to vary which certainly will influence biofilm mechanical properties and parameters. Moreover, single species may also regulate their EPS synthesis in dependence on cultivation conditions. So, the specific cultivation environment is likely to influence values of mechanical parameters.
Furthermore, some of the measurement techniques applied, only use small fractions of the biofilm (e.g. the microcantilever method in [180]), others need sample sizes of several square centimeters [223]. Thus, the measurement technique is likely to effect different results.
Concluding, there are only a few studies on biofilm mechanics. Several aspects like the role of microorganisms in determining mechanical properties in biofilms are unclear. Particularly, cells in the biofilm matrix might weaken the stability of the matrix. Furthermore, a cellular response to mechanical stresses is imaginable (cp. section 3.2.2).
Regarding the poor knowledge on biofilm mechanics, linear elastic behavior of biofilms is assumed in a first approach and the important parameters of strength and elastic modulus are ad hoc measured for the undefined mixed species biofilms as they are the object of investigation in this study.

6.1.1 Shear strength of biofilms

The method of Fluid Dynamic Gauging (FDG) [35] is applied to measure the strength of biofilms subjected to a fluid flow parallel to the substratum. This exposure is comparable to the one present in tube reactors. The results are presented and discussed in Möhle et al. [151]. Values of shear strength around $6 - 7Pa$ are found for heterotrophic biofilms growing on glucose. Interestingly, always a smooth and compact base biofilm remains on the substratum after enforced detachment by FDG.

6.1.2 Elastic Modulus of biofilm matrix

The Elastic Modulus E, also termed as Young's Modulus, relates normal stress σ to strain ε for solid bodies of linear elasticity ("Hooke's law") [42].

$$\sigma = E \cdot \varepsilon \tag{6.1}$$

Assuming linear elasticity of the biofilm, an apparent elastic modulus is measured using the Nanoindentation method (see section B.3). In order to cultivate biofilms for this measurement, a setup with two parallel biofilm tube reactors (BTRs) (section 4.2) connected by one mixing vessel is used. Special slide carriers come to application to later be dismounted and used in the Nanoindenter device. Two gear pumps are adjusted in a way that in one reactor a laminar flow regime ($Re = 1000$) and in the other one a turbulent flow regime ($Re = 3000$) is prevailing. Then, the system is inoculated with an undefined mixed species culture from sewage sludge (section 4.6). It is expected that the higher shear conditions select species/colonies from the inoculum which are better adapted to adhere to surfaces under high shear conditions by a more stable EPS-matrix. This should be seen in the higher stability (higher values of E) of the samples taken from the turbulent reactor. The direct connection of the reactors assures the same substrate conditions in the two tubes.
Figure 6.1 shows force-indentation curves of samples taken from the system. Here, several measurements on different spots of the sample are displayed of each tube. Albeit the indentations on different spots show deviating curves, they are found to be in the same range. In contrary to the hypothesis made above, samples of the reactor with turbulent flow are not showing a higher stability (steeper curves meaning less indentation depth at higher forces). The samples, however, are taken at different times. The sample subjected to laminar flow is taken after two days whereas the one grown under turbulent flow regime after one day. During the experiment glucose is supplied in order to maintain biomass viability in the reactor. It can thus be assumed that the adhered microorganisms start synthesis of EPS which in turn changes the mechanical properties distinctly. This observation indicates how sensitive mechanical parameters can be to the conditions under which the samples are taken.
Using the "Oliver-Pharr"-Model [165], values for the Elastic Modulus are derived from the force-indentation curves as listed in **table 6.1**.

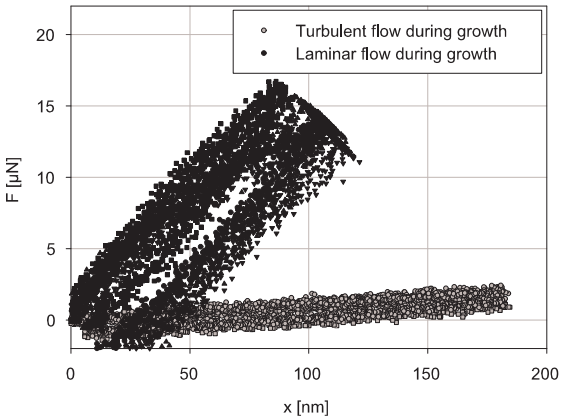

Figure 6.1: Nanoindentation of biofilms grown under laminar (black, taken at t=48h) and turbulent (gray, taken at t=24h) flow conditions

Table 6.1: Elastic moduli measured by Nanoindentation

t [h]	flow during growth	E [MPa]
24	turbulent	25 ± 9
48	laminar	662 ± 102
48	laminar(+ Fe)	1419 ± 862

The values of the laminar and the turbulent grown samples confirm the observations made above. The standard deviation of the measurements ranges from 15 to 36%. This result is not surprising regarding the heterogeneity of mixed culture biofilms. The contents of cells, amount and also type of EPS are likely to be spatially diverse. For different synthetic hydrogels Vidović [230] measures Elastic moduli and finds values in a broad range between 0.01 and 100MPa depending on the chemical structure of the gel-forming molecules. Thus, different types of EPS are expected to have a strong influence on the local mechanical properties of biofilms.

6.1.3 The role of multivalent ions in biofilm systems

Multivalent ions like $Mg^{2+}, Ca^{2+}, Fe^{2+}/Fe^{3+}$ are necessary for the cellular metabolism as functional elements of important enzymes. It is furthermore known that polymers in hydrogels can be cross-linked by addition of multivalent ions which leads to an increase in their mechanical stability. This can be also assumed for polysaccharids in the biofilm matrix which are suspected to play a central role in determining mechanical properties of the biofilm. Jiang et al. [106] demonstrate the influence of Ca^{++}-concentration on the properties of aerobic granules and Körstgens et al. [120, 119] show in Rheometer studies a strong influence of multivalent ion concentration on the rheological properties of monospecies biofilms.
As presented in Möhle et al. [151] the bulk concentration of iron strongly influences the stability of heterotrophic mixed species biofilms. Here, this effect is investigated by Nanoindentation. A biofilm sample grown under laminar flow conditions is indented before and after addition of a saturated $FeSO_4$-solution ($390 mg/l\, Fe$ as determined with a photometric iron cell test (Merck 14549)). The force-indentation curves are presented in **figure 6.2**. The measurements are performed with a stopping phase between indentation and withdrawing. Both curves show a creeping phenomenon during the stopping of the indenter which is typical for viscoelastic samples. The curve of the measurement with additional iron ions is much steeper and shows a bigger plastic deformation of the biofilm. This observation is confirmed by the E-Moduli presented in table 6.1.
It can be assumed that iron may precipitate in the biofilm and thereby effect a stabilization of the biofilm matrix. As already presented in section 4.5 iron concentration in solution remains constant over time in presence of oxygen and also other medium components. A precipitation in the biofilm is not expected in this experiment with very thin biofilms of low activity. Hence, these results confirm the assumption that biofilm mechanical properties are strongly influenced by the presence of multivalent ions due to cross-linking of matrix forming polymers. Higher ion concentrations result in a stabilization of the biofilm matrix.

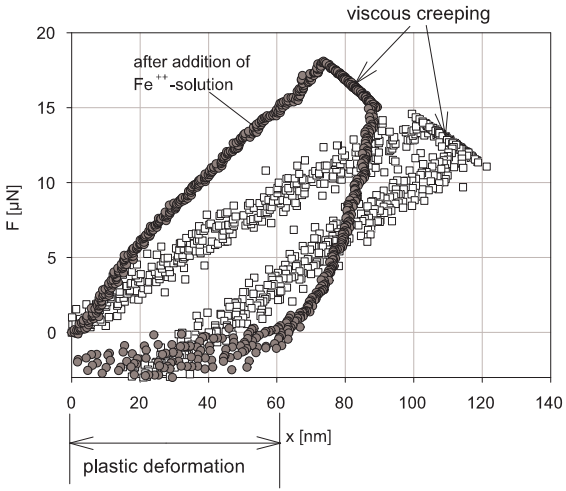

Figure 6.2: Nanoindentation before and after addition of iron solution

6.2 An analytical model of fluid-structure interactions in biofilm systems

A simple mechanical model is developed describing the interaction of fluid flow and biofilm structures of different shapes. Two aims are pursued with this approach. Firstly, an analytical expression shall be developed which provides the possibility to analyze which parameters biofilm detachment may depend on. Secondly, the validity of the numerical model as presented in section 6.3 can be tested in a direct comparison.

Figure 6.3 visualizes the structure of the model. The model is developed for laminar flow conditions in tube reactors yielding an axisymmetric flow profile of parabolic shape (1). An artificial biofilm structure is represented by a cylinder situated on the inner wall of the tube and subjected to fluid flow (2). A cylindrical shape is chosen in order to represent exposed biofilm structures which can often be observed by CLSM investigations. When growing into the flowing liquid these structures are

subjected to drag forces caused by frictional resistance and pressure drag. For flat biofilm geometries, however, shear forces predominate.

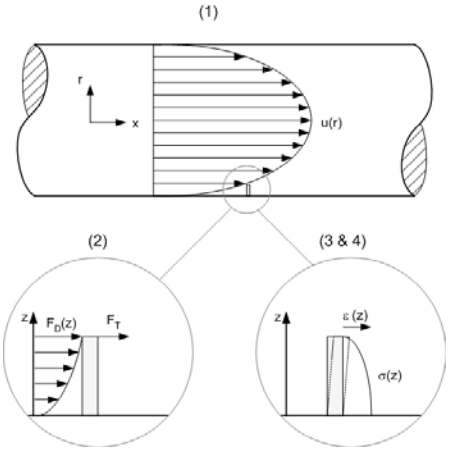

Figure 6.3: Approach of the elastostatic model: (1) Macroscopic flow field in tube, (2) External stresses on cylindrical structure (3 & 4), Internal stresses and deformation (for detailed information see Appendix D)

The fluid-induced external load leads to internal stresses $\sigma(z)$ and a deformation of the structure $\varepsilon(z)$ (3). In terms of temporal biofilm development the model is quasi-static. It can only regard certain points of time of the cultivation and is thus applicable to subsequent steps in biofilm growth. The detailed derivation of the model developed in this work is presented in Appendix D. There, an expression for the maximum flow induced stress in a cylindrical biofilm structure is given. Equation (6.2) lists the parameters on which it is dependent according to equation D.18.

$$\sigma_{max} = f(H_{cyl}, D_{cyl}, \rho, \nu, Q, R_T) \tag{6.2}$$

It is assumed that the maximum structural stress is crucial for detachment events (see above). The influencing parameters can be grouped threefoldly: (1) structural parameters describing the geometrical structure of the biofilm element H_{cyl} and D_{cyl}, (2) parameters describing the fluid properties density ρ and viscosity ν, (3) operational or reactor parameters, respectively, as flow rate Q and tube radius

R_T. Interestingly, most of the parameters remain constant during biofilm cultivations, namely fluid properties, tube radius and flow rate. In the majority of cases flow subjected biofilms grow in aqueous environments where following values can be applied $\rho = 1000\frac{kg}{m^3}$ and $\nu = 10^{-6}\frac{m^2}{s}$. Flow rate is supposed to be constant when using gear pumps. It can however be observed that it decreases when biofilm growth is fast (high substrate supply) and the hydraulic diameter decreases. This is not the case in the experiments presented in this study with low substrate supply. So, solely height and width of the structure may vary during the cultivation. This change, however, is determined by an interaction of substrate supply, growth and also detachment. This complex interaction is only captured by a numerical solution of a multidimensional model as its basics are presented in section 6.3.
It is pointed out that reactor geometry also influences internal stresses in the biofilm. This can already be shown by a simple computation using *Re*-number as a Scale-Up criterion. For the same *Re*-number in tubes with different diameters different mean flow velocities and thus flow fields are found (equations in section 4.1).
Regarding shear and drag forces acting on biofilm structures when subjected to fluid flow this equation can vary depending on the assumptions (e.g. biofilm structures of spherical or streamlined shape). However, the general dependencies will be similar. Now, the question is how can the local maximum structural stress serve as a determinant of overall biofilm detachment rate. Detachment will definitely be influenced by the stresses in exposed biofilm structures but also by their numbers, sizes, etc. Latter are in turn determined by growth conditions. This again confirms the need for a structured model and indicates that maybe no simple empirical detachment function of the type $r_{det} = f(...)$ is valid as suggested in literature, e.g. [212, 170, 159, 93].
In order to analyze the dependencies of the maximum structural stress, **figure 6.4** gives σ_{max} calculated with equation (D.18) in dependency on *Re* for different shapes and sizes of the cylinder. Measured biofilm strength from Fluid Dynamic Gauging (FDG) [151] is found in the graph as horizontal line. If this threshold is reached by the internal stress, the structure is supposed to break and thereby detach.
As obvious in the figure, structural properties play a central role. High and narrow structures higher stresses and are therefore more sensitive to detachment forces. That the maximum stress in a structure reaches the strength threshold can happen

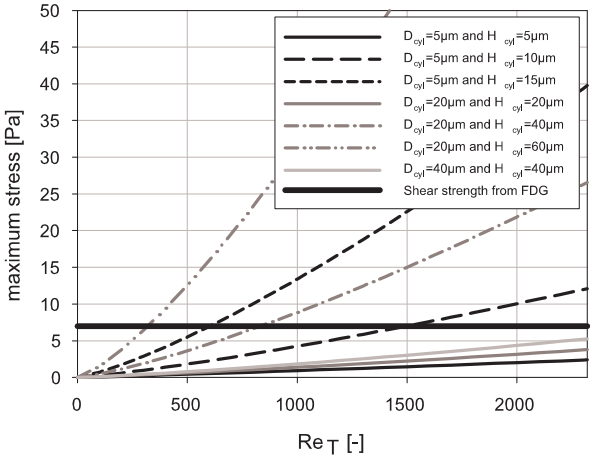

Figure 6.4: Dependence of highest stress in cylindrical biofilm structure on flow conditions

due to two changes - growth of the structure or an increase in flow rate. Hence, in biofilm cultivations with low substrate supply in which more structured biofilms develop, a higher detachment rate is supposed to be observable.
The observations of enforced detachment studies [218] can also be explained. When increasing Re_T, at first smaller structures are detaching and later bigger, more stable structures. Thus, detachment rate will increase with increasing Re_T. This will have more influence for structured, rough biofilms than for smooth biofilms. Latter are indeed very resistant against fluid-induced detachment due to the fact that pure shear forces are magnitudes lower in absolute value than additional drag forces (shown by the equations presented in Appendix D). These prognoses are in perfect accordance with the experimental observations made by Telgmann et al. [218].

6.3 Finite Element Method (FEM) simulations

A numerical multidimensional biofilm model regarding not only growth and diffusion processes but also fluid induced stresses and strains in biofilm structures is more complex and more computationally demanding. This may be the cause why only comparably few studies can hereto be found [178, 6, 222, 127]. Moreover, in these studies artificial biofilm structures are either provided as input data [6, 222] or develop from simulations [178, 127]. Here, realistic biofilm structures from CLSM pictures are used to reconstruct biofilm structure and are implemented in a FE model (section 3.3.3). Together with the mechanical parameters directly measured (section 6.1) this shall yield more reliable conclusions about detachment phenomena. At first, the analytical model in section 6.2 is compared quantitatively with a FE model assuming equal conditions and geometries in order to assure the validity of both modeling approaches mutually.

6.3.1 Comparison of analytical model and FEM simulation

For artificial cylindrical structures both the solution of the analytical model and the FEM simulation are compared using flow conditions in a FTBTR at $Re_T = 1500$ ($d_T = 10mm$) according to the cultivation in chapter 5. The elastic modulus is assumed to be at the lower boundary of values from section 6.1.2 with $E = 25MPa$ and the diameter of the cylinder is chosen to be $D_{cyl} = 20\mu m$. A lower E means in tendency a higher structural deformation and is thereby a harder test of the model's validity.
In **figure 6.5** the geometry is presented as it is used for the computations with a cylinder situated on the inner tube of the wall. For the computation of fluid-structure interactions a staggered approach is chosen because fluid and structure are weakly coupled [64]. On this account, the difference between the four iterations shown in (b) is small where the right structure is the converged solution. **Table 6.2** displays the absolute values of maximum shear stress as calculated by the analytical and FE model, respectively, in three cylinders with different heights together with the maximum deformation obtained. This comparison reveals very good matches -

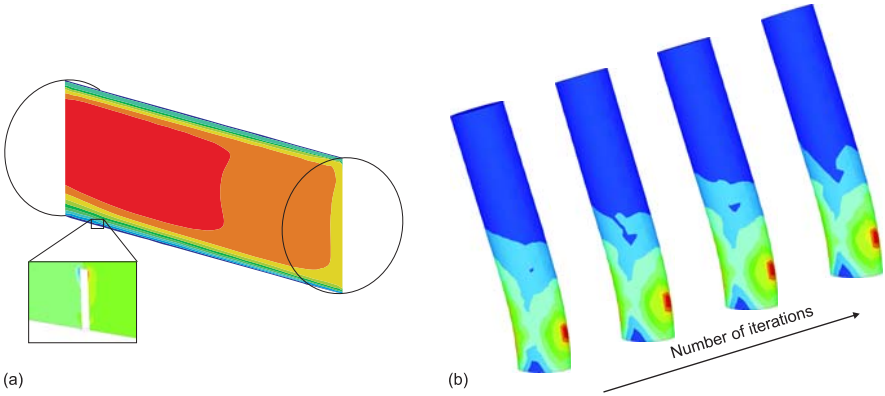

Figure 6.5: FEM simulation of cylindrical structure in tube: (a) flow field (high flow velocities in red); and (b) stresses as well as structural deformation of cylinder (compression stress in blue, tensile stress in red)

particularly for smaller structures. There are at least three causes why the results of the analytical and the FE model are not supposed to be identical. At first the overflow above the cylinder is not regarded in the analytical model which will affect the flow field. Secondly, the deformed cylinder obtains a different shape and thereby different flow resistance (change in c_D and A_{proj}). The analytical model, however, assumes the structure to be rigid. This effect is dependent on the value of the elastic modulus E: the higher E the less the structure is deformed. Moreover, the deformation is bigger for longer cylinders and thereby larger heights H_{cyl}. Thirdly, the stress distribution will change due to a change in structure.

6.3.2 Fluid-structure interactions in real biofilm structures

Reconstruction of biofilm structure from CLSM measurements

For the reconstruction of the biofilm volume the method developed by Böl and Reese [18, 19] for the reconstruction of sceletal muscles from Magnetic Resonance Imaging (MRI) measurements is used. **Figure 6.6** shows single pictures from a CLSM stack (a), the reconstructed biofilm volume (b) and its discretization with

Table 6.2: Comparison of the solutions for maximum stress and deformation ε in a cylindrical biofilm structure from analytical and numerical (FE) model

$H_{cyl}[\mu m]$	$\sigma_{max,an}[Pa]$	$\sigma_{max,FEM}[Pa]$	deviation [%]
25	3,91	3,87	1.0
50	30,02	27,75	8.2
100	287,38	223,91	28.3
$H_{cyl}[\mu m]$	$\varepsilon_{max,an}[m]$	$\varepsilon_{max,FEM}[m]$	deviation [%]
25	$4,44^{-10}$	$4,27^{-10}$	4.0
50	$1,78^{-8}$	$2,19^{-8}$	-18.7
100	$7,13^{-7}$	$2,63^{-7}$	171.1

finite elements (c). In this example CLSM data are used originating from the experiment presented in chapter 5 (see figure 5.2), sampled at $t = 38d$. Regarding the volume reconstruction (b) a rough surface structure with exposed structures rising upwards is visible. This structure is discretized by finite elements (c). The interaction of fluid flow and structure is computed in the same way as presented for the cylinder described above. The reconstructed biofilm structure is situated on the inner wall of a tube (10mm diameter to be comparable with FTBTR) and flow is computed for $Re_T = 1500$.

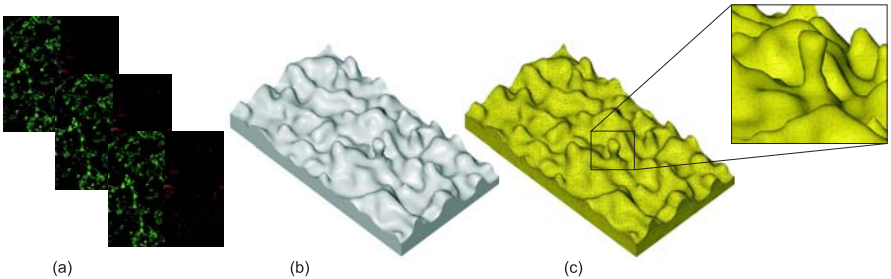

Figure 6.6: Reconstruction of CLSM stacks (a) into volume (b) and FE discretization (c)

Figure 6.7 shows the distribution of fluid pressure on the surface of the structure as a whole (a) and for slices along the biofilm (b). Highest pressures (red) are found at

exposed structures as visible in slices (b, III) and (b, IV) due to the ram pressure created by fluid flow against the structure. Flat areas, however, show lower pressures (blue and green).

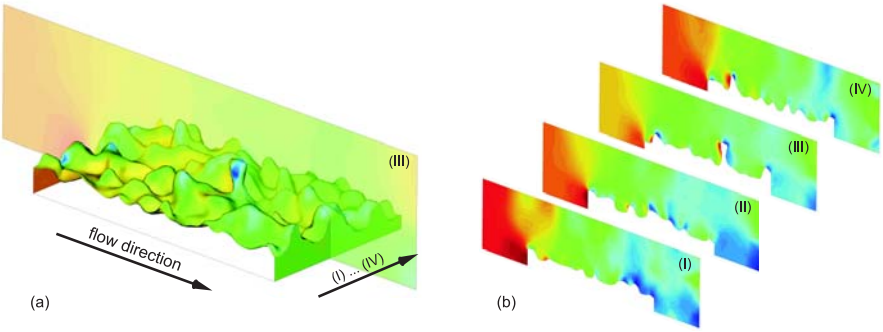

Figure 6.7: Fluid pressure distribution past real biofilm structure (high pressures in red, low in blue)

Stresses and strains in biofilm structure

The pressure distribution on the biofilm surface is now used to compute stresses and strains in the structure. Material behavior is linear elastic assuming an elastic modulus $E = 100Pa$. The converged solution is visualized in **figure 6.8**. As can be seen, highest stresses (red) occur at the bottom of exposed structures. They also reveal a high deformation which may become obvious in (b) compared with the undeformed structure in (c). This observation complies well with the results of the analytical model in section 6.2. Hence, exposed structures in biofilms yield high stresses when subjected to fluid flow and are thus likely to detach.

6.3.3 Stress induced detachment of biofilm structures

The FE model is now extended in order to simulate biofilm detachment. It is assumed that parts of the biofilm are disrupted when the local stress of a matrix element exceeds the strength σ_{crit} of the matrix. Several simulations are performed in

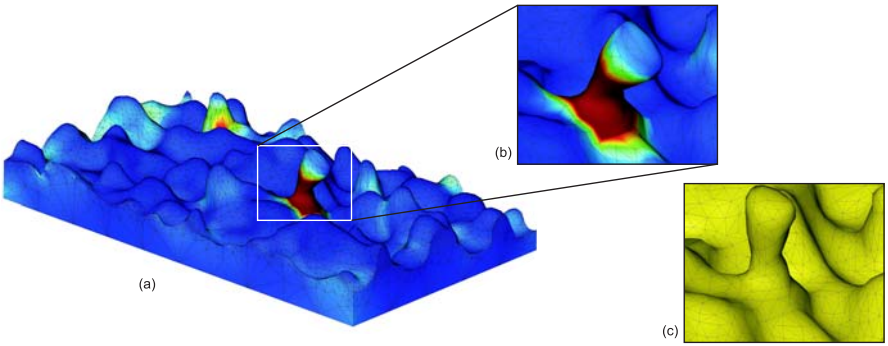

Figure 6.8: Deformation and highest stresses in real biofilm structure

order to investigate influences of structural and mechanical biofilm properties in the simulation outcome.

Influence of matrix strength on detachment

As already stated in section 6.2 the matrix strength σ_{crit} is a measure for biofilm stability and will centrally influence biofilm detachment. The structure already presented above is now used for the computation of detachment. Simulated structures after subjected to fluid flow for different values of σ_{crit} are shown in **figure 6.9**. For high values of σ_{crit}, i.e. a high matrix stability, only very exposed structures at the surface of the biofilm are detached. Low matrix stabilities - smaller values of σ_{crit} - on the other hand lead to the detachment of large portions from the top of the biofilm. Interestingly, a smooth surface structure remains after detachment. This observation is in compliance with the results presented in Möhle et al. [151] where smooth base biofilms remain after subjected to high shear stresses using the FDG technique. Nonetheless, the high sensitivity of the model to a variation of σ_{crit} is obvious which emphasizes the need for well measured mechanical parameters.

Influence of biofilm structure on detachment

Three different CLSM stacks of samples taken at $t = 10d$, $t = 24d$ and $t = 38d$ during the cultivation are now used for the reconstruction of the biofilm volume

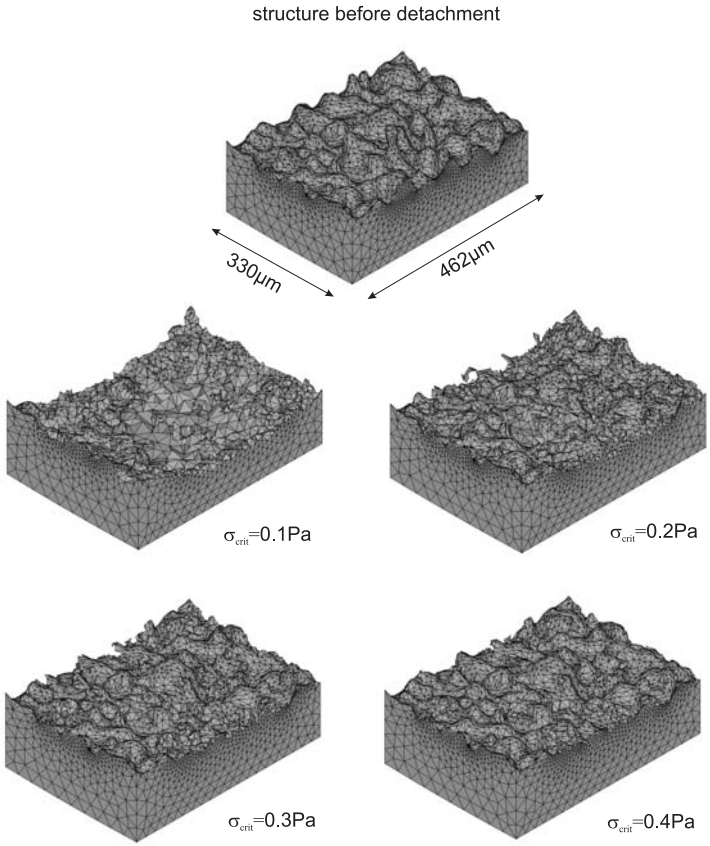

Figure 6.9: Biofilm structure before and after detachment at different strengths σ_{crit}

in order to investigate the effect of biofilm structure on detachment. The samples show heterogeneous structures and an increasing roughness by time.In **figure 6.10** detached biomass for the three samples at different σ_{crit} is presented. Regarding the values -especially for lower σ_{crit}- an increasing tendency over time can clearly be seen which complies well with the experimental observations presented in section 5.4. This increase is probably caused by the structural change occurring with progressing cultivation time. More exposed structures develop by time which in turn

are more sensitive to detachment forces. In that way, detachment could be deduced to the change of structure during biofilm development. Latter is, however, a result of the interaction of numerous processes.

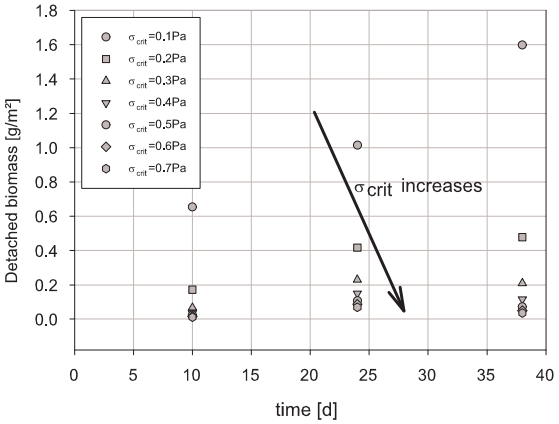

Figure 6.10: Detached biomass for different biofilm structures and matrix strengths σ_{crit}

6.4 Mechanics as explanation for biofilm detachment?

The results of this section indicate that detachment may be explicable by physical, i.e. mechanical, mechanisms. These theoretical considerations can give an imagination of how detachment may occur throughout biofilm development. This procedure is outlined in **figure 6.11** and is comparable to the results of a modeling study by Xavier et al. [256]. At the beginning of biofilm development (t_1) microcolonies are adhered to the substratum. Due to growth processes the structures can evolve in positive z-direction because substrates may be better available (t_2-t_4). At the same

time a smooth and thin base biofilm layer can develop by confluent growth on the substratum. For these considerations the occurence of a base biofilm is not necessarily needed but it is not contradictory to the hypothesis developed and found experimentally. If the structure reaches a shape so that internal stresses exceed its strength, it will detach (t_5). If this happens on several spots of the biofilm more or less subsequently, an average continuous detachment rate may result. When the detached structures are smaller than the exclusion size of a sieve analysis (e.g. $25\mu m$ as in section 5.4) this detached biomass is attributed to the eroded biomass whereas the mechanisms leading to its detachment could be described as sloughing. So, the distinction between erosion and sloughing is not only arbitrary but also seems less helpful for the explanation of detachment. Furthermore, the experimental differentiation is challenging. The development of specific biofilm structures is strongly dependent on the environmental conditions. For high substrate supplies smooth biofilm surfaces are expected which will show a higher resistance against detachment considering the results made above. Biofilm structures, however, emerge from interactions of processes like substrate supply, mass transfer and shear conditions. These processes cannot be separated. Thus, for an understanding of this interaction mathematical models are a great aid.

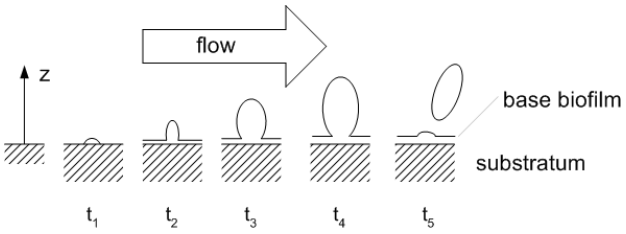

Figure 6.11: Image of "bubbling" biofilm detachment

A better understanding of biofilm development is approached by enlightening the interaction of fluid flow and biofilm structure. The distribution of stresses in the biofilm structure will determine detachment. Computation of the stress field in biofilms with well validated models needs a knowledge about mechanical properties of the biofilm and reliable values of the determining parameters. This, however, brings

the focus again on an aspect that may only be marginally considered in this chapter: the biology of the biofilm forming microorganisms. Mechanical properties of the biofilm matrix are determined by the EPS. Type and amount of produced EPS, in turn, depend on the specific species and their regulatory pathways. Assuming a heterogeneous distribution of species, a heterogeneous distribution of mechanical properties may as well be expected in biofilms. This will influence detachment behavior strongly. Regarding again figure 6.4, it is evident that a change of biofilm strength is effecting the occurrence of detachment events. In this regard, environmental conditions may serve as evolutionary pressure. Biofilm structures with stronger and stickier EPS have more stability, and this provides an evolutionary advantage in systems with high flow rates.

Nonetheless, at this point in time it is impossible to predict how single cells of specific species in a mixed culture biofilm will react to a change of environmental conditions, how it can compete with its concurrents and how this will effect the emergent properties of a whole biofilm. An insight into this topic might be given by systems biology with a focus on single cells. This approach, however, for natural biofilms with a plethora of different species and complex ecological interactions is a more than challenging task.

7 Concluding remarks

Biofilms are not stand-alone units. They develop in close interaction with their environment and simultaneously form this environment. Numerous processes determine this development. To capture the *complexity* thereby arising, mathematical modeling proves to be of big help. However, pure modeling might result in losing track of reality as well as pure experimental approaches yield few advances in terms of a better process understanding. Thus, an iterative method combining mathematical modeling and experimental validation is proposed, tested and proved to result in advances concerning a better understanding of biofilm processes and interactions with its environment.

This study shows that several aspects are of central importance for biofilm development. Experimental evidence is presented for the utmost significance of *biofilm detachment* phenomena. Though intensive research in the last years biofilm detachment phenomena are still not well understood and the question of how to mathematically describe detachment is not yet solved. Common modeling approaches for detachment seem too simplistic and reveal the need for more structured models regarding the complexity of fluid-structure interactions. *Structural heterogeneity* is the result as well as the cause for several phenomena which emphasizes its relevance and the demand for its experimental investigation. CLSM is a promising tool to investigate biofilm structure and the spatial distribution of biofilm constituents. However, as one result of this work the need for improvements of the CLSM methodology emerges. Structural properties on the *mesoscale* can be of importance but are usually neglected due to the analytical techniques applied.

Using the current knowledge biofilm development can well be described on the scale of the reactor with 1D modeling approaches. This, however, is only easily possible if erosion is the predominant detachment process. Sloughing is a stochastic event that is hard if not impossible to predict.

Concluding this work, more open questions seem to have emerged than been solved. Nevertheless, the method proposed proved to be helpful concerning a structured proceeding in research on complex natural systems. Mathematical Modeling is not

intended to be capable of 1:1 mirroring of the real world but of big help in process understanding. By means of the topic of biofilm detachment it is revealed that the recent empirical approaches are not sufficient to describe and understand the relevant processes. Therefore, a more detailed investigation is needed and a systematic approach like the one suggested is pursued. When the interactions will be better understood in the future, simplifications can be developed and also integrated in 1D-approaches with the aim of having simple and reliable models. The latter may also be used for an aimed reactor design in wastewater treatment. As next step, it may also be helpful not to search for a universal biofilm model but to develop models for specific conditions. Moreover, the increase of computational power makes simulations possible regarding fluid-structure interaction. Nevertheless, it becomes obvious that biology cannot be any more disregarded in the explanation of biofilm development. Microorganisms spent more than 3 billions years of evolution in biofilms. Hence, it cannot be expected that biofilms in all their diverse environments will be completely understood after 30 years of biofilm research.

A Numerical solutions of biofilm growth models

A.1 One dimensional biofilm model

For the numerical solution (simulation) of the 1D model presented in chapter 5 the software AQUASIM [189] is applied using the biofilm reactor compartment whose equations are described in Wanner and Reichert [237]. There, mass balances of solutes (equation (3.16)) and solids (equation (3.17)) are implemented in the program. Biofilm growth velocity u_F (equation (3.19)) is determined by the user-defined processes and is computed numerically. In this study the processes of growth and decay are used as presented in the stoichiometric matrix, table 5.1. Biofilm detachment is recognized as being dependent on u_F according to equation (3.13). The particular biofilm structure of hemispherical colonies in this model is recognized using a function for the biofilm area A_F which is dependent on the space coordinate z perpendicular to the substratum (equation (5.1)). EPS production is modeled using a growth coupled approach as in equation (3.10) with $\beta = 0$. The decay process follows equation (3.9). Thickness of concentration boundary layer is set to zero. All further parameters and initial conditions are listed in table 5.2.

A.2 Multidimensional biofilm model

The numerical simulations with the particle-based model shown in section 5.6 are performed with the framework developed by Xavier et al. [255]. The software is written by João Xavier in JAVA object oriented source code and is compiled using eclipse SDK version 3.1.0 (*http://www.eclipse.org/platform*). A minimized JAVA applet of the software can be tested under *http://www.biofilms.bt.tudelft.nl/frameworkMaterial/monospecies2d.html (03/17/08).* The same processes and parameters come to application as in the 1D model described above. Due to the discrete nature of the model initial biofilm thickness cannot directly be taken over from the 1D model. Initial biofilm volume in the particle-based model can be computed from

initial biofilm thickness in AQUASIM.

$$V_{F,ini} = L_{F,ini} \cdot A_F \tag{A.1}$$

The biofilm volume is determined by the number $n_{particles}$ and volume $V_{particle}$ of the particles.

$$V_F = n_{particles} \cdot V_{particle} = n_{particles} \cdot \frac{\pi}{48} r_{particle}^3 \tag{A.2}$$

The initial number of particles $n_{particles,ini}$ and initial radius of particles $r_{particle,ini}$ must be provided in the model. For the simulations shown in section 5.6 $n_{particles,ini} = 7$ is chosen in order to obtain a small number of colonies yielding a colony-like growth.

B Experimental methods

B.1 Confocal Laser Scanning Microscopy

Confocal Laser Scanning Microscopy CLSM is recently the state-of-the-art tool for the investigation of biofilms. Biofilms can be examined in fully hydrated, living stage and three dimensional structure of the biofilm can be obtained, visualized and also analyzed by Digital Image Analysis Tools.
All microscopic investigations shown in this study are performed by Marian Haesner at the Helmholtz Centre for Environmental Research (UFZ) in Magdeburg, Germany in the working group of Dr. Thomas Neu. A specific staining method as presented in Staudt et al. 2004 is applied. Lectins from *Aleuria aurantia* (Molecular Probes, Eugene, Oregon) are used for staining of EPS glycoconjugates. For the cells SYTO 60 nucleic acid stain (Molecular Probes) is applied. The samples are investigated with a TCS SP-1 (Leica, Germany) confocal laser scanning microscope. EPS and cell volumes are computed as average from three image stacks recorded with a 20x 0.5 NA objective lens using JImageAnalyze software. For image visualization the software Imaris 4.2 (Bitplane, Switzerland) is used. An extensive elaboration on the CLSM methodology is presented in Haesner 2008.

B.2 Laser diffraction spectroscopy

The analysis of particle size distribution of sewage sludge samples presented in section 4.6 is performed with a MasterSizer 2000 (Malvern Systems). Measurement principle is the diffraction of laser light at small particles. Diffraction patterns are analyzed by the software associated to the device (version 5.40) using the Fraunhofer model.

B.3 Nanoindentation

Force-Indentation curves as presented in section 6.1.2 are recorded with a TriboIndenter (Hysitron) using a "Berkovich" tip. E-Modulus is determined by curve fitting applying the model developed by Oliver and Pharr 1992 [165].

C The Rotating Disc Reactor (RDR)

A further biofilm reactor system is developed in order to provide biofilms on planar substrata grown under defined hydrodynamic conditions (cp. sec 6.1.1). The Rotating Disc Reactor (RDR) uses rotating discs in a quasi-stagnant solution. Thus, a gradient of flow velocity and wall shear stress develops along the radial coordinate which allows a simultaneous cultivation of biofilms under different but defined hydrodynamic conditions. Rotating disc systems have found their applications in different fields [62, 194, 72]. In biofilm research rotating disc assays come to application with a focus on action of antibiotics on biofilms [88, 61]. In this study, however, the focus lies on the question of how environmental conditions, like flow, influence biofilm development. Moreover, this reactor is applied for measurements of shear strength of biofilms which is presented in detail elsewhere [151].

C.1 Flow field above rotating discs

For the case of rotating discs in a stagnant fluid an analytical solution of Navier-Stokes-equations is available [36, 202]. So, the velocity field above the discs can be computed. Here, especially the theoretical wall shear stress τ_W is of interest assuming that it might serve as a measure for the mechanical exposure on the biofilm [8]. An approximate solution for τ_W on the disc surface depending linearly on radial coordinate r is found [36, 202] and shown in equation (C.1).

$$|\tau_W| = 0.8\rho\sqrt{\nu}\omega^{\frac{3}{2}}r \tag{C.1}$$

Here, τ_W is dependent on angular velocity ω and fluid properties density ρ and viscosity ν. Further studies also focusing on external mass transfer in rotating disc systems are found in literature [62, 194].

C.2 Characterization and test of RDR system

Reactor design and operation is described in Möhle et al. 2007. Residence time distribution and mixing behavior (data not shown) revealed a behavior similar to a continuously stirred tank reactor with a retardation of mixing time [126]. Several cultivations under heterotrophic conditions were conducted and are presented elsewhere [151]. In the following, an experiment with chemoautotrophic biofilms with NH_4^+ as energy source is presented. The development of biofilm thickness is given in **figure C.1**. Gravimetrically determined biofilm thickness is revealing the typical behavior of biofilm growth curves without reaching steady state. The small deviation between the thickness values of the two discs might derive from nutrient gradients (oxygen, glucose) perpendicular in the reactor but are neglected. Outlet samples are tested for the concentrations of NH_4^+, NO_2^- and NO_3^{2-}. Their temporal development shows the expected behaviour of a nitrifying biofilm cultivation with a maximum of Nitrite concentration around $t = 70d$ (data not shown).

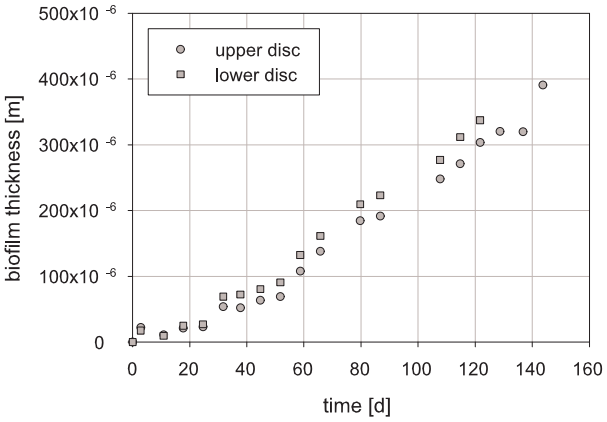

Figure C.1: Development of biofilm thickness in Rotating Disc Reactor

It is commonly accepted that biofilm thickness depends on flow conditions in a way that higher flow rates effect thinner biofilms and vice versa [250]. Having in mind the distribution of flow velocity along the radial coordinate in the RDR (cp. section C.1) thinner biofilms

at the outer edges and thicker biofilms toward the middle of the disc are expected. At two points of time (t = 121d and 147d) samples were taken from the reactor and investigated by CLSM (see App. B.1). Biofilm thickness is determined as height of CLSM stacks at different positions on the disc and presented in **figure C.2**. No dependency of biofilm thickness on radial coordinate r can be identified - L_F even seems to be constant. Chemoautotrophic bacteria grow comparatively slow and form dense as well as compact and stable biofilms. So, the fluid shear acting on the biofilm might not play such a big role in the development of biofilm structure. This observation could also be explained by one of the drawbacks of the CLSM-method [76]: the limited penetration depth of the laser or the stains, respectively.

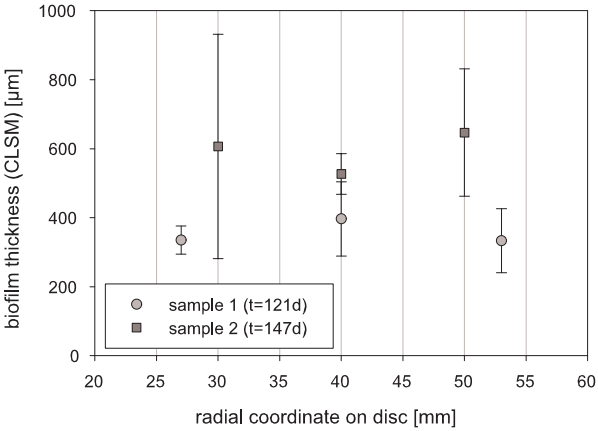

Figure C.2: Biofilm thickness from CLSM in dependence on radial position of disc in RDR

Another explanation approach, however, becomes evident when regarding an image of the biofilm as shown in **figure C.3**. A ripple mark-like surface of the biofilm is clearly visible whose structure is of larger spatial dimensions[1] than the microscopic view field of $0.5mm \times 0.5mm$. This spatial scale is subsequently termed as mesoscale (cp. section 2.1.2). Hence, it is plausible that thickness as determined by CLSM strongly depends on the position - CLSM stacks recorded on "valleys" deliver lower thicknesses than on "hills" of the ripples. This explanation is confirmed by the large standard deviation of the values.

[1]The distance from the edge left in the picture to the outer edge of the disc is 40mm.

This gives a first indication that mesoscale structure should not be neglected in biofilm cultivations (see also section 5.2.1). An adequate experimental method to tackle this challenge is presented by Milferstedt et al. 2006 which uses a commercial flatbed scanner to visualize biofilm structure [153, 154] and which is perfectly applicable to the RDR system. A better resolution and 3D information is, however, provided by mosaic scans with CLSM. In that connection not the maximum height of CLSM stacks should be used but Digital Image Analysis (DIA) tools could be useful [76] in order to gain mean values for biofilm thickness and their deviation (e.g. surface roughness R_a).

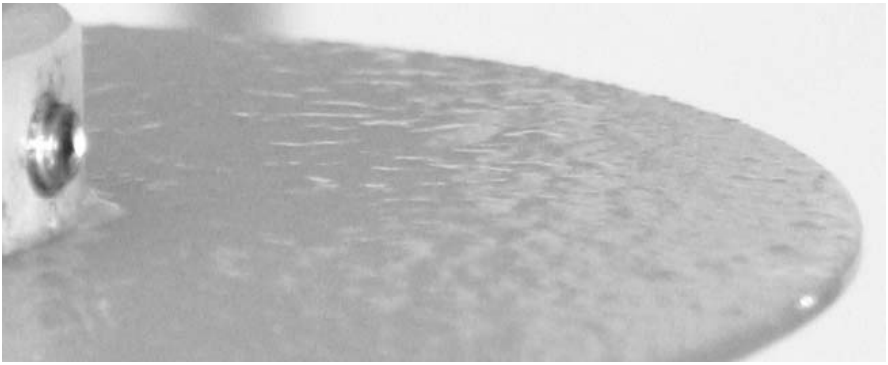

Figure C.3: Detail of disc in RDR with chemoautotrophic biofilm; photograph taken at $t = 122d$

D Analytical model of fluid-structure interactions in biofilm systems

Below, the analytical model discussed in section 6.2 is developed. Precisely, it is derived in four steps: (1) characterisation of the macroscopic flow field , (2) description of fluid-structure interaction, i.e. which forces act externally on the biofilm structure due to fluid flow, (3) derivation of internal stress distribution in the structure caused by external fluid-induced stresses and (4) estimation of structural deformation. Figure 6.3 shall visualise this approach.

(1) Macroscopic flow field

To be found in section 4.1.

(2) Fluid-structure interaction

The fluid-induced stresses can be separated according to two different modes of action: (a) shear at the top of the structure and (b) drag stress that is caused by the fluid approaching the structure perpendicularly and flowing around it. Equation (4.9) for the computation of shear stress (a) is introduced in section 4.1. The drag force F_D (b) acting on a cylinder with a diameter D_{cyl} can be calculated using equation (D.1) when subjected to a perpendicular flow with the free-stream velocity u_D of a fluid with the density ρ [242]. A_{proj} is the projection area of the cylinder ($A_{proj,cyl} = H_{cyl} \cdot D_{cyl}$).

$$F_D = \frac{1}{2} c_D \rho u_D^2 A_{proj} \tag{D.1}$$

For the drag coefficient c_D several empirical relationships depending on the drag Reynolds number (equation (D.2)) can be found.

$$Re_D = \frac{u_D D_{cyl}}{\nu} \tag{D.2}$$

Equation (D.3) [242] is in excellent accordance for our Re_D-region.

$$c_D = 1 + \frac{10}{Re_D^{\frac{2}{3}}} \tag{D.3}$$

Combining equations (D.1) - (D.3) yields equation (D.4) showing F_D depending on the free-stream velocity u_D.

$$F_D(u_D) = \frac{1}{2}\rho H_{cyl} D_{cyl} u_D^2 + 5\rho H_{cyl} D_{cyl}^{\frac{1}{3}} \nu^{\frac{2}{3}} u_D^{\frac{4}{3}} \tag{D.4}$$

For tubular flows the macroscopic flow field can well be described under laminar conditions implying a dependency of u_D on the radial coordinate r (equation (4.4)). Turbulent flows are not regarded in this case study. The radial coordinate r is substituted by $r = R_T - z$ which gives equation (D.5) depending on z.

$$u_D(z) = \frac{4Q}{\pi R^3} z - \frac{2Q}{\pi R^4} z^2 \tag{D.5}$$

This formula could now be inserted in (D.4) in order to gain a relationship specifying the load on the cylindrical structure in dependence on z. However, this would lead amongst others to a term of the shape $(\frac{4Q}{\pi R^3} z - \frac{2Q}{\pi R^4} z^2)^{\frac{4}{3}}$. The solution of this term is a progression with an infinite number of terms. On this account a linear approximation is introduced revealing good accordance in the region near the substratum surface. The equation for the flow velocity then is only dependent on z and has a structure like in equation (D.6).

$$u_D(z) = f_{flow} \cdot z \tag{D.6}$$

The proportionality factor f_{flow} is dependent on the volume flux in the tube Q (on Re, respectively) and is derived from the slope of the parabolic function at $z = \frac{H_{cyl}}{2}$ which yields good results. The slope is given by the first derivative of equation (D.5) in (D.7).

$$f_{flow}(Q) = (u_D(z))' = \frac{4Q}{\pi R^3}\left(1 - \frac{H_{cyl}}{2R}\right) \tag{D.7}$$

Applying equation (D.6) under knowledge of (D.7) results in equation (D.8) which shows the drag force depending on the coordinate z perpendicular to the substratum.

$$F_D(z) = \frac{1}{2}\rho H_{cyl} D_{cyl} f_{flow}^2 z^2 + 5\rho H_{cyl} D_{cyl}^{\frac{1}{3}} \nu^{\frac{2}{3}} f_{flow}^{\frac{4}{3}} z^{\frac{4}{3}} \tag{D.8}$$

Substituting $A = \frac{1}{2}\rho H_{cyl} D_{cyl} f_{flow}^2$ and $B = 5\rho H_{cyl} D_{cyl}^{\frac{1}{3}} \nu^{\frac{2}{3}} f_{flow}^{\frac{4}{3}}$ yields the simplified equation (D.9) which describes the external fluid-induced stress perpendicular to a cylindrical structure and is further used in the following steps.

$$F_D(z) = Az^2 + Bz^{\frac{4}{3}} \tag{D.9}$$

(3) Internal stress distribution

The cylinder already introduced in the last section is now regarded as a cantilever (see Figure 6.3) - a beam fixed on one side. The drag forces cause a load which is given by $p(z) = \frac{d(F_D)}{dz}$ resulting in equation (D.10).

$$p(z) = 2Az + \frac{4}{3}Bz^{\frac{1}{3}} \tag{D.10}$$

The internal stress distribution is subsequently computed according to the method as it is found in any teaching book about technical mechanics (elastostatics/deflection of beams as for example in Craig 1996). Aim of this investigation is to determine the highest stresses which in beam-like structures are found as normal stresses in axial direction σ (D.11) depending on the momentum M around the bearing point of the cantilever.

$$\sigma(x) = \frac{M}{I}x \tag{D.11}$$

The coordinate x perpendicular to the beam is zero in the central fiber of the cylinder. So, the highest internal stress can be found in the outer fiber of the beam. The moment of inertia I of a circular cross sectional area is presented in (equation D.12) [42].

$$I = \frac{\pi}{64}D_{cyl}^4 \tag{D.12}$$

The momentum M is determined using the differential equations for the deflection of linearly elastic beams (equation D.13) with the flexural rigidity EI consisting of the elastic modulus E and the areal moment of inertia I and deformation ε.

$$\begin{aligned}(EI\varepsilon'')'' &= p \\ EI\varepsilon'' &= M\end{aligned} \tag{D.13}$$

After two integration steps of equation (D.10) the distribution of momentum in the cantilever (equation (D.14)) is derived.

$$-M(z) = \frac{1}{3}Az^3 + \frac{3}{7}Bz^{\frac{7}{3}} + C_1z + C_2 \tag{D.14}$$

The integration constants C_1 and C_2 are calculated with the use of the boundary conditions for a cantilever with a force F_t at its tip.

$$V(z = H_{cyl}) = F_t \rightarrow C_1 = -AH_{cyl}^2 - BH_{cyl}^{\frac{4}{3}} - F_t \tag{D.15}$$

$$M(z = H_{cyl}) = 0 \rightarrow C_2 = \frac{2}{3}AH_{cyl}^3 + \frac{4}{7}BH_{cyl}^{\frac{7}{3}} + F_tH_{cyl} \tag{D.16}$$

Shear force F_t at the top of the structure is derived from shear stress (4.9) under knowledge of the surface area exposed to the shear (cross sectional area of cylinder).

$$F_t = \frac{\eta Q D_{cyl}^2}{R_T^4}(R - H) \tag{D.17}$$

The highest stress in the structure is found at the bottom of the cantilever ($z = 0$). Using (D.11) as well as (D.12) and inserting (D.14) - (D.17) gives equation (D.18) which is showing the dependencies of σ_{max}.

$$\begin{aligned}
\sigma_{max} &= \frac{M(z=0)D_{cyl}}{2I} \\
&= -\frac{512}{3\pi^3}\frac{H_{cyl}^4}{D_{cyl}^2}\rho\frac{Q^2}{R_T^6}\left(1 - \frac{H_{cyl}}{2R_T}\right)^2 \\
&\quad -\frac{640\sqrt[3]{256}}{7\pi^{\frac{7}{3}}}\frac{H_{cyl}^{\frac{10}{3}}}{D_{cyl}^{\frac{8}{3}}}\rho\nu^{\frac{2}{3}}\frac{Q^{\frac{4}{3}}}{R_T^4}\left(1 - \frac{H_{cyl}}{2R_T}\right)^{\frac{4}{3}} \\
&\quad -\frac{32}{\pi}\frac{H_{cyl}}{D_{cyl}}\rho\nu\frac{Q}{R_T^4}(R_T - H_{cyl})
\end{aligned} \tag{D.18}$$

A detailed discussion on the behavior of this function is found in section 6.2.

(4) Structural deformation

In step (3) the actual aim to derive the maximum stress in the structure is already reached. However, one criterion for the validity of the computation is that the deformation is small. This shall be tested in this step. Moreover, the structural deformation can be compared with the results of the numerical simulation in order to validate the FEM-model (see section 6.3). According to (D.13) the deflection v of the cylindrical cantilever can be derived by two further integration steps of the momentum M of the cantilever (equation (D.19)).

$$EI\varepsilon(z) = \frac{1}{60}Az^5 + \frac{27}{910}Bz^{\frac{13}{3}} + \frac{1}{6}C_1z^3 + \frac{1}{2}C_2z^2 + C_3z + C_4 \tag{D.19}$$

The integration constants C_3 and C_4 are again determined using the boundary conditions of a cantilever.

$$\varepsilon'(z = 0) = 0 \rightarrow C_3 = 0 \tag{D.20}$$

$$\varepsilon(z = 0) = 0 \rightarrow C_4 = 0 \tag{D.21}$$

The maximum deformation ε_{max} is found at the top of the cylinder at $z = H_{cyl}$.

$$\begin{aligned}\varepsilon_{max} \quad = \quad & \frac{1}{EI}\left[\frac{22}{15\pi^2}D_{cyl}H_{cyl}^6\rho\frac{Q^2}{R_T^6}\left(1-\frac{H_{cyl}}{2R_T}\right)^2\right. \\ & +\frac{29\sqrt[3]{256}}{39\pi^{\frac{4}{3}}}D_{cyl}^{\frac{1}{3}}H_{cyl}^{\frac{16}{3}}\rho\nu^{\frac{2}{3}}\frac{Q^{\frac{4}{3}}}{R_T^4}\left(1-\frac{H_{cyl}}{2R_T}\right)^{\frac{4}{3}} \\ & \left.+\ \frac{1}{3}D_{cyl}^2H_{cyl}^3\rho\nu\frac{Q}{R_T^4}(R_T-H_{cyl})\right] \end{aligned} \tag{D.22}$$

List of Symbols

Latin Symbols

A	$[m^2]$	area
B	$[\frac{g}{m^2 \cdot d}]$	loading
c	$[\frac{g}{m^3}]$	concentration
c_D	$[-]$	drag coefficient
d	$[m]$	diameter
D_i	$[\frac{m^2}{d}]$	diffusion coefficient of substance i
E	$[\frac{N}{m^2}]$	elastic modulus
F	$[N]$	force
f_D	$[-]$	ratio of diffusion coefficients in biofilm and water
f_{flow}	$[s^{-1}]$	approximation factor of laminar flow profile near walls
H	$[m]$	height
I	$[m^4]$	moment of inertia
j	$[\frac{g}{m^2 \cdot d}]$	flux
k	$[d^{-1}]$	reaction constant
L	$[m]$	length
M	$[Nm]$	momentum
m	$[g]$	mass
n	$[-]$	number
p	$[\frac{N}{m}]$	line load
Q	$[\frac{m^3}{d}]$	volumetric flow rate
r	$[\frac{g}{m^3 \cdot d}]$	rate
r	$[m]$	radial coordinate
R	$[m]$	radius
Re	$[-]$	Reynolds number
Sc	$[-]$	Schmidt number
Sh	$[-]$	Sherwood number
t	$[d]$	time
u	$[\frac{m}{d}]$	flow velocity
V	$[m^3]$	volume
x	$[m]$	coordinate parallel to the substratum

X	$[\frac{g}{m^3}]$	concentration of particulate component/biomass
Y	$[\frac{kg}{kg}]$	yield coefficient
z	$[m]$	coordinate perpendicular to the substratum

Greek Symbols

α	$[\frac{gEPS}{gX}]$	growth coupled production coefficient
β	$[\frac{gEPS}{gXd}]$	biomass coupled production coefficient
ε	$[-]$	strain
η	$[Pa \cdot s]$	dynamic viscosity
μ	$[\frac{1}{d}]$	growth rate
ν	$[\frac{m^2}{d}]$	kinematic viscosity
ρ	$[\frac{g}{m^3}]$	density
σ	$[\frac{N}{m^2}]$	normal stress
τ	$[\frac{N}{m^2}]$	shear stress
ϕ	$[-]$	fraction

Indices

A	area
D	drag
$crit$	critical
cyl	cylinder
d	dry
det	detachment
i	compound i
ini	initial
l	liquid
F	biofilm
m	maintenance
max	maximum
O_2	oxygen
$proj$	projection
S	substrate

$surf$	surface
T	tube
t	tangential
w	wet

Abbreviations

BTR	Biofilm Tube Reactor
CLSM	Confocal Laser Scanning Microscopy
COD	Chemical Oxygen Demand
CSTR	Continuous Stirred Tank Reactor
DGGE	Denaturing Gradient Gel Analysis
DIA	Digital Image Analysis
EPS	Extracellular Polymeric Substances
FDG	Fluid Dynamic Gauging
FEM	Finite Element Method
FTBTR	Flow-Through Biofilm Tube Reactor
HPLC	High Pressure Liquid Chromatography
MRI	Magnetic Resonance Imaging
RAR	Rotating Annular Reactor
RDR	Rotating Disc Reactor

Bibliography

[1] Ahn, Y., Park, E., Oh, Y., Park, S., Webster, G., and Weightman, A. Biofilm microbial community of a thermophilic trickling biofilter used for continuous biohydrogen production. *FEMS Microbiology Letters 249*, 1 (2005), 31–8.

[2] Allison, D., Evans, D., Brown, M., and Gilbert, P. Possible involvement of the division cycle in dispersal of *Escherichia coli* from biofilms. *Journal of Bacteriology 172*, 3 (1990), 1667–1669.

[3] Alpkvist, E. *Mathematical Modeling of Biofilms: Theory, Numerics and Applications*. PhD thesis, University of Malmö, 2006.

[4] Alpkvist, E., Bengtsson, J., Overgaard, N., Christensson, M., and Heyden, A. Simulation of nitrification of municipal wastewater in a Moving Bed(tm) biofilm process: a bottom-up approach based on a 2D-continuum model for growth and detachment. *Water Science and Technology 55*, 8-9 (2007), 247–255.

[5] Alpkvist, E., and Klapper, I. A multidimensional multispecies continuum model for heterogeneous biofilm development. *Bulletin of Mathematical Biology 69*, 2 (2007), 765–789.

[6] Alpkvist, E., Picioreanu, C., van Loosdrecht, M., and Heyden, A. Three-dimensional biofilm model with individual cells and continuum EPS matrix. *Biotechnology and Bioengineering 94*, 5 (2006), 961–79.

[7] ATV. *Biologische und weitergehende Abwasserreinigung*, vol. 4. Ernst und Sohn, 1997.

[8] Bakke, R. *Biofilm Detachment*. PhD thesis, Montana State University, 1986.

[9] Bakke, R., Trulear, M., Robinson, J., and Characklis, W. Activity of *Pseudomonas aeruginosa* in biofilms: Steady state. *Biotechnology and Bioengineering 26*, 12 (1984), 1418–1424.

[10] Bakken, L., and Olsen, R. Buoyant densities and dry-matter contents of microorganisms: Conversion of measured biovolume into biomass. *Applied and Environmental Microbiology 45*, 4 (1983), 1188–1195.

[11] Bakker, D., van der Plaats, A., Verkerke, G., Busscher, H., and van der Mei, H. Comparison of velocity profiles for different flow chamber designs used in studies

of microbial adhesion to surfaces. *Applied and Environmental Microbiology 69*, 10 (2003), 6280–7.

[12] Batstone, D., Picioreanu, C., and van Loosdrecht, M. Multidimensional modelling to investigate interspecies hydrogen transfer in anaerobic biofilms. *Water Research 40*, 16 (2006), 3099–3108.

[13] Baty, A., Eastburn, C., Techkarnjanaruk, S., Goodman, A., and Geesey, G. Spatial and temporal variations in chitinolytic gene expression and bacterial biomass production during chitin degradation. *Applied and Environmental Microbiology 66*, 8 (2000), 3574–85.

[14] Bester, E., Wolfaardt, G., Joubert, L., Garny, K., and Saftic, S. Planktonic-cell yield of a Pseudomonad biofilm. *Applied and Environmental microbiology 71*, 12 (2005), 7792–8.

[15] Beukes, N. Biogeochemistry: Early options in photosynthesis. *Nature 431* (2004), 522–3.

[16] Bishop, P., and Rittmann, B. Modelling heterogeneity in biofilms: Report of the discussion session. *Water Science and Technology 32*, 8 (1995), 263–265.

[17] Böl, M., Möhle, R., Haesner, M., Neu, T., Horn, H., Hempel, D., and Krull, R. Finite Element modeling of fluid-structure interaction in biofilm systems using real biofilm structures from CLSM data. *Biotechnology and Bioengineering* ((in preparation)).

[18] Böl, M., and Reese, S. Micromechanical modelling of skeletal muscles based on the finite element method. *Computer Methods in Biomechanics and Biomedical Engineering* (2007). (accepted).

[19] Böl, M., and Reese, S. A new approach for the simulation of skeletal muscles using the tool of statistical mechanics. *Materials Science and Engineering Technology* (2007). (accepted).

[20] BMBF(ed.). Systems biology, 2002.

[21] Boessmann, M., Neu, T., Horn, H., and Hempel, D. Growth, structure and oxygen penetration in particle supported autotrophic biofilms. *Water Science and Technology 49*, 11-12 (2004), 371–7.

[22] Boessmann, M., Staudt, C., Neu, T., Hempel, D., and Horn, H. Investigation and modeling of growth,structure and oxygen penetration in particle supported biofilms. *Chemical Engineering and Technology 26*, 2 (2003), 219–222.

[23] Boll, R., and Barjenbruch, M. Biofilmreaktoren. Tech. rep., Institut für Siedlungswasserwirtschaft, 1998.

[24] Bond, P., Smriga, S., and Banfield, J. Phylogeny of microorganisms populating a thick, subaerial, predominantly lithotrophic biofilm at an extreme acid mine drainage site. *Applied and Environmental Microbiology 66*, 9 (2000), 3842–3849.

[25] Branda, S., Vik, S., Friedman, L., and Kolter, R. Biofilms: the matrix revisited. *Trends in Microbiology 13*, 1 (2005), 20–6.

[26] Bryers, J. Modeling biofilm accumulation. In *Physiological models in microbiology*, M. Bazin and J. Prosser, Eds. CRC press, 1988, pp. 109–144.

[27] Bryers, J. *Biofilms II: Process analysis and applications*. Wiley-Liss, New York, 2000.

[28] Carnazza, S., Satriano, C., Guglielmino, S., and Marletta, G. Fast exopolysaccharide secretion of *Pseudomonas aeruginosa* on polar polymer surfaces. *Journal of Colloid and Interface Science 289*, 2 (2005), 386–93.

[29] Casey, E. Tracer measurements reveal experimental evidence of biofilm consolidation. *Biotechnology and Bioengineering 98*, 4 (2007), 913–918.

[30] Cerca, N., Jefferson, K., Oliveira, R., Pier, G., and Azeredo, J. Comparative antibody-mediated phagocytosis of *Staphylococcus epidermidis* cells grown in a biofilm or in the planktonic state. *Infection and Immunity 74*, 8 (2006), 4849–55.

[31] Chambless, J., and Stewart, P. A 3D computer model analysis of three hypothetical biofilm detachment mechanisms. *Biotechnology and Bioengineering 97*, 6 (2007), 1573–1584.

[32] Characklis, W., and Cooksey, K. Biofilms and microbial fouling. *Advances in Applied Microbiology 29* (1983), 93–138.

[33] Characklis, W., and Marshall, K. *Biofilms*. Wiley, 1989.

[34] Chen, S., and Huang, S. Shear stress effects on cell growth and L-Dopa production by suspension culture of *Stizolobium hassjoo* cells in an agitated bioreactor. *Bioprocess Engineering 22* (2000), 5–12.

[35] Chew, J., Höfling, V., Augustin, W., Paterson, W., and Wilson, D. A method for measuring the strength of scale deposits on heat transfer surfaces. *Developments in Chemical and Mineral Processing 13*, 1/2 (2005), 21–30.

[36] Cochran, W. The flow due to a rotating disc. *Proceedings of the Cambridge Philosophical Society 30* (1934), 365 – 375.

[37] Cohen, I., and Harel, D. Explaining a complex living system: dynamics, multi-scaling and emergence. *Journal of The Royal Society Interface 4*, 13 (2007), 175–182.

[38] Costerton, J. A short history of the development of the biofilm concept. In *Microbial biofilms*, H. Lappin-Scott and J. Costerton, Eds. Cambridge University Press, 2004.

[39] Costerton, J., Geesey, G., and Cheng, K.-J. How bacteria stick. *Scientific American 238*, 1 (1978), 86–95.

[40] Costerton, J., Lewandowski, Z., DeBeer, D., Caldwell, D., Korber, D., and James, G. Biofilms, the customized microniche. *Journal of Bacteriology 176*, 8 (1994), 2137–2142.

[41] Costerton, J., Stewart, P., and E.P., G. Bacterial biofilms: A common cause of persistent infections. *Science 284*, 5418 (1999), 1318–22.

[42] Craig, R. *Mechanics of Materials*. Wiley, 1996.

[43] Damveld, R., vanKuyk, P., Arentshorst, M., Klis, F., van den Hondel, C., and Ram, A. Expression of agsA, one of five 1,3-α-D-glucan synthase-encoding genes in *Aspergillus niger* is induced in response to cell wall stress. *Fungal Genetics and Biology 42*, 2 (2005), 165–77.

[44] Davies, D., Chakrabarty, A., and Geesey, G. Exopolysaccharide production in biofilms: substratum activation of alginate gene expression by *Pseudomonas aeruginosa*. *Applied and Environmental Microbiology 59*, 4 (1993), 1181–6.

[45] Davies, D., and Geesey, G. Regulation of the alginate biosynthesis gene algC in *Pseudomonas aeruginosa* during biofilm development in continuous culture. *Applied and Environmental Microbiology 61*, 3 (1995), 860–7.

[46] Davies, D., Parsek, M., Pearson, J., Iglewski, B., Costerton, J., and Greenberg, E. The involvement of cell-to-cell signals in the development of a bacterial biofilm. *Science 280*, 5361 (1998), 295–8.

[47] de Beer, D., and Schramm, A. Micro-environments and mass transfer phenomena in biofilms studied with microsensors. *Water Science and Technology 39*, 7 (1999), 173–178.

[48] de Beer, D., Stoodley, P., and Lewandowski, Z. Liquid flow in heterogeneous biofilms. *Biotechnology and Bioengineering 44*, 5 (1994), 636–641.

[49] de Duve, C. *Aus Staub geboren - Leben als kosmische Notwendigkeit (en.:Vital dust. Life as a cosmic imperative.)*. Spektrum, 1995.

[50] de Haan, J. How emergence arises. *Ecological Complexity 3*, 4 (2006), 293–301.

[51] de Kreuk, M., Heijnen, J., and van Loosdrecht, M. Simultaneous COD, nitrogen, and phosphate removal by aerobic granular sludge. *Biotechnology and Bioengineering 90*, 6 (2005), 761–9.

[52] Diekmann, R., Naujoks, M., Gerdes-Kühn, M., and Hempel, D. Effects of suboptimal environmental conditions on immobilized bacteria growing in continuous culture. *Bioprocess and Biosystems Engineering 5*, 1 (1990), 13–17.

[53] Dockery, J., and Klapper, I. Finger formation in biofilm layers. *SIAM Journal for applied Mathematics 62*, 3 (2001), 853–869.

[54] Dreger, M. *Produktion und Aufarbeitung des Exopolysaccharids PS-EDIV aus Sphingomonas pituitosa.* Doctorate thesis, Technische Universität Braunschweig, 2008.

[55] Dreger, M., Schultheis, E., Jansen, A., Hempel, D., and Nörtemann, B. Production of exopolysaccharide PS-EDIV by Sphingomonas pituitosa.

[56] Eberl, H. A deterministic continuum model for the formation of EPS in heterogeneous biofilm architectures. In *Biofilms 2004: Structure and Activity of Biofilms* (Las Vegas, NV, USA, 2004).

[57] Eberl, H., Morgenroth, E., Noguera, D., Picioreanu, C., Rittmann, B., van Loosdrecht, M., and Wanner, O. *Mathematical Modeling of Biofilms.* IWA Publishing, London, 2006.

[58] Eberl, H., Parker, D., and van Loosdrecht, M. A new deterministic spatio- temporal continuum model for biofilm development. *Journal of Theoretical Medicine 3* (2001), 161–175.

[59] Eberl, H., Picioreanu, C., Heijnen, J., and van Loosdrecht, M. A three-dimensional numerical study on the correlation of spatial structure, hydrodynamic conditions, and mass transfer and conversion in biofilms. *Chemical Engineering Science 55*, 24 (2000), 6209–6222.

[60] Ebrahimi, S., Picioreanu, C., Xavier, J., Kleerebezem, R., Kreutzer, M., Kapteijn, F., Moulijn, J., and van Loosdrecht, M. Biofilm growth pattern in honeycomb monolith packings: Effect of shear rate and substrate transport limitations. *Catalysis Today 105*, 3-4 (2005), 448–454.

[61] Eckert, R., Brady, K., Greenberg, E., Qi, F., Yarbrough, D., He, J., McHardy, I., Anderson, M., and Shi, W. Enhancement of antimicrobial activity against *Pseudomonas*

aeruginosa by co-administration of G10KHc and tobramycin. *Antimicrobial Agents and Chemotherapy 50*, 11 (2006), 3833–3838.

[62] Elimelech, M., Gregory, J., Jia, X., and R.A., W. *Particle Deposition and Aggregation - Measurement, Modelling and Simulation*. Elsevier, 1998.

[63] Fan, L.-S., Leyva-Ramos, R., Wisecarver, K., and Zehner, B. Diffusion of phenol through a biofilm grown on activated carbon particles in a draft-tube three-phase fluidized-bed bioreactor. *Biotechnology and Bioengineering 35*, 3 (1990), 279–286.

[64] Felippa, C., and Park, K. Staggered transient analysis procedures for coupled mechanical systems: Formulation. *Computer Methods in Applied Mechanics and Engineering 24*, 1 (1980), 61–111.

[65] Flemming, H. Sorption sites in biofilms. *Water science and technology 32*, 8 (1995), 27–34.

[66] Flemming, H. Biofouling in water systems–cases, causes and countermeasures. *Applied and Environmental Microbiology 59*, 6 (2002), 629–40.

[67] Flemming, H., Neu, T., and Wozniak, D. The EPS matrix: The "house of biofilm cells". *Journal of Bacteriology* (2007).

[68] Flemming, H., and Wingender, J. Relevance of microbial extracellular polymeric substances (EPSs) – Part I: Structural and ecological aspects. *Water Science and Technology 43*, 6 (2001), 1–8.

[69] Fux, C., Costerton, J., Stewart, P., and Stoodley, P. Survival strategies of infectious biofilms. *Trends in Microbiology 13*, 1 (2005), 34–40.

[70] Ghigo, J. Natural conjugative plasmids induce bacterial biofilm development. *Nature 412*, 6845 (2001), 442–5.

[71] Gjaltema, A., Arts, P., van Loosdrecht, M., Kuenen, J., and Heijnen, J. Heterogeneity of biofilms in rotating annular reactors: Occurrence, structure, and consequences. *Biotechnology and Bioengineering 44*, 2 (1994), 194–204.

[72] Goeres, D., Loetterle, L., Hamilton, M., Murga, R., Kirby, D., and Donlan, R. Statistical assessment of a laboratory method for growing biofilms. *Microbiology 151*, Pt 3 (2005), 757–62.

[73] Gross, R., Hauer, B., Otto, K., and Schmid, A. Microbial biofilms: New catalysts for maximizing productivity of long-term biotransformations. *Biotechnology and Bioengineering 98*, 6 (2007), 1123–1134.

[74] Guerrero, R., Piqueras, M., and Berlanga, M. Microbial mats and the search for minimal ecosystems. *International Microbiology 5*, 4 (2002), 177–88.

[75] Habash, M., and Reid, G. Microbial biofilms: Their development and significance for medical device-related infections. *Journal of clinical pharmacology 39*, 9 (1999), 887–98.

[76] Haesner, M. *Einfluss der Kultivierungsbedingungen auf die Entwicklung von Biofilmen in Rohrreaktoren*. Doctorate thesis, Technische Universität Braunschweig, (in preparation). in Hempel, D.C. (ed.): ibvt-Schriftenreihe, FIT-Verlag Paderborn.

[77] Haesner, M., Horn, H., Neu, T., and Hempel, D. Biofilm development in tube reactors - effect of increasing and decreasing substrate conditions on biofilm structure and reproducibility, (in preparation).

[78] Hage, K. *Untersuchung des Abbaus von Feststoffen durch mikrobielle Biofilme*. Diploma thesis, Technische Universität Braunschweig, 2007.

[79] Hall-Stoodley, L., and Stoodley, P. Biofilm formation and dispersal and the transmission of human pathogens. *Trends in Microbiology 13*, 1 (2005), 7–10.

[80] Hansen, S., Rainey, P., Haagensen, J., and Molin, S. Evolution of species interactions in a biofilm community. *Nature 445* (2007), 533–536.

[81] Haselrieder, W. *Utilization/Design of sludge microbial fuel cells for sewage treatment and simultaneous electricity generation*. Student research paper, Technische Universität Braunschweig, 2005.

[82] Heitz, E., Flemming, H.-C., and Sand, W. *Microbially influenced corrosion of materials : scientific and engineering aspects ; with 56 tables ; [papers from a Symposium on Microbial Degradation of Materials in Lahnstein, Germany ; in 1993]*. Springer, 1996.

[83] Hempel, D., and Krull, R. Biologische Behandlung von Abwässern mit schwerabbaubaren Inhaltsstoffen. In *Handbuch des Umweltschutzes und der Umweltschutztechnik*, H. Brauer, Ed. Springer, 1996.

[84] Henneken, L., Klüner, T., Nörtemann, B., and Hempel, D. Abbau von EDTA mit freien und immobilisierten Bakterien. *GWF Wasser Abwasser 135*, 6 (1994), 354–358.

[85] Henrichsen, J. Twitching motility. *Annual Review of Microbiology 37* (1983), 81–93.

[86] Hentzer, M., Eberl, L., Nielsen, J., and Givskov, M. Quorum sensing - a novel target for the treatment of biofilm infections. *BioDrugs : clinical immunotherapeutics, biopharmaceuticals and gene therapy 17*, 4 (2003), 241–50.

[87] Hentzer, M., Riedel, K., Rasmussen, T., Heydorn, A., Andersen, J., Parsek, M., Rice, S., Eberl, L., Molin, S., Hoiby, N., Kjelleberg, S., and Givskov, M. Inhibition of quorum sensing in *Pseudomonas aeruginosa* biofilm bacteria by a halogenated furanone compound. *Microbiology 148*, Pt 1 (2002), 87–102.

[88] Hentzer, M., Teitzel, G., Balzer, G., Heydorn, A., Molin, S., Givskov, M., and Parsek, M. Alginate overproduction affects *Pseudomonas aeruginosa* biofilm structure and function. *Journal of Bacteriology 183*, 18 (2001), 5395–401.

[89] Hermanowicz, S. A model of two-dimensional biofilm morphology. *Water Science and Technology 37*, 4-5 (1998), 219–222.

[90] Hille, A., Neu, T., Hempel, D., and Horn, H. Oxygen profiles and biomass distribution in biopellets of *Aspergillus niger*. *Biotechnology and Bioengineering 92*, 5 (2005), 614–23.

[91] Horn, H. Dynamics of nitrifying bacteria population in a biofilm controlled by an oxygen microelectrode. *Water Science and Technology 29*, 10-11 (1994), 69–76.

[92] Horn, H. *Substratumsatz und Stofftransport in Biofilmsystemen: Quantitative Messungen und Modellierung*. Doctorate thesis, University of Kassel, 1995.

[93] Horn, H. *Substrate conversion and mass transport in biofilm systems : experiment and modelling (in german: Modellierung von Stoffumsatz und Stofftransport in Biofilmsystemen)*. Habilitationsschrift, Technische Universität Braunschweig, 2004. Vol. 17 in Hempel, D.C. (ed.): ibvt-Schriftenreihe, FIT-Verlag Paderborn.

[94] Horn, H., and Hempel, D. Mass transfer coefficients for an autotrophic and a heterotrophic biofilm system. *Water Science and Technology 32*, 8 (1995), 199–204.

[95] Horn, H., and Hempel, D. Growth and decay in an auto-heterotrophic biofilm. *Water Research 31*, 9 (1997), 2243–2252.

[96] Horn, H., and Hempel, D. Substrate utilization and mass transfer in an autotrophic biofilm system: Experimental results and numerical simulation. *Biotechnology and Bioengineering 53*, 4 (1997), 363–371.

[97] Horn, H., and Hempel, D. Modeling mass transfer and substrate utilization in the boundary layer of biofilm systems. *Water Science and Technology 37*, 4-5 (1998), 139–147.

[98] Horn, H., and Morgenroth, E. Transport of oxygen, sodium chloride, and sodium nitrate in biofilms. *Chemical Engineering Science 61*, 5 (2006), 1347–1356.

[99] Horn, H., Neu, T., and Wulkow, M. Modelling the structure and function of extracellular polymeric substances in biofilms with new numerical techniques. *Water Science and Technology 43*, 6 (2001), 121–127.

[100] Horn, H., Reiff, H., and Morgenroth, E. Simulation of growth and detachment in biofilm systems under defined hydrodynamic conditions. *Biotechnology and Bioengineering 81*, 5 (2003), 607–617.

[101] Horn, H., Wäsche, S., and Hempel, D. Simulation of biofilm growth, substrate conversion and mass transfer under different hydrodynamic conditions. *Water Science and Technology 46*, 1-2 (2002), 249–252.

[102] Hu, Z., Hidalgo, G., Houston, P., Hay, A., Shuler, M., Abruna, H., Ghiorse, W., and Lion, L. Determination of spatial distributions of zinc and active biomass in microbial biofilms by two-photon laser scanning microscopy. *Applied and Environmental Microbiology 71*, 7 (2005), 4014–21.

[103] Huber, B., Eberl, L., Feucht, W., and Polster, J. Influence of polyphenols on bacterial biofilm formation and quorum-sensing. *Zeitschrift für Naturforschung 58*, 11-12 (2003), 879–84.

[104] Hunt, S., Werner, E., Huang, B., Hamilton, M., and Stewart, P. Hypothesis for the role of nutrient starvation in biofilm detachment. *Applied and Environmental Microbiology 70*, 12 (2004), 7418–25.

[105] Huws, S., McBain, A., and Gilbert, P. Protozoan grazing and its impact upon population dynamics in biofilm communities. *Journal of Applied Microbiology 98*, 1 (2005), 238–244.

[106] Jiang, H.-L., Tay, J.-H., Liu, Y., and Tay, S.-L. Ca^{++} augmentation for enhancement of aerobically grown microbial granules in sludge blanket reactors. *Biotechnology Letters 25* (2003), 95–99.

[107] Kessin, R. *Dictyostelium: Evolution, cell biology, and the development of multicellularity*. Cambridge University Press, 2001.

[108] Kim, G., Webster, G., Wimpenny, J., Kim, B., Kim, H., and Weightman, A. Bacterial community structure, compartmentalization and activity in a microbial fuel cell. *Journal of Applied Microbiology 101*, 3 (2006), 698–710.

[109] Kjelleberg, S., Steinberg, P., Givskikov, M., Gram, L., Manefield, M., and de Nys, R. Do marine natural products interfere with prokaryotic AHL regulatory systems? *Aquatic Microbial Ecology 13* (1997), 85–93.

[110] Klapper, I., Rupp, C., Cargo, R., Purvedorj, B., and Stoodley, P. Viscoelastic fluid description of bacterial biofilm material properties. *Biotechnology and Bioengineering 80*, 3 (2002), 289–96.

[111] Klausen, M., Heydorn, A., Ragas, P., Lambertsen, L., Aaes-Jorgensen, A., Molin, S., and Tolker-Nielsen, T. Biofilm formation by *Pseudomonas aeruginosa* wild type, flagella and type IV pili mutants. *Molecular Microbiology 48*, 6 (2003), 1511–24.

[112] Kleerebezem, R., and van Loosdrecht, M. Mixed culture biotechnology for bioenergy production. *Current Opinions in Biotechnology 18*, 3 (2007), 207–12.

[113] König, J. Reinigung von fauligem Abwasser aller Art durch Zuführung von Luft beim Herabrieseln an einem Drahtnetz. *Gesundheitsingenieur 4* (1883), 121–123.

[114] Koch, B., Ostermann, M., Hoke, H., and Hempel, D. Sand and activated carbon as biofilm carriers for microbial degradation of phenols and nitrogen-containing aromatic compounds. *Water Research 25*, 1 (1991), 1–8.

[115] Kolter, R. Surfacing views of biofilm biology. *Trends in Microbiology 13*, 1 (2005), 1–2.

[116] Kommedal, R., Bakke, R., Dockery, J., and Stoodley, P. Modelling production of extracellular polymeric substances in a *Pseudomonas aeruginosa* chemostat culture. *Water Science and Technology 43*, 6 (2001), 129–34.

[117] Kowalewski, M. *Untersuchung von Abtragsereignissen in mikrobiellen Biofilmen unter kontrollierten hydrodynamischen Bedingungen.* Master thesis, Hochschule Magdeburg-Stendal, 2006.

[118] Kreft, J., Picioreanu, C., Wimpenny, J., and van Loosdrecht, M. Individual-based modelling of biofilms. *Microbiology 147*, Pt 11 (2001), 2897–912.

[119] Körstgens, V. *Die mechanische Stabilität bakterieller Biofilme: Ein Untersuchung verschiedener Einflüsse auf Biofilme von Pseudomonas aeruginosa.* Doctorate thesis, Universität Duisburg - Essen, 2003.

[120] Körstgens, V., Flemming, H., Wingender, J., and Borchard, W. Influence of calcium ions on the mechanical properties of a model biofilm of mucoid *Pseudomonas aeruginosa*. *Water Science and Technolgy 43*, 6 (2001), 49–57.

[121] Krull, R., and Hempel, D. Biodegradation of naphthalenesulphonic acid-containing sewages in a two-stage treatment plant. *Bioprocess Engineering 10* (1994), 229–234.

[122] Krumbein, W., Paterson, D., and Zavarzin, G. *Fossil and recent biofilms - A natural history of life on earth*. Kluwer, Dordrecht, 2003.

[123] Kupriyanova, E., Villarejo, A., Markelova, A., Gerasimenko, L., Zavarzin, G., Samuelsson, G., Los, D., and Pronina, N. Extracellular carbonic anhydrases of the stromatolite-forming cyanobacterium *Microcoleus chthonoplastes*. *Microbiology 153*, 4 (2007), 1149–1156.

[124] La Motta, E. External mass transfer in a biological film reactor. *Biotechnology and Bioengineering 18*, 10 (1976), 1359–1370.

[125] Landa, A., van der Mei, H., and Busscher, H. Detachment of linking film bacteria from enamel surfaces by oral rinses and penetration of sodium lauryl sulphate through an artificial oral biofilm. *Advances in Dental Research 11*, 4 (1997), 528–538.

[126] Langemann, T. *Untersuchung des Zusammenhangs von Biofilmstruktur und -festigkeit mit Hilfe des Fluid Dynamic Gauging*. Student research paper, Technische Universität Braunschweig, 2006.

[127] Laspidou, C., and Aravas, N. Variation in the mechanical properties of a porous multi-phase biofilm under compression due to void closure. *Water Science and Technology 55*, 8-9 (2007), 447–453.

[128] Laspidou, C., and Rittmann, B. Modeling the development of biofilm density including active bacteria, inert biomass, and extracellular polymeric substances. *Water Research 38*, 14-15 (2004), 3349–3361.

[129] Lawrence, J., and Neu, T. Microscale analyses of the formation and nature of microbial biofilm communities in river systems. *Reviews in Environmental Science and Biotechnology 2*, 2 (2003), 85–97.

[130] Lawrence, J., Scharf, B., Packroff, G., and Neu, T. Microscale evaluation of the effects of grazing by invertebrates with contrasting feeding modes on river biofilm architecture and composition. *Microbial Ecology 44*, 3 (2002), 199–207.

[131] Leff, L., McArthur, V., and Shimkets, L. Information spiraling: movement of bacteria and their genes in streams. *Microbial ecology 24* (1992), 11–24.

[132] Leid, J., Willson, C., Shirtliff, M., Hassett, D., Parsek, M., and Jeffers, A. The exopolysaccharide alginate protects *Pseudomonas aeruginosa* biofilm bacteria from

IFN-γ mediated macrophage killing. *The Journal of Immunology 175*, 11 (2005), 7512–8.

[133] León Ohl, A. *Wechselwirkungen von Stofftransport und Wachstum in Biofilmsystemen*. Doctorate thesis, Technische Universität Braunschweig, 2007. Vol. 28 in Hempel, D.C. (ed.): ibvt-Schriftenreihe, FIT-Verlag Paderborn.

[134] León Ohl, A., Horn, H., and Hempel, D. Behaviour of biofilm systems under varying hydrodynamic conditions. *Water Science and Technology 49*, 11-12 (2004), 345–351.

[135] Lewandowski, Z., and Stoodley, P. Flow induced vibrations, drag force, and pressure drop in conduits covered with biofilm. *Water Science and Technology 32*, 8 (1995), 19–26.

[136] Liu, H., Ramnarayanan, R., and Logan, B. Production of electricity during wastewater treatment using a single chamber microbial fuel cell. *Environmental Science and Technology 38*, 7 (2004), 2281–2285.

[137] Liu, Y., and Tay, J.-H. Metabolic response of biofilm to shear stress in fixed-film culture. *Journal of Applied Microbiology 90* (2001), 337–342.

[138] Liu, Y., and Tay, J.-H. Review: The essential role of hydrodynamic shear force in the formation of biofilm and granular sludge. *Water Research 36* (2002), 1653–1665.

[139] Liu, Z., Du, Z., Lian, J., Zhu, X., Li, S., and Li, H. Improving energy accumulation of microbial fuel cells by metabolism regulation using *Rhodoferax ferrireducens* as biocatalyst. *Letters in Applied Microbiology 44*, 4 (2007), 393–8.

[140] Lovley, D., Holmes, D., Nevin, K., and Poole. Dissimilatory Fe(III) and Mn(IV) Reduction. In *Advances in Microbial Physiology*, vol. 49. Academic Press, 2004, pp. 219–286.

[141] Madigan, M., Martinko, J., and Brock, T. *Brock - Biology of microorganisms*. Pearson, Prentice Hall, 2006.

[142] Manefield, M., Harris, L., Rice, S., de Nys, R., and Kjelleberg, S. Inhibition of luminescence and virulence in the black tiger prawn (*Penaeus monodon*) pathogen *Vibrio harveyi* by intercellular signal antagonists. *Applied and Environmental Microbiology 66*, 5 (2000), 2079–84.

[143] Marshall, K., Stout, R., and Mitchell, R. Mechanis of the initial events in the sorption of marine bacteria to surfaces. *Journal of General Microbiology 68* (1971), 337–348.

[144] Marshall, K., Stout, R., and Mitchell, R. Selective sorption of bacteria from seawater. *Canadian Journal of Microbiology 17*, 11 (1971), 1413–6.

[145] Martins, A., Heijnen, J., and van Loosdrecht, M. Bulking sludge in biological nutrient removal systems. *Biotechnology and Bioengineering 86*, 2 (2004), 125–35.

[146] Matsumoto, S., Terada, A., Aoi, Y., Tsuneda, S., Alpkvist, E., Picioreanu, C., and van Loosdrecht, M. Experimental and simulation analysis of community structure of nitrifying bacteria in a membrane-aerated biofilm. *Water Science and Technology 55*, 8-9 (2007), 283–290.

[147] Matz, C., and Kjelleberg, S. Off the hook - how bacteria survive protozoan grazing. *Trends in Microbiology 13*, 7 (2005), 302–7.

[148] Mechias, J. *Simulation and Modelling of the Influence of Biofilm Structure on Molecular Diffusion with AQUASIM*. Student research paper, TU Braunschweig, Inst. of Biochemical Engineering, 2005.

[149] Medilanski, E., Kaufmann, K., Wick, L., Wanner, O., and Harms, H. Influence of the surface topography of stainless steel on bacterial adhesion. *Biofouling 18*, 3 (2002), 193–203.

[150] Möhle, R. *Simulation der Biomasseverteilung in Biofilmen bei variierender hydrodynamischer Beanspruchung*. Diploma thesis, Technische Universität Braunschweig, 2004.

[151] Möhle, R., Langemann, T., Haesner, M., Augustin, W., Scholl, S., Neu, T., Hempel, D., and Horn, H. Structure and shear strength of microbial biofilms as determined with confocal laser scanning microscopy and fluid dynamic gauging using a novel rotating disc biofilm reactor. *Biotechnology and Bioengineering 98*, 4 (2007), 747–755.

[152] Möhle, R., Zapf, K., Kowalewski, M., Neu, T., Horn, H., and Hempel, D. A novel flow-through biofilm tube reactor (FTBTR) for the investigation of growth and detachment in biofilm cultivations. *Biotechnology and Bioengineering* (in preparation).

[153] Milferstedt, K., Pons, M., and Morgenroth, E. Abrasion as a major source of macroscale heterogeneity in biofilm development in an annular reactor. In *Biofilms 2004: Structure and Activity of Biofilms* (Las Vegas, 2004), vol. 392.

[154] Milferstedt, K., Pons, M., and Morgenroth, E. Optical method for long-term and large-scale monitoring of spatial biofilm development. *Biotechnology and Bioengineering 94*, 4 (2006), 773–82.

[155] Molina-Höppner, A., Sato, T., Kato, C., Ganzle, M., and Vogel, R. Effects of pressure on cell morphology and cell division of lactic acid bacteria. *Extremophiles 7*, 6 (2003), 511–6.

[156] Monod, J. The growth of bacterial cultures. *Annu. Rev. Microbiol. 3* (1949), 371–394.

[157] Moreira, J., and Alves, P. Hydrodynamic effects on BHK cells grown as suspended natural aggregates. *Biotechnology and Bioengineering 46* (1995), 351–360.

[158] Morgenroth, E. *Enhanced biological phosphorous removal in biofilm reactors*. Doctorate thesis, Technische Universität München, 1998.

[159] Morgenroth, E. Detachment: an often-overlooked phenomenon in biofilm research and modeling. In *Biofilms in wastewater treatment*, S. Wuertz, P. Bishop, and P. Wilderer, Eds. IWA Publishing, 2003, pp. 264–290.

[160] Neu, T. Significance of bacterial surface-active compounds in interaction of bacteria with interfaces. *Microbiological Reviews 60*, 1 (1996), 151–66.

[161] Nicolella, C., van Loosdrecht, M., and Heijnen, J. Particle-based biofilm reactor technology. *Trends in Biotechnology 18*, 7 (2000), 312–320.

[162] Nicolella, C., van Loosdrecht, M., van der Lans, R., and Heijnen, J. Hydrodynamic characteristics and gas-liquid mass transfer in a biofilm airlift suspension reactor. *Biotechnology and Bioengineering 60*, 5 (1998), 627–35.

[163] Nollert, M., Diamond, S., and McIntire, L. Hydrodynamic shear stress and mass transport modulation of endothelian cell metabolism. *Biotechnology and Bioengineering 38* (1991), 588–602.

[164] Ohashi, A., and Harada, H. Characterization of detachment mode of biofilm developed in an attached-growth reactor. *Water Science and Technology 30*, 11 (1994), 35–45.

[165] Oliver, W., and Pharr, G. An improved technique for determining hardness and elastic modulus using load and displacement sensing indentation experiments. *Journal of Materials Research 7*, 6 (1992), 1564–1583.

[166] Olson, G., Brierley, J., and Brierley, C. Bioleaching review part B. *Applied Microbiology and Biotechnology 63*, 3 (2003), 249–257.

[167] Otto, P. *Entwicklung eines chemisch-biologischen Verfahrens zur Reinigung EDTA enthaltender Abwässer*. Doctorate thesis, Technische Universität Braunschweig, 2003. Vol.16 in Hempel, D.C. (ed.): ibvt-Schriftenreihe, FIT-Verlag Paderborn.

[168] Parsek, M., and Greenberg, E. Sociomicrobiology: the connections between quorum sensing and biofilms. *Trends in Microbiology 13*, 1 (2005), 27–33.

[169] Perez, J., Picioreanu, C., and van Loosdrecht, M. Modeling biofilm and floc diffusion processes based on analytical solution of reaction-diffusion equations. *Water Research 39*, 7 (2005), 1311–23.

[170] Peyton, B., and Characklis, W. A statistical analysis of the effect of substrate utilization and shear stress on the kinetics of biofilm detachment. *Biotechnology and Bioengineering 41*, 7 (1993), 728–735.

[171] Picioreanu, C., Head, I., Katuri, K., van Loosdrecht, M., and Scott, K. A computational model for biofilm-based microbial fuel cells. *Water Research 41*, 13 (2007), 2921–2940.

[172] Picioreanu, C., Kreft, J., Klausen, M., Haagensen, J., Tolker-Nielsen, T., and Molin, S. Microbial motility involvement in biofilm structure formation - a 3D modelling study. *Water Science and Technology 55*, 8-9 (2007), 337–343.

[173] Picioreanu, C., Kreft, J., and van Loosdrecht, M. Particle-based multidimensional multispecies biofilm model. *Applied and Environmental Microbiology 70*, 5 (2004), 3024–3040.

[174] Picioreanu, C., and van Loosdrecht, M. A mathematical model for initiation of microbiologically influenced corrosion by differential aeration. *Journal of the Electrochemical Society 149*, 6 (2002), 211–223.

[175] Picioreanu, C., and van Loosdrecht, M. Use of mathematical modelling to study biofilm development and morphology. In *Biofilms in Medicine, Industry and Environmental Biotechnology*, P. Lens, A. Moran, T. Mahony, P. Stoodley, and V. O´Flaherty, Eds. IWA Publishing, London, 2003, pp. 413–437.

[176] Picioreanu, C., van Loosdrecht, M., and Heijnen, J. Mathematical modeling of biofilm structure with a hybrid differential-discrete cellular automaton approach. *Biotechnology and Bioengineering 58*, 1 (1998), 101–16.

[177] Picioreanu, C., van Loosdrecht, M., and Heijnen, J. A theoretical study on the effect of surface roughness on mass transport and transformation in biofilms. *Biotechnology and Bioengineering 68*, 4 (2000), 355–69.

[178] Picioreanu, C., van Loosdrecht, M., and Heijnen, J. Two-dimensional model of biofilm detachment caused by internal stress from liquid flow. *Biotechnology and Bioengineering 72* (2001), 205–218.

[179] Pirt, S. *Principles of microbe and cell cultivation*. Blackwell, London, 1975.

[180] Poppele, E., and Hozalski, R. Micro-cantilever method for measuring the tensile strength of biofilms and microbial flocs. *Journal of Microbiological Methods 55*, 3 (2003), 607–15.

[181] Popper, K. *Logik der Forschung (en.:The logic of scientific discovery)*. Mohr, 1934. 10th edition 1994.

[182] Prigent-Combaret, C., Vidal, O., Dorel, C., and Lejeune, P. Abiotic surface sensing and biofilm-dependent regulation of gene expression in *Escherichia coli*. *Journal of Bacteriology 181*, 19 (1999), 5993–6002.

[183] Pross, A. On the emergence of biological complexity: Life as a kinetic state of matter. *Origins of Life and Evolution of Biospheres 35*, 2 (2005), 151–166.

[184] Purevdorj-Gage, B., Costerton, W., and Stoodley, P. Phenotypic differentiation and seeding dispersal in non-mucoid and mucoid *Pseudomonas aeruginosa* biofilms. *Microbiology 151* (2005), 1569–1576.

[185] Queck, S., Weitere, M., Moreno, A., Rice, S., and Kjelleberg, S. The role of quorum sensing mediated developmental traits in the resistance of *Serratia marcescens* biofilms against protozoan grazing. *Environmental Microbiology 8*, 6 (2006), 1017–25.

[186] Rabaey, K., and Verstraete, W. Microbial fuel cells: novel biotechnology for energy generation. *Trends in Biotechnology 23*, 6 (2005), 291–8.

[187] Raven, P., Johnson, G., Losos, J., and Singer, S. *Biology*, vol. 7. Lange, New York, 2005.

[188] Reguera, G., McCarthy, K., Mehta, T., Nicoll, J., Tuominen, M., and Lovley, D. Extracellular electron transfer via microbial nanowires. *Nature 435*, 7045 (2005), 1098–1101.

[189] Reichert, P. *AQUASIM 2.0 - User Manual*. EAWAG, Dübendorf (CH), 1998.

[190] Reid, G. Biofilms in infectious disease and on medical devices. *International journal of antimicrobial agents 11*, 3-4 (1999), 223–6.

[191] Reis, M., Serafim, L., Lemos, P., Ramos, A., Aguiar, F., and Van Loosdrecht, M. Production of polyhydroxyalkanoates by mixed microbial cultures. *Bioprocess and Biosystems Engineering 25*, 6 (2003), 377–85.

[192] Rittmann, B. Detachment from biofilms. In *Structure and Function of Biofilms*, W. Characklis and P. Wilderer, Eds. Wiley, 1989.

[193] Rittmann, B. The membrane biofilm reactor: the natural partnership of membranes and biofilm. *Water Science and Technology 53*, 3 (2006), 219–25.

[194] Roberge, P. *Corrosion testing made easy: Erosion-corrosion*. National Association of Corrosion, 2004.

[195] Rode, A. *Isolierung und Charakterisierung von bakteriellen extrazellulären polymeren Substanzen aus Biofilmen*. Doctorate thesis, Universität Duisburg-Essen, 2004.

[196] Rohwerder, T., Gehrke, T., Kinzler, K., and Sand, W. Bioleaching review part a. *Applied Microbiology and Biotechnology 63*, 3 (2003), 239–248.

[197] Rupp, C., Fux, C., and Stoodley, P. Viscoelasticity of *Staphylococcus aureus* biofilms in response to fluid shear allows resistance to detachment and facilitates rolling migration. *Applied and environmental microbiology 71*, 4 (2005), 2175–2178.

[198] Ryder, M. Catheter-related infections: it's all about biofilm. *Medscape 5*, 3 (2005).

[199] Sahoo, S., Verma, R., Suresh, A., Rao, K., Bellare, J., and Suraishkumar, G. Macro-level and genetic-level responses of *Bacillus subtilis* to shear stress. *Biotechnology Progress 19*, 6 (2003), 1689–96.

[200] Salem, S., Moussa, M., and van Loosdrecht, M. Determination of the decay rate of nitrifying bacteria. *Biotechnology and Bioengineering 94*, 2 (2006), 252–62.

[201] Schlegel, H. *Geschichte der Mikrobiologie*, vol. 28 of *Acta historica Leopoldina*. Deutsche Akademie der Naturforscher Leopoldina, Halle (Saale), 1999.

[202] Schlichting, H., and Gersten, K. *Boundary layer theory*, 8th ed. Springer, 2000.

[203] Schooling, S., and Beveridge, T. Membrane vesicles: an overlooked component of the matrices of biofilms. *Journal of Bacteriology 188*, 16 (2006), 5945–57.

[204] Schwarz, W. The cellulosome and cellulose degradation by anaerobic bacteria. *Applied Microbiology and Biotechnology 56*, 5 (2001), 634–649. 0175-7598.

[205] Service, R. Complex systems:exploring the systems of life. *Science 284*, 5411 (1999), 80a–83.

[206] Seviour, R., and Blackall, L. *The microbiology of activated sludge*. Kluwer, Dordrecht, 1999.

[207] Shapiro, J. *Bacteria as multicellular organism*. Scientific American. Oxford University Press, 1988.

[208] Siboni, N., Lidor, M., Kramarsky-Winter, E., and Kushmaro, A. Conditioning film and initial biofilm formation on ceramics tiles in the marine environment. *FEMS Microbiology Letters 274*, 1 (2007), 24–9.

[209] Siegrist, H., and Gujer, W. Mass transfer mechanisms in a heterotrophic biofilm. *Water Research 19*, 11 (1985), 1369–1378.

[210] Staudt, C. *Entwicklung der Struktur von Biofilmen*. Doctorate thesis, Technical University Braunschweig, 2005. Vol. 22 in Hempel, D.C. (ed.): ibvt-Schriftenreihe, FIT-Verlag Paderborn.

[211] Staudt, C., Horn, H., Hempel, D., and Neu, T. Volumetric measurements of bacterial cells and EPS glycoconjugates in biofilms. *Biotechnology and Bioengineering* (2004).

[212] Stewart, P. A model of biofilm detachment. *Biotechnology and Bioengineering 41* (1993), 111–117.

[213] Stickler, D. Bacterial biofilms and the encrustation of urethral catheters. *Biofouling 9*, 4 (1996), 293–305.

[214] Stoodley, P., Lewandowksi, Z., Boyle, J., and Lappin-Scott, H. Structural deformation of bacterial biofilms caused by short-term fluctuations in fluid shear: An in situ investigation of biofilm rheology. *Biotechnology and Bioengineering 65*, 1 (1999), 83–92.

[215] Stoodley, P., Wilson, S., Hall-Stoodley, L., Boyle, J., Lappin-Scott, H., and Costerton, J. Growth and detachment of cell clusters from mature mixed-species biofilms. *Applied and environmental microbiology 67*, 12 (2001), 5608–5613.

[216] Sutherland, I. Biofilm exopolysaccharides: a strong and sticky framework. *Microbiology 147*, 1 (2001), 3–9.

[217] Symmons, S., Allison, D., Smith, A., and Gilbert, P. Protozoan grazing on biofilm communities. In *Biofilm Communities: Order from Chaos? Contributions made at the Sixth Meeting of the Biofilm Club*, A. McBain, D. Allison, M. Brading, A. Rickard, V. Joanna, and J. Walker, Eds. BioLine, 2003, pp. 351–358.

[218] Telgmann, U., Horn, H., and Morgenroth, E. Influence of growth history on sloughing and erosion from biofilms. *Water Research 38*, 17 (2004), 3671–84.

[219] Terada, A., Lackner, S., Tsuneda, S., and Smets, B. Redox-stratification controlled biofilm (ReSCoBi) for completely autotrophic nitrogen removal: the effect of co- versus counter-diffusion on reactor performance. *Biotechnology and Bioengineering 97*, 1 (2007), 40–51.

[220] Tice, M., and Lowe, D. Photosynthetic microbial mats in the 3,416-myr-old ocean. *Nature 431* (2004), 549–552.

[221] Tijhuis, L., van Loosdrecht, M., and Heijnen, J. Dynamics of biofilm detachment in biofilm airlift suspension reactors. *Biotechnology and Bioengineering 45*, 6 (1995), 481–487.

[222] Towler, B., Cunningham, A., Stoodley, P., and McKittrick, L. A model of fluid-biofilm interaction using a burger material law. *Biotechnology and Bioengineering 96*, 2 (2007), 259–271.

[223] Towler, B., Rupp, C., Cunningham, A., and Stoodley, P. Viscoelastic properties of a mixed culture biofilm from rheometer creep analysis. *Biofouling 19*, 5 (2003), 279–285.

[224] van Benthum, W., van Loosdrecht, M., Tijhuis, L., and Heijnen, J. Solid retention time in heterotrophic and nitrifying biofilms in a biofilm airlift suspension reactor. *Water Science and Technology 32* (1995), 53–60.

[225] van Loosdrecht, M., Eikelboom, D., Gjaltema, A., Mulder, A., Tijhuis, L., and Heijnen, J. Biofilm structures. *Water Science and Technology 32*, 8 (1995), 35–44.

[226] Van Loosdrecht, M., and Henze, M. Maintenance, endogeneous respiration, lysis, decay and predation. *Water Science and Technology 39*, 1 (1999), 107–117.

[227] van Loosdrecht, M., Lyklema, J., Norde, W., Schraa, G., and Zehnder, A. The role of bacterial cell wall hydrophobicity in adhesion. *Applied and Environmental Microbiology 53*, 8 (1987), 1893–1897.

[228] Vandamme, E. *Biopolymers*, vol. 1. Wiley-VCH, 2005.

[229] Verran, J., and Hissett, T. The effect of substratum surface defects upon retention of, and biofilm formation by, microorganisms from potable water. *Special publication, Royal Society of Chemistry 242* (1999), 25–33.

[230] Vidović, E. *The development of bioabsorbable hydrogels on the basis of polyester grafted poly(vinyl alcohol)*. PhD thesis, Rheinisch-Westfälischen Technischen Hochschule Aachen, 2006.

[231] Vinogradov, A., Winston, M., Rupp, C., and Stoodley, P. Rheology of biofilms formed from the dental plaque pathogen *Streptococcus mutans*. *Biofilms 1* (2004), 49–56.

[232] Vollmer, G., and Lorenz, K. *Die Natur der Erkenntnis : Beiträge zur evolutionären Erkenntnistheorie : mit 12 Tabellen*. Was können wir wissen? Vol. I. Hirzel, 1988.

[233] Wagner, K., and Hempel, D. Biodegradation by immobilized bacteria in an airlift-loop reactor - influence of biofilm diffusion limitation. *Biotechnology and Bioengineering 31*, 6 (1988), 559–566.

[234] Walker, J., Surman, S., and Jass, J. *Industrial biofouling; detection, prevention and control*. Wiley, Chichester, 2000.

[235] Wanner, O., and Gujer, W. A multispecies biofilm model. *Biotechnology and Bioengineering 28* (1986), 314–328.

[236] Wanner, O., and Morgenroth, E. Biofilm modeling with AQUASIM. *Water Science and Technology 49*, 11-12 (2004), 137–44.

[237] Wanner, O., and Reichert, P. Mathematical modeling of mixed-culture biofilms. *Biotechnology and Bioengineering 49*, 2 (1996), 172–184.

[238] Watnick, P., and Kolter, R. Biofilm, city of microbes. *Journal of Bacteriology 182*, 10 (2000), 2675–2679.

[239] Weiss, R., and Ollis, D. Extracellular microbial polysaccharides. I. Substrate, biomass, and product kinetic equations for batch xanthan gum fermentation. *Biotechnology and Bioengineering 22*, 4 (1980), 859–873.

[240] Weitere, M., Bergfeld, T., Rice, S., Matz, C., and Kjelleberg, S. Grazing resistance of *Pseudomonas aeruginosa* biofilms depends on type of protective mechanism, developmental stage and protozoan feeding mode. *Environ Microbiol 7*, 10 (2005), 1593–601.

[241] Whitchurch, C., Tolker-Nielsen, T., Ragas, P., and Mattick, J. Extracellular DNA required for bacterial biofilm formation. *Science 295* (2002), 1487.

[242] White, F. *Viscous fluid flow*. McGraw-Hill, New York, 1991.

[243] White, F. *Fluid mechanics*, 5th ed. McGraw-Hill, New York, 2003.

[244] Whitfield, C., and Keenleyside, W. Regulation of expression of group IA capsular polysaccharides in *Escherichia coli* and related extracellular polysaccharides in other bacteria. *Journal of industrial microbiology 15*, 4 (1995), 361–71.

[245] Wiesmann, U. *Fundamentals of biological wastewater treatment*. Wiley-VCH, Weinheim, 2007.

[246] Wimpenny, J., Manz, W., and Szewzyk, U. Heterogeneity in biofilms. *FEMS Microbiology Reviews 24* (2000), 661–671.

[247] Wolf, G., Picioreanu, C., and van Loosdrecht, M. Kinetic modelling of phototrophic biofilms - the PHOBIA model. *Biotechnology and Bioengineering 97*, 5 (2007), 1064–1079.

[248] Worlitzsch, D., Tarran, R., Ulrich, M., Schwab, U., Cekici, A., Meyer, K., Birrer, P., Bellon, G., Berger, J., Weiss, T., Botzenhart, K., Yankaskas, J., Randell, S., Boucher, R., and Doring, G. Effects of reduced mucus oxygen concentration in airway *Pseudomonas* infections of cystic fibrosis patients. *Journal of Clinical Investigations 109*, 3 (2002), 317–25.

[249] Wäsche, S. *Einfluss der Wachstumsbedingungen auf Stoffübergang und Struktur von Biofilmsystemen*. Doctorate thesis, Technische Universität Braunschweig, 2002. Vol.14 in Hempel, D.C. (ed.): ibvt-Schriftenreihe, FIT-Verlag Paderborn.

[250] Wäsche, S., Horn, H., and Hempel, D. Influence of growth conditions on biofilm development and mass transfer at the bulk/biofilm interface. *Water research 36*, 19 (2002), 4775–4784.

[251] Xavier, J., and Foster, K. Cooperation and conflict in microbial biofilms. *Proceedings of the National Academy of Sciences USA 104*, 3 (2007), 876–81.

[252] Xavier, J., Picioreanu, C., Rani, S., van Loosdrecht, M., and Stewart, P. Biofilm control strategies based on enzymatic disruption of the eps matrix - a modelling study. *Microbiology 151* (2005), 3817–3832.

[253] Xavier, J., Picioreanu, C., and van Loosdrecht, M. Assessment of three-dimensional biofilm models through direct comparison with confocal microscopy imaging. *Water Science and Technology 49*, 11-12 (2004), 177–185.

[254] Xavier, J., Picioreanu, C., and van Loosdrecht, M. A modelling study of the activity and structure of biofilms in biological reactors. *Biofilms 1* (2004), 377–391.

[255] Xavier, J., Picioreanu, C., and van Loosdrecht, M. A framework for multidimensional modelling of activity and structure of multispecies biofilms. *Environmental Microbiology 7*, 8 (2005), 1085–1103.

[256] Xavier, J., Picioreanu, C., and van Loosdrecht, M. A general description of detachment for multidimensional modelling of biofilms. *Biotechnology and Bioengineering 91*, 6 (2005), 651–69.

[257] Zapf, K. *Untersuchung von Wachstum und Abtrag bei der Strukturentwicklung heterotropher Biofilme*. Student research paper, Technische Universität Braunschweig, 2006.

[258] Zhang, T., and Bishop, P. Density, porosity and pore structure of biofilms. *Water Research 28*, 11 (1994), 2267–2277.

[259] Zhang, T., and Bishop, P. Evaluation of tortuosity factors and effective diffusivities. *Water Research 28*, 11 (1994), 2279–2287.

[260] Zienkiewicz, O., Taylor, R., and Zhu, J. *The finite element method: its basis and fundamentals*. Elsevier Butterworth-Heinemann, 2005. Literaturangaben.

[261] Zimmer, C. Complex systems:life after chaos. *Science 284*, 5411 (1999), 83–86.

[262] Zobell, C. The effect of solid surfaces upon bacterial activity. *Journal of Bacteriology 46*, 1 (1943), 39–56.

Zusammenfassung

Das Leben in sessilen Gemeinschaften bietet Mikroorganismen in zahlreichen Habitaten entscheidende evolutionäre Vorteile. In dieser als Biofilm bezeichneten Form mikrobiellen Lebens lassen sich Organismen verschiedenster Reiche, wie z.B. Bacteria, Fungi, Archaea, Protistae, etc. in einer Matrix aus biogenen extrazellulären polymeren Substanzen (EPS) immobilisiert vorfinden. Diese Matrix bietet einerseits Schutz gegenüber externen Störungen, verursacht andererseits durch Stofftransporteffekte aber auch eine räumliche Heterogenität zahlreicher Eigenschaften. Das konzertierte Wirken der Zellen im Biofilm sowohl auf intra- als auch auf interspezifischer Ebene lässt den Vergleich mit multizellulären Organismen zu und bietet einen Erklärungsansatz für den eingangs genannten evolutionären Erfolg von Biofilmen. So verwundert es nicht, dass sich Biofilme vielerorts in Natur, Technik und sogar in Form hartnäckiger Infektionen auf medizinischen Implantaten finden lassen.

Basierend auf der erfahrungswissenschaftlichen Methode von Hypothese und experimenteller Prüfung wird in dieser Arbeit eine iterative Methodik vorgestellt, welche die mathematische Modellierung mit Experimenten kombiniert und so zu einem fokussierten Arbeiten und besserem Verständnis von Biofilmen in Wechselwirkung mit ihrer Umwelt führt. Auf diese Weise konnte das Versuchssytem zur gezielten Kultivierung von Biofilmen im Labor derart weiterentwickelt werden, dass es die benötigten Daten für eine breite Modellvalidierung liefert. In Form des Flow-through Biofilm Tube Reactor (FTBTR) liegt ein Biofilmreaktorsystem vor, das einerseits die definierte Einstellung der Kultivierungsparameter, wie Substratversorgung und Strömungsbedingungen erlaubt, aber auch vollständig bilanzierbar ist. Zentrales Ziel dieser Arbeit ist es, ein mehrdimensionales Modell zu entwickeln, das in der Lage ist, die Strukturentwicklung von Biofilmen zu prognostizieren. Basierend auf experimentellen Daten wird mit einem zunächst eindimensionalen Modellansatz versucht, die zeitliche Entwicklung des Biofilms auf Ebene des Reaktors zu beschreiben. Die während der Biofilmentwicklung beobachteten steigenden Raten von Biomasseproduktion und Substratverbrauch können im Modell durch das

Wachstum des Biofilms in Form halbkugeliger Kolonien sehr gut wiedergegeben werden. Der so entwickelte Satz von Parametern und Prozessen wird nun in ein partikelbasiertes mehrdimensionales Biofilmmodell integriert mit dem Ziel, die im Experiment beobachteten Strukturen auf der Mikroebene als emergente Eigenschaft in den Simulationen wiederzufinden. Die nicht erfolgreiche Durchführung dieses Vorhabens hat deutlich aufgezeigt, dass die empirischen Ansätze zur Beschreibung von Abtragsphänomenen in Biofilmsystemen nicht hinreichend die reale Komplexität dieser Prozesse beschreiben können.

Basierend auf diesen Erkenntnissen wird ein mechanischer Modellansatz konzipiert, der die komplexe Interaktion von Fluidströmung und Biofilmstruktur berücksichtigt. Die zunächst analytische Annäherung a priori an diese Fragestellung zeigt, von welchen Parametern Abtragsereignisse abhängen. Ein darauf basierendes Finite Elemente Modell führt den Abtrag von Biomasse aus dem Biofilm auf das strukturelle Versagen der Matrix zurück und erlaubt so eine detailliertere Analyse der Abtragsphänomene. Dieser neue Modellansatz bietet ein flexibles Rahmenwerk, das es erlaubt, beliebige weitere relevante Prozesse zu implementieren.

Die künftige Weiterentwicklung dieses Modells in engem Wechselspiel mit seiner experimentellen Validierung lässt ein deutlich besseres Verständnis von Biofilmen in ihrer Umwelt erhoffen. Die so gewonnenen Erkenntnisse können für den Menschen dann insbesondere für die Vermeidung und Kontrolle unerwünschter Biofilme, aber auch bei der gezielteren Auslegung und Optimierung von effizienten Abwasserbehandlungsanlagen nützlich sein.